

# *Shallow groundwater geochemistry in the Española Basin, Rio Grande rift, New Mexico: Evidence for structural control of a deep thermal source*

P.S. Johnson  
D.J. Koning

New Mexico Bureau of Geology and Mineral Resources, New Mexico Institute of Mining and Technology,  
801 Leroy Place, Socorro, New Mexico 87801, USA

F.K. Partey  
Agrium, Inc., Soda Springs, Idaho 83276, USA

## ABSTRACT

We have developed a conceptual model for the Tesuque aquifer system in the southeastern Española Basin near Santa Fe, New Mexico, based on measurements of chemical, isotopic, and thermal properties of groundwater from 120 wells. This study concentrates on a single groundwater-flow unit (GFU) of the Tesuque aquifer associated with the Santa Fe River drainage, where groundwater flows east to west across north-trending rift structures. We examine links between groundwater flow, temperature, water chemistry, and major fault structures. Hydrologic and hydrochemical processes are assessed through spatial mapping of temperature and chemical composition (Ca:Na ratios, F, As, B, Li,  $\delta^2\text{H}$ , and  $\delta^{18}\text{O}$ ), Piper and bivariate plots, Spearman rank-order correlations, and flow-line modeling of mineral saturation (PHREEQC software). Results help delineate recharge and discharge areas and demonstrate spatial correspondence of major rift structures with changes in chemical and thermal data. Thermal wells with anomalous discharge temperatures and regional thermal gradients exceeding  $40\text{ }^\circ\text{C/km}$  align with structural boundaries of the Cañada Ancha graben and Caja del Rio horst. Mg-Li geothermometry characterizes temperatures associated with deep circulating groundwater. Important features of the conceptual model are (1) a forced convection system in the Tesuque aquifer associated with the Caja del Rio horst drives upward flow and discharge of warm, Na-rich groundwater in the western half of the Cañada Ancha graben; and (2) major horst-graben structures concentrate upward flow of deep,  $\text{NaSO}_4$  thermal waters from underlying bedrock. Both features likely contribute to chemical anomalies and thermal disturbances in the shallow Tesuque aquifer.

## INTRODUCTION

Groundwater conditions in the Santa Fe Group aquifer of the Española Basin, northern New Mexico, have been studied for several decades but in some areas are still poorly understood. In the southern Española Basin near Santa Fe, complex groundwater flow patterns have been documented (Spiegel and Baldwin, 1963; Mourant, 1980; Johnson, 2009) but not explained, and the geochemical characteristics of groundwater have not been thoroughly examined. Since 2002, the New Mexico Bureau of Geology and Mineral Resources (NMBGMR) and Office of the State Engineer have conducted hydrologic and geochemical field studies in the Santa Fe area to better understand the regional aquifer system and its geochemical characteristics. One product is a large geochemical data set generated from existing data and new samples collected in 2005 (Johnson et al., 2008). Researchers have also generated new geologic maps (Koning and Read, 2010) and a geophysical data model (Grauch et al., 2009), which have refined depositional and tectonic interpretations and updated the geologic framework of the basin (e.g., Koning et al., this volume). The primary goal of this study is to integrate these data to better understand the region's groundwater resources. In this paper, we combine geochemical data from Johnson et al. (2008) pertaining to a local groundwater-flow unit (GFU) associated with the Santa Fe River drainage (Johnson, 2009) with hydrologic, thermal, and structural data to examine links between groundwater flow, temperature, water chemistry, and Rio Grande rift structures. Based on interpretations of these data, we propose a conceptual model for the Tesuque aquifer system. Important features of the conceptual model are the following: (1) the buried Caja del Rio horst creates a forced convection system in the Tesuque aquifer that drives upward flow and discharge of warm, sodium-rich water in the Cañada Ancha graben; and (2) upwelling of deep thermal fluids along horst-graben structures contributes to shallow-water quality degradation in the discharge area of the Santa Fe GFU. Results of this study enhance understanding of geologic controls on regional groundwater flow, heat transport, and groundwater quality in the Tesuque aquifer system near Santa Fe.

## PHYSICAL AND GEOLOGIC SETTING

The Española Basin, one of a series of extensional basins in the Rio Grande rift, lies between the east-dipping San Luis Basin to the northeast and the Santo Domingo and east-dipping Albuquerque Basins to the southwest (Fig. 1). The Española Basin is topographically situated between two mountainous terrains—the Sangre de Cristo Mountains on the east and the Jemez volcanic field on the west. The Rio Grande flows southwestward along the axis of the basin. In the southeastern portion of the basin, the Santa Fe River flows southwest from the Sangre de Cristo Mountains, cuts through the Cerros del Rio volcanic field, and discharges into the Rio Grande at Cochiti Reservoir. The following geologic overview of the Santa Fe area is synthesized from

more-detailed descriptions of the basin and mountain-block geology presented by Spiegel and Baldwin (1963), Galusha and Blick (1971), Manley (1978, 1979), Bauer et al. (1997), Read et al. (2003), Koning and Hallett (2001), Koning and Maldonado (2003), Myer and Smith (2006), and Koning and Read (2010). General geologic features, principal rock types, and stratigraphy are shown in Figures 2 and 3.

## Stratigraphy

The Tesuque aquifer system consists of basin fill and overlies bedrock comprising Proterozoic crystalline rocks, Pennsylvanian strata, early Neogene sedimentary rocks, and Eocene–Oligocene volcanic and volcanioclastic rocks. The upper Santa Fe River drainage in the Sangre de Cristo Mountains consists primarily of Proterozoic granitic gneiss and schist that are rich in quartz, potassium feldspar, plagioclase, and biotite, and local amphibolite dikes. These Proterozoic rocks are locally overlain by thin

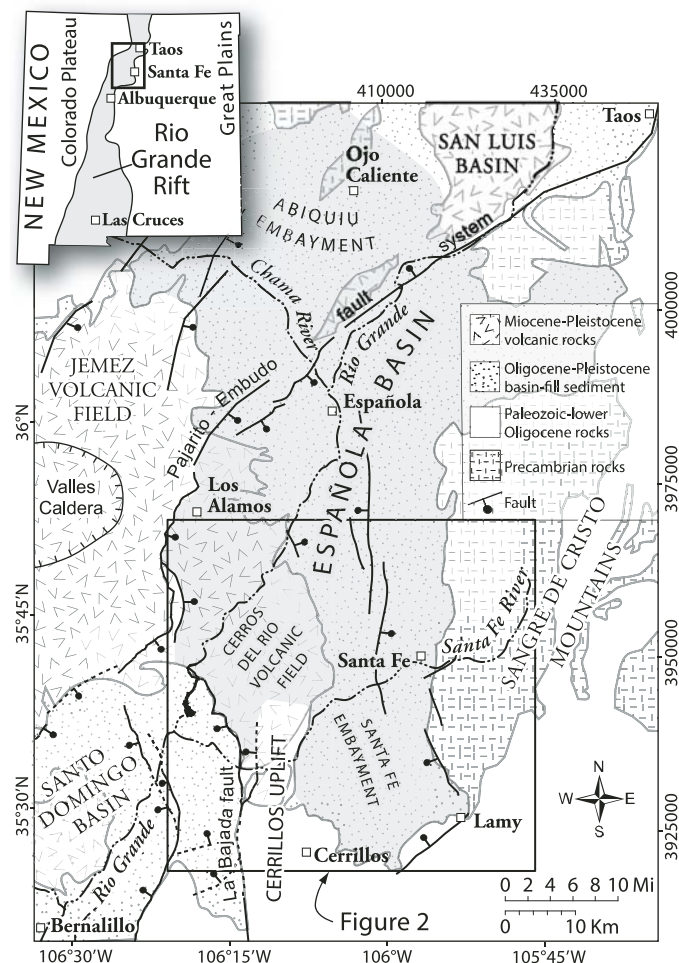


Figure 1. Regional geologic setting of the Española Basin. Structural features and faults are modified from Koning and Read (2010) and Minor et al. (2006). Española Basin is shaded gray.

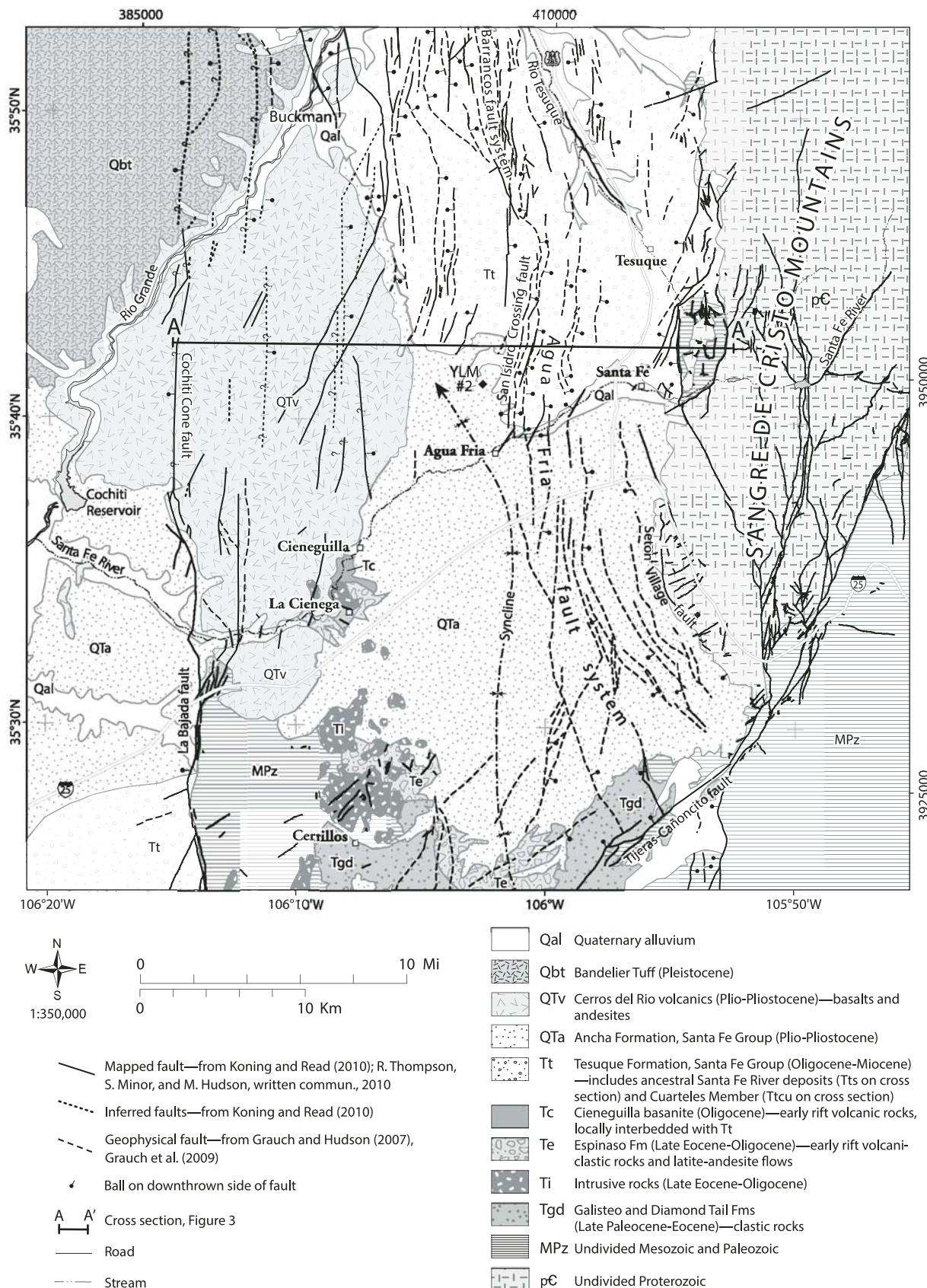


Figure 2. Generalized geology of the study area. Geologic contacts and mapped faults are generalized from Koning and Read (2010). Faults inferred from geophysical data are from Grauch et al. (2009). Cross section A–A' is shown in Figure 3. YLM#2—Yates La Mesa No. 2 exploration well.

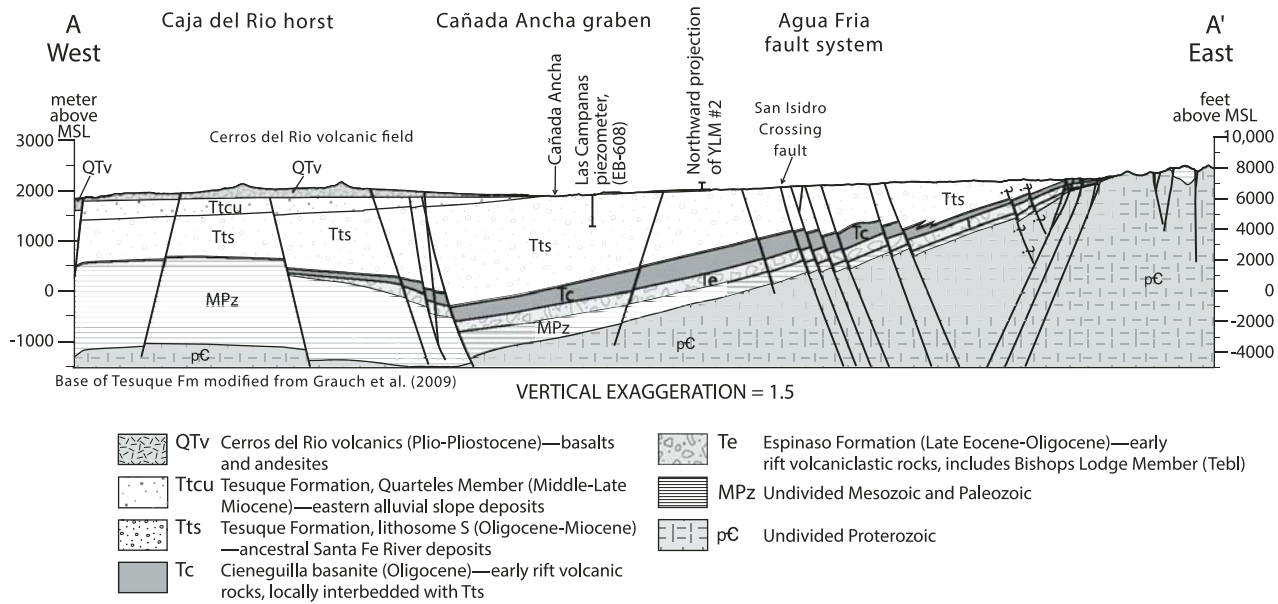


Figure 3. Geologic cross section, west to east, north of the Santa Fe River. Line of cross section is shown in Figure 2 (modified from section D-D' of Koning and Read, 2010). YLM#2—Yates La Mesa No. 2 exploration well.

(<60 m), limestone-dominated Pennsylvanian strata. Mesozoic to Upper Permian strata do not exist along the mountain front near Santa Fe, where the Late Eocene–Oligocene Espinoso Formation unconformably overlies Proterozoic and Pennsylvanian units (Figs. 2 and 3). Cuttings from the Yates La Mesa No. 2 exploration well (YLM#2) west of Santa Fe (Fig. 2) document a similar sequence of strata underlying basin-fill sediments: Proterozoic granitic rocks overlain by 462 m of interbedded Pennsylvanian limestone and clastic sedimentary strata, 307 m of the Espinoso Formation, and 318 m of the Cieneguilla basanite (Myer and Smith, 2006). East of YLM#2, the Cieneguilla basanite thins dramatically and crops out north of Santa Fe as a single, 1–2-m-thick flow (Read et al., 2003). West of YLM#2, interpretations of geophysical data indicate thickening of upper Paleozoic and Mesozoic strata over the Cerrillos uplift (Fig. 3) (Myer and Smith, 2006; Rodriguez and Sawyer, this volume).

The Espinoso Formation, where exposed on the southern and western margins of the basin, mostly consists of alluvial fan deposits of volcaniclastic conglomerate and sandstone. Minor monzonite, latite, and andesite flows and ash-flow tuffs surround vents distributed in a zone from what is now the Cerrillos Hills to north of Cieneguilla (Fig. 4) (Smith et al., 1991; Erskine and Smith, 1993; Kautz et al., 1981; Grauch et al., 2009). Local hydrothermal alteration and related vein deposits are noted near La Cienega but are relatively uncommon. At least one interbedded tuff, ~30 m thick, has been reported in logs from YLM#2 (David Sawyer, 2008, personal commun.).

In YLM#2, the Oligocene-age Cieneguilla basanite appears as interbedded mafic lava flows and sedimentary layers rich in pyroxene and plagioclase, with varying degrees of calcite or zeo-

lite replacement (Myer and Smith, 2006). Near La Cienega, outcrop exposures consist of basanite, basalt, and phreatomagmatic basaltic breccias (Stearns, 1953; Sun and Baldwin, 1958; Koning and Hallett, 2001). In the type section for the Cieneguilla basanite 3 km north of La Cienega, we have noted local hydrothermal alteration, calcite veins, and vugs filled with calcite (Fig. 5).

Erosion of Proterozoic and Pennsylvanian units during rift tectonism is primarily responsible for generating the siliciclastic sediments that fill the Española Basin and form the productive aquifers in the Santa Fe area. Collectively referred to as the Santa Fe Group, these basin-fill alluvial units include the Late Oligocene–Miocene Tesuque Formation and the Plio-Pleistocene Ancha Formation. All data presented in this study originate from wells completed in the Tesuque Formation, which consists of arkosic sandstone with minor conglomerate, siltstone, and claystone (Spiegel and Baldwin, 1963; Koning et al., 2007; Koning and Read, 2010). The Tesuque Formation is <600 m thick at the base of the Sangre de Cristo Mountains, but increases to 2000–2800 m in thickness in the Cañada Ancha graben northwest of Santa Fe (Fig. 4) (Biehler et al., 1991; Grauch et al., 2009). In YLM#2, Myer and Smith (2006) documented 1210 m of subarkosic sand and mudstone. The sand is composed of abundant quartz and feldspar, minor quartz-muscovite aggregates and quartzite, and scarce limestone. Because of the regional westward dip, the oldest Tesuque Formation strata are found near the mountain front and the youngest strata are exposed to the west near Buckman.

In the Santa Fe area, the Tesuque Formation has been subdivided into four interfingering map units called lithosomes (Read et al., 2005; Koning and Read, 2010) that correspond to

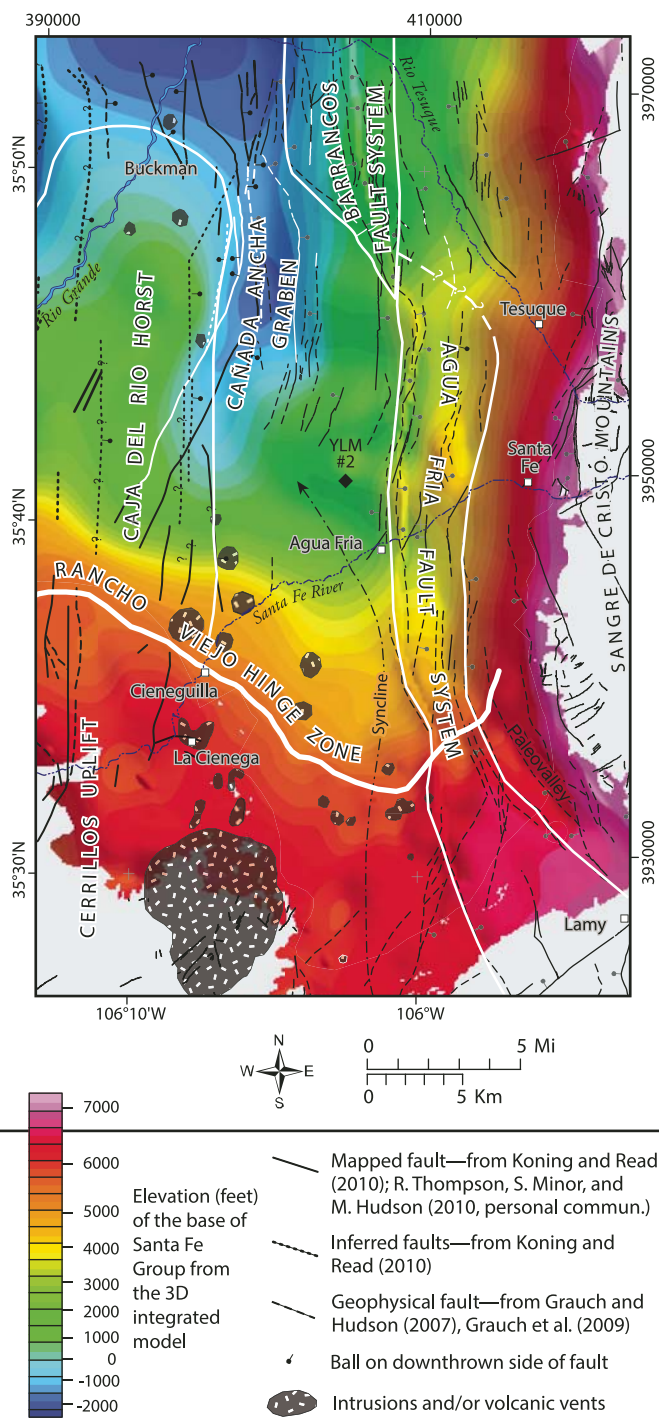


Figure 4. Major structural features of the southeastern Española Basin. Structural features, the lateral limits of the Cerros del Rio volcanic field, and Oligocene volcanic intrusions and vents are superimposed on the three-dimensional (3D) geophysical model from Grauch et al. (2009). The model defines the elevation (in feet) of the top of Oligocene volcanic rocks (base of the Santa Fe Group). Structural features (Barrancos and Agua Fria fault systems, Cañada Ancha graben, Cerillos uplift and Caja del Rio horst) are used for spatial reference in subsequent figures.

depositional facies of contributing paleodrainage systems. For this paper, the most significant of these is lithosome S (Tts in Fig. 3), deposited by a west-flowing, ancestral Santa Fe River during the latest Oligocene to Middle Miocene (Koning et al., 2004; Koning and Read, 2010). Lithosome S is a coarse, pebbly sand that becomes increasingly finer grained to the north, west, and south. The coarse-grained facies of lithosome S forms the most productive zone of the Tesuque aquifer, with a mean hydraulic conductivity of 2 m/d (Koning and Johnson, 2006). The Tesuque Formation generally overlies pre-rift volcanic rocks of the Cieneguilla basanite and Espinaso Formation (Koning and Read, 2010; Myer and Smith, 2006), but its base probably interfingers with the upper Cieneguilla basanite in the subsurface (Koning and Read, 2010; Koning et al., this volume). The Tesuque Formation is locally overlain by Plio-Pleistocene basalts of the Cerros del Rio volcanic field and the Ancha Formation (Spiegel and Baldwin, 1963).

### Structural Features

The southern Española Basin is structurally bounded on the northwest by the Pajarito-Embudo fault system, on the southwest by the La Bajada and Cochiti Cone faults (Minor et al., 2006; Grauch et al., 2009), and on the east by a few discontinuous, small-displacement faults and monoclines along the base of the Sangre de Cristo Mountains (Koning and Read, 2010) (Figs. 1 and 2). New aeromagnetic and gravity data and interpretations (Grauch et al., 2009) have refined our understanding of the basin's structural and tectonic features and their hydrogeologic significance (Fig. 4). The following overview summarizes the



Figure 5. Photograph of hydrothermal alteration in the Oligocene Cieneguilla basanite north of La Cienega. This exposure of altered, brecciated basalt contains abundant calcium-carbonate-filled vugs, vesicles, and veins up to 50 cm wide. Results of bulk-rock analysis of vein calcite are presented in Table 7 (sample Ci-6). Notebook is 4.75 in.  $\times$  7.5 in. Photo by D. Koning.

major rift structures that deform basement, bedrock, and overlying Tesuque Formation sediments.

The rift-related geometry at the base of the Santa Fe Group near Santa Fe is a deep, west-tilted half graben called the Cañada Ancha graben (Koning et al., this volume), which assumes a synclinal form on its southern end. There, the graben is bounded on its south side by a curvilinear (concave to the north), north-dipping flexure called the Rancho Viejo hinge zone (Biehler et al., 1991; Grauch et al., 2009). South of the Rancho Viejo hinge zone is a broad, folded platform (Fig. 4). Santa Fe Group sediments thicken northward by 1200–1700 m across the hinge zone and into the Cañada Ancha graben. The hinge zone is hydrologically important because it represents the southern extent of a relatively thick Santa Fe Group aquifer. Grauch et al. (2009) theorized that the Rancho Viejo hinge zone may represent a long-lived crustal weakness associated with multiple episodes of deformation that extended into the Late Miocene or early Pliocene after deposition of the Tesuque Formation.

The basin model of Grauch et al. (2009) portrays the Cañada Ancha graben as a narrow, west-tilted half graben bounded to the west by the Caja del Rio horst, a north- to northeast-elongated bedrock high that plunges gently to the north (Fig. 4). The Caja del Rio horst is buried beneath the Cerros del Rio volcanic field and delineated by gravity and magnetotelluric data as a northern extension of the Cerrillos uplift (Minor, 2006; Grauch et al., 2009; Rodriguez and Sawyer, this volume). Koning and Read (2010) depicted the eastern horst boundary as a series of east-down faults with a cumulative throw of up to 600–800 m (Fig. 3), consistent with geophysical interpretations of Grauch et al. (2009). Koning et al. (this volume) interpret that most of this deformation occurred prior to the late Pliocene.

Numerous normal faults are exposed within the Tesuque Formation in the middle of the basin (Fig. 2) and many concealed faults were interpreted from the geophysical studies of Grauch et al. (2009). Many of the faults are categorized into two major fault systems, the Barrancos and Agua Fria fault systems, which collectively traverse the entire basin in a generally north-south direction (Figs. 2, 4). The Barrancos fault system forms a zone 3–5 km wide consisting of east- and west-down faults across a large-scale, west-dipping monocline that forms the eastern edge of the Cañada Ancha graben (Koning et al., this volume). The Agua Fria fault system consists of a 3–5-km-wide zone of mostly east-down faults that bound west-tilted fault blocks (Grauch et al., 2009). Within the Santa Fe GFU, the western boundary of the Agua Fria fault system corresponds to the San Isidro Crossing fault. Grauch et al. (2009) hypothesized that these basement-piercing faults may serve as partial flow barriers, compartmentalize aquifers, or possibly control upwelling of deep groundwater from fractured basement. Similar intrabasin and basin-boundary structures have been shown to have a major effect on groundwater flow, heat flow, and geochemistry in other basins of the Rio Grande rift (Witcher et al., 2004).

## THE HYDROLOGIC SYSTEM

Groundwater flow in the Santa Fe Group aquifer near Santa Fe has been discussed generally by Spiegel and Baldwin (1963), Mourant (1980), and McAda and Wasiolek (1988). A regional water-table map depicting groundwater flow conditions for the period 2000–2005 by Johnson (2009) refined water-level elevation contours for the Santa Fe area (Fig. 6). Assuming the Tesuque aquifer is isotropic, the horizontal groundwater flow direction is perpendicular to the elevation-head contours. Based on this simplifying assumption, Johnson (2009) generated flow lines, normal to equipotential lines, that approximate the direction of horizontal flow and, following Spiegel and Baldwin (1963), delineated local groundwater flow units with flow-line boundaries that encompass recharge and discharge zones. One such local GFU was defined for the area between Santa Fe and Tesuque (Fig. 6) (Johnson, 2009; Spiegel and Baldwin, 1963). Named the Santa Fe GFU, this area is the focus of the geochemical data collection, analysis, and interpretation presented here.

In the Santa Fe GFU, groundwater flows through the Tesuque Formation from the mountains on the east, westward toward the Rio Grande. Horizontal hydraulic gradients vary from 0.04 to 0.08 at the mountain front, steepen to as much as 0.12 at the San Isidro Crossing fault on the west boundary of the Agua Fria fault system, and flatten to 0.007 west of Agua Fria and north of the Santa Fe River (Fig. 6). The San Isidro Crossing fault coincides with a drop in the water table and appears to locally impede groundwater flow. The gradient anomaly associated with the San Isidro Crossing fault has been a consistent feature of historic water-level maps (Spiegel and Baldwin, 1963; Mourant, 1980) and required inclusion of a low-permeability zone in the groundwater flow model of McAda and Wasiolek (1988).

Depth-specific water-level measurements from multi-level piezometers provide information on the magnitude and direction of vertical hydraulic gradients in the upper 700 m of the Tesuque aquifer (Johnson, 2009). Upward hydraulic gradients dominate the Santa Fe GFU (Fig. 6, Table 1) and often match or exceed the magnitude of horizontal gradients. Near the mountain front, upward gradients vary in magnitude from 0.06 (piezometer C) to 0.16 (piezometer A). Piezometer E, adjacent to the Santa Fe River west of the San Isidro Crossing fault, has a downward gradient of 0.02 coincident with a water-table high over the river (Fig. 6) that demonstrates river recharge to the Tesuque aquifer. Basin-floor recharge from channel infiltration has also been demonstrated along the Cañada Ancha and other streams and arroyos traversing the basin (Manning, 2009; Moore, 2007; Thomas et al., 2000; Anderholm, 1994). Elsewhere west of the San Isidro Crossing fault, in the Cañada Ancha graben, upward hydraulic gradients ranging from 0.03 (piezometer D) to 0.13 (piezometer B) drive upward flow of groundwater toward the water table and create an anomalously low horizontal gradient on the water-table surface (Table 1, Fig. 6).

Pervading upward hydraulic gradients establish the Cañada Ancha graben as a discharge zone for regional

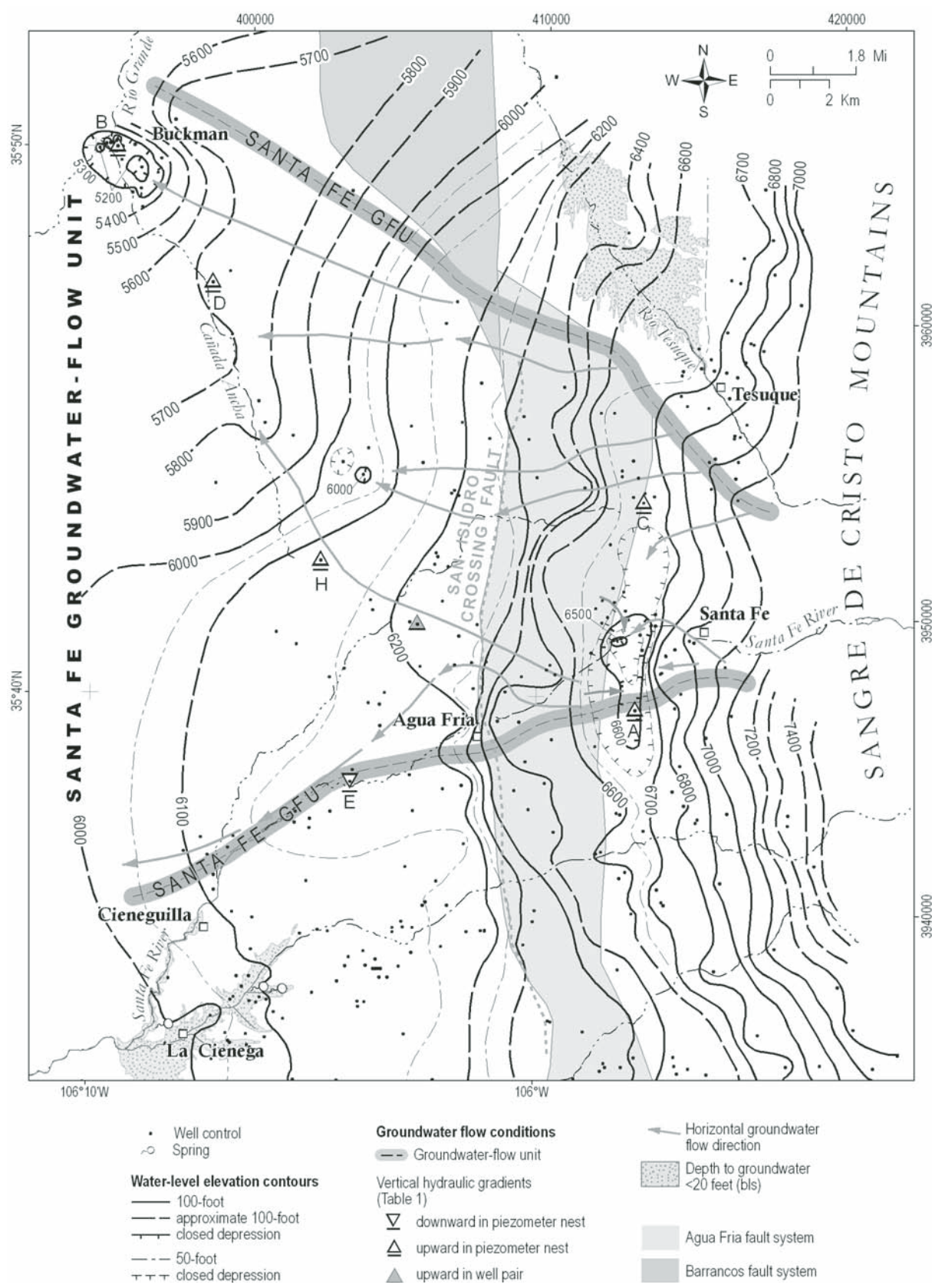


Figure 6. Groundwater-level elevation contours in the southern Española Basin. Small black dots indicate locations of measurements taken during 2000–2005. Downward- and upward-pointing triangles depict direction (downward or upward) of vertical hydraulic gradients (see Table 1 for well information and magnitude of hydraulic gradient). Gray bands denote boundaries for the Santa Fe groundwater-flow unit (GFU). Modified from Johnson (2009). bls—below sea level.

TABLE 1. VERTICAL HYDRAULIC GRADIENTS IN THE SANTA FE GROUNDWATER-FLOW UNIT

Site name	Location (UTM, NAD83)		Surface elevation (m asl)	Well depths (shallow–deep, m bls)	Water-level elevation (shallow–deep, m asl)	Vertical hydraulic gradient (+ up, – down)
	Easting (m)	Northing (m)				
SF-1 piezometer A	412838	3946969	2097	204–585	2003–2065	+0.16
SF-2 piezometer B	395376	3966090	1683	100–565	1614–1674	+0.13
Archery piezometer C	413149	3953989	2193	192–331	2036–2044	+0.06
Buckman SF6 piezometer D	398587	3961476	1818	114–736	1759–1779	+0.03
SF River piezometer E	403199	3944575	1939	180–576	1883–1876	-0.02
Las Campanas piezometer H	402225	3952079	1946	125–600	1860–1879	+0.04
Peters well pair (611/164)	405489	3949905	2004	226–610	1893–1898	+0.04

Key: asl—above sea level; bls—below land surface.

westward groundwater flow within the Santa Fe GFU. Adjusted radiocarbon ages from Manning (2009) indicate that groundwater ages in the Cañada Ancha graben range from 18,700 to 35,400 years. The recharge zone lies east of the San Isidro Crossing fault in the Sangre de Cristo mountains and along the Santa Fe River channel.

### Groundwater and Heat Flow in the Rio Grande Rift

For most of its length, the Rio Grande rift system is characterized by high heat flow and conductive thermal gradients, extension tectonics, fault-block mountains and deep sedimentary basins, Quaternary volcanism, and numerous Quaternary faults (Reiter *et al.*, 1975; Seager, 1975; Swanberg and Morgan, 1978; Chapin and Cather, 1994). Conductive temperature gradients in the Rio Grande rift, calculated from bottomhole temperatures in 2-km-deep wells, range from 25 to 55 °C/km (Goff *et al.*, 1981). Reiter *et al.* (1975) defined regional geothermal trends associated with the northern Rio Grande rift based on heat-flow data and recognized a major geothermal anomaly with heat-flow values greater than 2.5 HFU (heat-flow unit,  $\mu\text{cal}/\text{cm}^2 \cdot \text{s}$ ). This thermal anomaly coincides with the western part of the rift in northern New Mexico and the Española Basin, and in this study area is documented by a thermal gradient of 34.9 °C/km (1.9 HFU) measured at Buckman (Reiter *et al.*, 1975). Three low-temperature geothermal reservoirs with calculated temperatures of 27–58 °C were also identified southwest of the study area near the southern margin of the Valles caldera (Pearson and Goff, 1981). Two of these thermal reservoirs discharge along strands of the Jemez fault zone.

Thermal anomalies due to convection are commonly observed in basins with permeable aquifers, faulting and fracture zones, and recharge and discharge of groundwater. Examples of convective heat transfer have been described for numerous hydrogeologic settings (Anderson, 2005; Kilty and Chapman, 1980) including the Rio Grande rift (Mailloux *et al.*, 1999). The deep interconnected sedimentary basins, complex basement faulting, and bedrock constrictions common in the rift create hydrogeologic conditions that may sustain either local or basin-scale forced convection systems. Such systems involve deep cir-

culation and heating of groundwater under approximately normal subsurface temperature conditions. After groundwater has been heated at great depths, hydrogeologic conditions force groundwater to flow upward toward the surface where water temperatures become significantly warmer than expected.

Numerous studies have presented evidence that geothermal anomalies along the Rio Grande rift may be associated with forced convection driven by inter- and intrabasin groundwater flow (Harder *et al.*, 1980; Morgan *et al.*, 1981; Witcher *et al.*, 1992; Mailloux *et al.*, 1999) or with upflow along fault zones (Trainer and Lyford, 1979; Plummer *et al.*, 2004a, 2004b). The La Bajada constriction at the southern terminus of the Española Basin, bounded on its east side by the Cerrillos uplift and Caja del Rio horst (Sawyer and Minor, 2006; Koning *et al.*, this volume), has been proposed as one setting that could generate groundwater convection and thermal anomalies (Morgan *et al.*, 1981; Swanberg, 1984). Basement-piercing faults and volcanic features associated with the Cerros del Rio volcanic field have been linked to upward migration of deep mantle fluids and anomalously high  $^3\text{He}/^4\text{He}$  ratios in groundwater in the Española Basin (Manning, 2009). Elevated water temperatures and high Cl and As concentrations have been observed in close proximity to major faults in the Albuquerque Basin to the south (Plummer *et al.*, 2004a, 2004b).

## METHODS

### Data Used in the Investigation

The data used in this investigation include new data collected by NMBGMR in 2005 and historical data from published and unpublished sources. The entire data set for the southeastern Española Basin near Santa Fe was presented in Johnson *et al.* (2008). A subset of geochemical data from 120 samples for the Santa Fe GFU (Figs. 6 and 7) are used in this study. Measurements of major and trace elements in rock samples of Espinosa Formation (Te) and the Cieneguilla basanite (Tc) collected near Cieneguilla are used to evaluate chemistry of hydrothermal deposits. Details about site characteristics, sample collection, and sample analysis for these data are described below.

## Sample Collection and Analysis

Forty-six groundwater samples were collected in the Santa Fe River GFU from wells completed in the Tesuque Formation and analyzed for major- and minor-ion and trace-element chemistry, oxygen and hydrogen isotopes, and field measurements of

specific conductance, dissolved oxygen, pH, and temperature. Sample locations are shown on Figure 7 and site information is presented in Table 2. Sampled well types include test wells (for domestic and public supply), monitoring wells (including depth-specific piezometers), supply wells (public, community, and commercial), domestic wells, and windmills. Sample depths

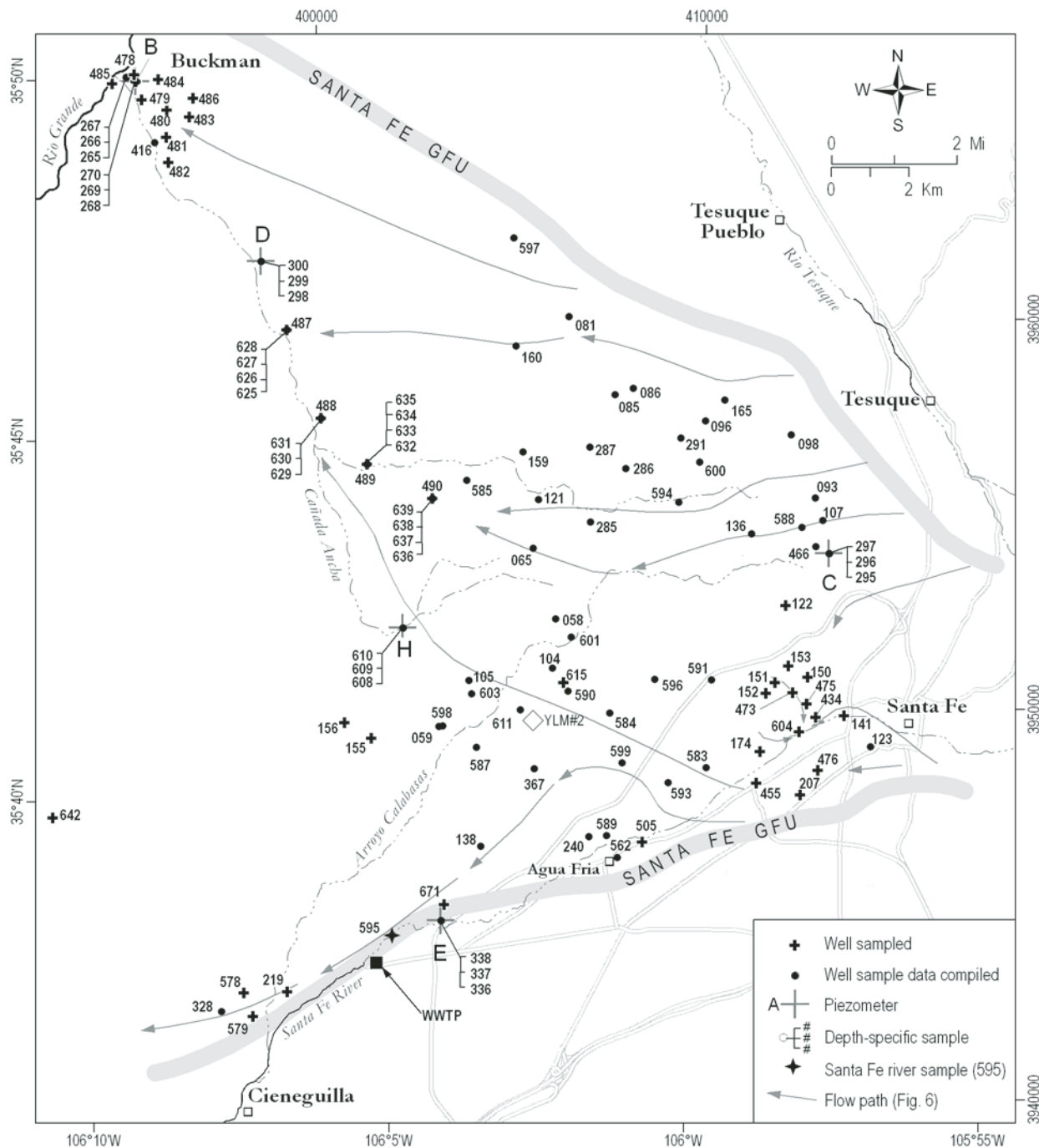


Figure 7. Locations of groundwater and surface-water samples collected and data compiled in the Santa Fe groundwater-flow unit (GFU). Site, sample, and chemical data from these locations are presented in Tables 2–6. YLM#2—Yates La Mesa No. 2 exploration well; WWTP—wastewater treatment plant.

TABLE 2. WELL AND SAMPLE INFORMATION

Site name	Location (UTM, NAD83)						Samples collected and analyzed											
	Well number	Well type	Easting (m)	Northing (m)	Surface elevation (ft asl)	Surface elevation (m asl)	Well depth (m bsl)	Screen top (m bsl)	Screen bottom (m bsl)	Screen length (m)	Sample MAT (°C)	Sample number	Sample date (mm/dd/yy)	Field parameters	Major ions	Trace elements	H and O isotopes	
El Prado Leyba	058	Test	406139	3952312	6678	1981	247	198	241	43	9.6	EB-058A	08/24/94	220	x	x	x	
La Tierra 16	059	Domestic	403151	3949549	6497	2035	244	183	244	61	9.9	EB-059A	06/02/05	213	x	x	x	
HDC1	065	Test	405560	3954130	6676	1997	239	197	239	43	9.6	EB-065A	11/30/78	218	+	x	x	
La Dos No. 1	081	Domestic	406473	3960661	6549	2016	288	209	287	78	9.8	EB-081A	05/10/05	248	x	x	x	
Los Dos No. 2	085	Domestic	407663	3958820	6612	2035	236	195	234	39	9.7	EB-085C	06/10/05	214	x	IB	x	
Sharp	086	Test	408125	3958220	6674	2035	235	184	228	45	9.6	EB-086A	11/14/77	206	+	x	x	
Conron No. 2	093	Domestic	412294	3955412	7105	2166	198	183	198	15	8.7	EB-093A	05/11/05	191	x	x	x	
Tano Vista	096	Test	409975	3957390	6922	2110	237	U	U	9.1	EB-096A	06/20/85	212	x	x	x		
Los Sueños Expl Ninos	098	Domestic	412169	3957033	6923	2111	256	207	250	43	9.1	EB-098C	05/25/05	229	x	x	x	
Cuervos	104	Test	406047	3951057	6659	2030	258	221	252	30	9.6	EB-104A	04/04/94	236	x	x	x	
Test	105	Test	403911	3950729	6574	2004	260	183	220	37	9.8	EB-105B	04/09/99	201	x	x	x	
Test	107	Test	412977	3954837	7162	2184	195	183	195	12	8.6	EB-107A	05/01/86	189	x	x	x	
SF Ranch HQ1	121	Test	405692	3955377	6554	1998	184	160	179	19	9.8	EB-121A	05/28/75	169	x	IB	x	
Northwest	122	Supply	412030	3952550	7160	2183	610	305	604	299	8.6	EB-122E	06/30/05	454	x	x	x	
New Hickox No. 2	123	Test	414198	3949035	6963	2123	262	222	256	134	9.0	EB-123A	02/19/99	189	x	x	x	
Hearststone1	136	Test	411150	3954500	7059	2152	262	244	262	18	8.8	EB-136A	10/25/01	253	+	x	x	
SF Shelter MWA	138	Test	404216	3946481	6455	1968	224	213	220	6	10.0	EB-138A	05/02/02	216	x	x	x	
Monitoring	141	Monitoring	413528	3949830	6895	2102	11	8	11	3	9.1	EB-141A	06/14/05	9	IB	x	x	
Monitoring	150	Monitoring	412592	3950613	7025	2142	115	100	112	12	9.2	EB-150B	02/01/02	106	IB	x	x	
Monitoring	151	Monitoring	411757	3950685	6956	2121	111	95	108	12	9.0	EB-151B	01/08/04	102	IB	x	x	
Monitoring	152	Monitoring	411521	3950411	6931	2113	113	104	110	6	9.1	EB-152B	01/08/04	107	x	x	x	
Monitoring	153	Monitoring	412105	3951100	7014	2139	107	98	107	9	8.9	EB-153A	01/06/04	103	IB	x	x	
Monitoring	155	Monitoring	401411	3949249	6436	1962	102	80	102	21	10.0	EB-155A	09/24/03	91	IB	x	x	
Monitoring	156	Monitoring	400727	3949653	6439	1963	107	99	107	8	10.0	EB-156A	09/24/03	103	x	x	x	
Domestic	159	Domestic	402295	3956594	6501	1982	U	U	U	U	9.9	EB-159A	05/10/05	113	x	x	x	
Windmill	160	Windmill	405117	3959307	6395	1950	107	93	105	12	10.1	EB-160A	06/06/05	99	x	x	x	
Domestic	165	Domestic	410472	3957919	6827	2081	245	184	221	37	9.3	EB-165A	03/01/06	203	x	x	x	
Domestic	174	Domestic	411371	3948913	6843	2086	107	U	U	U	9.2	EB-174A	07/01/05	79	x	x	x	
Supply	207	Supply	412401	3947501	6845	2087	77	U	U	U	9.2	EB-207H	11/06/91	73	x	x	x	
Domestic	219	Domestic	399467	3942749	6215	1895	74	23	72	49	10.5	EB-219B	09/13/84	48	x	x	x	
Commercial	240	Commercial	406983	3946736	6588	2009	183	131	183	52	9.7	EB-240A	05/12/05	157	x	x	x	
Monitoring	265	Monitoring	395131	3966203	5469	1667	90	84	87	3	11.9	EB-265A	03/31/05	85	x	x	x	
Monitoring	266	Monitoring	395137	3966202	5477	1670	52	45	48	3	11.9	EB-266A	03/30/05	47	x	x	x	
Monitoring	267	Monitoring	395127	3966201	5469	1667	18	12	15	3	11.9	EB-267A	03/31/05	14	x	x	x	
Monitoring	268	Monitoring	398376	3966090	5521	1683	568	564	567	3	11.8	EB-268A	07/27/86	566	+x	x	x	
Monitoring	269	Monitoring	395390	3966086	5522	1684	251	245	248	3	11.8	EB-269A	04/05/05	246	x	x	x	
Monitoring	270	Monitoring	395376	3966092	5522	1684	105	99	102	3	11.8	EB-270A	04/06/05	100	x	x	x	
Test	285	Test	407026	3954795	6705	2044	227	176	225	48	9.5	EB-285A	05/28/75	200	IB	x	x	
Test	286	Test	407931	3956170	6721	2049	213	99	208	109	9.5	EB-286A	12/20/74	154	x	x	x	
Test	287	Test	407017	3956720	6664	2032	256	134	253	119	9.6	EB-287A	05/28/75	194	IB	x	x	
Test	291	Test	409947	3956549	6815	2078	171	208	37	9.3	EB-291A	04/14/77	189	x	x	x		
Monitoring	295	Monitoring	413152	3953889	7200	2195	335	329	332	3	8.6	EB-295A	04/04/05	331	x	x	x	
Archery 1b (piezometer C)	296	Monitoring	413146	3953983	7200	2195	284	277	3	8.6	EB-296A	04/05/05	276	x	x	x	x	
Archery 1c (piezometer C)	297	Monitoring	413146	3953983	7200	2195	154	200	46	8.6	EB-297A	04/04/05	177	x	x	x	x	
Archery 1c (piezometer C)	298	Monitoring	398587	3961476	5965	1819	761	732	741	9	11.0	EB-298A	03/29/05	736	x	x	x	x
Buckman SF-6a (piezometer D)	299	Monitoring	398587	3961476	5965	1819	405	396	405	9	11.0	EB-299A	03/30/05	401	x	x	x	x
Buckman SF-6b (piezometer D)	300	Monitoring	398587	3961476	5965	1819	155	85	143	58	11.0	EB-300A	04/06/05	114	x	x	x	x
Buckman SF-6c (piezometer D)	328	Test	397578	3942243	6368	1941	155	125	155	30	10.2	EB-328A	06/07/05	140	x	x	x	x

(Continued)

TABLE 2. WELL AND SAMPLE INFORMATION (Continued)

Site name	Location (UTM, NAD83)										Samples collected and analyzed						
	Well number	Well type	Easting (m)	Northing (m)	Surface elevation (ft asl)	Surface elevation (m asl)	Well depth (m)	Screen top (m bsl)	Screen bottom (m bsl)	Screen length (m)	MAT (°C)	Sample number	Sample date (mm/dd/yy)	Sample depth (m bsl)	Field parameters	Major ions	Trace elements
SFR a (piezometer E)	336	Monitoring	403199	3944575	6366	1941	579	579	6	10.2	EB-336A	4/8/2005	576	x	x	x	x
SFR b (piezometer E)	337	Monitoring	403199	3944575	6366	1941	325	319	325	6	10.2	EB-337A	4/8/2005	322	x	x	x
SFR c (piezometer E)	338	Monitoring	403199	3944575	6366	1941	183	177	183	6	10.2	EB-338A	4/9/2005	180	x	x	x
Gold	367	Domestic	405580	3948470	6536	1993	155	117	151	34	9.8	EB-367A	05/12/05	134	x	x	x
Weil PNM	416	Test	395864	3964520	5605	1709	354	U	U	117	EB-416A	05/02/04	187	x	x	x	x
Ferguson	434	Supply	412808	3949782	6865	2093	229	53	227	174	9.2	EB-434A B	06/05/97	140	x	x	x
Osage	455	Supply	411283	3948102	6755	2059	235	64	232	168	9.4	EB-455A B	06/17/97	148	x	x	x
Estancia Subdiv	466	Test	412797	3954172	7143	2178	244	195	244	49	8.7	EB-466A	11/22/04	220	IB	+	+
Santa Fe MW-7	473	Monitoring	412209	3950426	7029	2143	133	108	133	24	8.9	EB-473A	03/10/05	120	x	x	x
Santa Fe Ortiz-1	475	Monitoring	412564	3950130	6999	2134	140	107	140	34	8.9	EB-475A	07/29/04	123	x	x	x
Santa Fe	476	Supply	412862	3948426	6868	2094	221	61	221	160	9.2	EB-476B	05/17/00	141	IB	+	+
Buckman No. 1	478	Supply	395333	3966270	5479	1670	334	78	333	255	11.9	EB-478A D	10/22/03	206	x	x	x
Buckman No. 2	479	Supply	395525	3965621	5524	1684	486	71	481	410	11.8	EB-479A B	10/22/03	276	x	x	x
Buckman No. 3A	480	Supply	396172	3965366	5614	1712	457	152	454	302	11.6	EB-	12/03/96	303	x	x	x
Buckman No. 4	481	Supply	396164	3964658	5635	1718	372	140	372	232	11.6	EB-481A B	10/02/96	256	x	x	x
Buckman No. 5	482	Supply	396210	3964020	5671	1729	360	76	284	11.5	EB-482A B	12/03/96	218	x	x	x	x
Buckman No. 6	483	Supply	396748	3965176	5697	1737	352	88	283	196	11.5	EB-483A C	10/02/96	185	x	x	x
Buckman No. 7	484	Supply	395955	3966140	5595	1706	431	213	427	214	11.7	EB-484A C	10/02/96	320	x	x	x
Buckman No. 8	485	Supply	394780	3966031	5528	1685	277	116	274	159	11.8	EB-485A C	10/22/03	195	x	x	x
Buckman No. 9	486	Supply	396848	3965659	5726	1746	416	98	407	310	11.4	EB-486B	12/02/02	252	x	x	x
Buckman No. 10	487	Supply	399250	3959720	6044	1843	610	154	604	450	10.8	EB-487A	09/21/03	379	x	x	x
Buckman No. 11	488	Supply	400130	3957460	6149	1875	610	137	604	466	10.6	EB-488A	07/19/03	370	x	x	x
Buckman No. 12	489	Supply	401300	3956280	6245	1904	585	122	579	457	10.4	EB-489A	07/06/03	351	x	x	x
Buckman No. 13	490	Supply	402980	3955400	6413	1955	610	122	604	482	10.1	EB-490A	09/14/03	363	IB	+	+
Agua Fria No. 1	505	Supply	408355	3946591	6607	2014	29	9	27	18	9.7	EB-505E	06/08/05	18	IB	x	x
Village MHP No. 1	562	Test	407717	3946197	6579	2006	U	U	U	9.8	EB-562B	09/03/97	U	x	x	x	x
Hyde Park, Yellow Cat	571	Test	419795	3952766	7933	2419	111	U	U	U	7.1	EB-571A	07/01/78	95	x	x	x
SF Horse Park North	578	Domestic	398152	3942717	6207	1892	98	91	98	6	10.5	EB-578B	06/19/00	95	x	x	x
SF Horse Park South	579	Domestic	398379	3942119	6191	1887	73	55	67	12	10.5	EB-579B	06/21/00	61	x	x	x
Althouse	583	Domestic	409986	3948497	6840	2085	137	U	U	9.3	EB-583A	06/03/05	120	x	x	x	x
Leibman	584	Domestic	407524	3949892	6728	2051	232	195	232	37	9.5	EB-584A	05/26/05	213	x	x	x
La Tierra Henry	585	Domestic	403853	3955866	6457	1969	U	U	U	10.0	EB-585A	05/24/05	152	x	x	x	x
Travis Ranch	587	Domestic	404110	3949025	6528	1990	293	122	287	165	9.9	EB-587A	05/24/05	204	x	x	x
C. Henry	588	Domestic	412444	3954655	7125	2172	207	238	238	30	8.7	EB-588A	05/25/05	223	x	x	x
Leyba Agua Fria	589	Domestic	407442	3946750	6607	2014	183	159	177	18	9.7	EB-589A	06/02/05	168	x	x	x
Constant 1	590	Domestic	406448	3950465	6687	2039	195	U	U	9.6	EB-590A	05/25/05	177	x	x	x	x
Homans	591	Domestic	410125	3950744	6912	2107	189	174	189	15	9.1	EB-591A	05/26/05	181	x	x	x
Heartstone2	592	Domestic	411191	3954720	7036	2145	262	219	238	18	8.9	EB-592A	05/25/05	228	x	x	x
Sugarmen	593	Domestic	409294	3955311	6741	2055	140	125	137	12	9.4	EB-593A	05/26/05	131	x	x	x
Tujillo	594	Domestic Stream	401950	3944200	6302	2086	263	232	238	6	9.3	EB-594A	06/01/05	235	x	x	x
Santa Fe River above WWTP	595	Monitoring	405006	3936039	6337	1932	402	372	399	27	10.2	EB-605A	09/24/06	386	x	x	x
Centaurus Ranch	596	Domestic	408677	3950763	6827	2081	200	151	194	43	9.3	EB-596A	06/01/05	172	x	x	x
Mariyah Ranch	597	Domestic	405067	3962076	6668	2033	268	226	265	40	9.6	EB-597A	06/03/05	245	x	x	x
Leyba 600	598	Domestic	403236	3949568	6504	1983	183	159	177	18	9.9	EB-598A	05/10/05	168	x	x	x
Terwilliger	599	Domestic	407830	3948618	6700	2043	177	155	177	21	9.5	EB-599A	06/02/05	166	x	x	x
Preston	600	Domestic	409825	3956335	6927	2112	291	250	290	40	9.1	EB-600A	06/01/05	270	x	x	x
O'Neill	601	Domestic	406530	3951847	6651	2028	233	201	233	U	9.6	EB-601A	06/01/05	183	x	x	x
Borrego	603	Domestic Supply	403984	3950389	6565	2001	375	125	369	18	9.8	EB-603A	06/07/05	186	x	x	x
Torreón No. 2	604	Monitoring	412377	3949416	6825	2081	375	125	369	244	9.3	EB-604D	06/30/05	247	x	x	x
Jail Deep, Espinazo Fm	605	Monitoring	405006	3936039	6337	1932	402	372	399	27	10.2	EB-605A	09/24/06	386	x	x	x

(Continued)

TABLE 2. WELL AND SAMPLE INFORMATION (Continued)

Site name	Well number	Location (UTM, NAD83)		Surface elevation (ft asl) (m asl)	Well depth (m bsls)	Screen top (m bsls)	Screen bottom length (m)	MAT (°C)	Sample number	Sample date (mm/dd/yy)	Sample depth (m bsls)	Field parameters	Major ions	Samples collected and analyzed		
		Well type	Easting (m)	Northing (m)										H and O isotopes	Trace elements	
Las Campanas a (piezometer H)	608	Monitoring	402225	3952079	6383	1946	607	598	604	6	10.1	EB-608A	09/28/06	601	x	x
Las Campanas b (piezometer H)	609	Monitoring	402225	3952079	6383	1946	402	393	399	6	10.1	EB-609A	09/27/06	396	x	x
Las Campanas c (piezometer H)	610	Monitoring	402225	3952079	6383	1946	137	116	134	18	10.1	EB-610A	09/26/06	125	x	x
Peters Expl.	611	Test	405227	3949987	6575	2004	610	363	607	244	9.8	EB-611A	08/02/04	485	x	x
Constant 2	615	Domestic Test	406339	3950675	6678	2036	274	220	268	49	9.6	EB-615A	05/21/04	244	+	IB
Buckman No. 10 zone 1900–1920	625	Test	399250	3959720	6038	1841	585	579	585	6	10.8	EB-625A	08/12/03	582	x	+
Buckman No. 10 zone 1650–1670	626	Test	399250	3959720	6038	1841	509	503	509	6	10.8	EB-626A	08/14/03	506	x	+
Buckman No. 10 zone 1080–1100	627	Test	399250	3959720	6038	1841	335	329	335	6	10.8	EB-627A	08/15/03	332	x	IB
Buckman No. 10 zone 797–817	628	Test	399250	3959720	6043	1842	249	243	249	6	10.8	EB-628A	08/16/03	246	x	IB
Buckman No. 11 zone 1900–1920	629	Test	400130	3957460	6138	1871	585	579	585	6	10.6	EB-629A	06/14/03	582	x	+
Buckman No. 11 zone 1620–1640	630	Test	400130	3957460	6138	1871	500	494	500	6	10.6	EB-630A	06/16/03	497	x	+
Buckman No. 11 zone 820–840	631	Test	400130	3957460	6138	1871	256	250	256	6	10.6	EB-631A	06/18/03	253	x	+
Buckman No. 12 zone 1780–1800	632	Test	401300	3956280	6247	1905	549	543	549	6	10.4	EB-632A	05/28/03	546	x	+
Buckman No. 12 zone 1430–1450	633	Test	401300	3956280	6247	1905	442	436	442	6	10.4	EB-633A	05/31/03	439	x	IB
Buckman No. 12 zone 1110–1130	634	Test	401300	3956280	6247	1905	345	335	345	9	10.4	EB-634A	06/02/03	340	x	IB
Buckman No. 12 zone 770–790	635	Test	401300	3956280	6247	1905	241	235	241	6	10.4	EB-635A	06/03/03	238	x	IB
Buckman No. 13 zone 2002–1982	636	Test	402980	3955400	6413	1955	610	604	610	6	10.1	EB-636A	07/29/03	607	x	+
Buckman No. 13 zone 1290–1310	637	Test	402980	3955400	6413	1955	399	393	399	6	10.1	EB-637A	07/31/03	396	x	+
Buckman No. 13 zone 900–920	638	Test	402980	3955400	6413	1955	280	274	280	6	10.1	EB-638A	07/31/03	277	x	+
Buckman No. 13 zone 691–711	639	Test	402980	3955400	6413	1955	217	211	217	6	10.1	EB-639A	08/01/03	214	x	+
USFS 1200 ft well Parker	642	Domestic	393253	3947208	6730	2052	364	321	367	46	9.5	EB-642A	06/09/03	344	x	+
	671	Domestic	403283	3944985	6394	1949	213	116	207	91	10.1	EB-671A	04/06/07	162	+	x

Key: asl—above sea level; bsls—below land surface; U—undetermined; WWTP—wastewater treatment plant; MAT—mean annual temperature; x—full analysis; +—partial analysis; IB—ion balance exceeds quality criteria ±5.0%.

ranged from 9 to 736 m, with a median of 206 m. One grab sample of stream flow from the Santa Fe River was taken above the wastewater treatment plant (WWTP in Fig. 7) in May 2005. Well samples were collected using dedicated submersible pumps or a portable, air-operated, submersible piston pump (Bennett pump). Sample locations include five nested piezometers lettered B, C, D, E, and H (Fig. 7). Each nest has three depth-specific piezometers indicated by an “a” (deep), “b” (intermediate), or “c” (shallow) next to the site name (Tables 2–6). Piezometer B located at Buckman consists of two adjacent nests, SF-2 and SF-3, which tap six separate depth intervals ranging from 18 to 568 m.

### Field Parameters

Groundwater discharge temperature, specific conductance (SC), pH, and dissolved oxygen (DO) were measured using a YSI 556 multi-probe system. The probe has a rated accuracy of 0.15 °C for temperature, 0.5% for SC, 0.2 units for pH, and 2% for DO. Field parameters were measured in a bucket filled with purge water at the time of sample collection. Field parameters, general chemistry, and site location relative to the San Isidro Crossing fault are presented in Table 3.

### Major Ions and Trace Elements

Samples were collected following a borehole purge and stabilization of the field parameters. Purge volumes varied between one and three casing volumes. Samples were collected in 125 mL (trace elements) or 500 mL (ions) polyethylene bottles that were triple-rinsed with purge water prior to filling. All samples were stored on ice and in the dark and transported to the laboratory within 24–36 h of collection. Samples were filtered prior to analysis using a 0.45-micron filter. Alkalinity was determined by titration within 36 h of sample collection. Major anions were analyzed by ion chromatography (IC), major cations by inductively coupled plasma-optical emission spectroscopy (ICP-OES), and trace elements by inductively coupled plasma–mass spectrometry (ICP-MS). Analytical error for major ions and trace elements is generally <10% using IC, ICP-OES, and ICP-MS. Major-ion and trace-element data are presented in Tables 4 and 5.

### Hydrogen and Oxygen Isotopes

Samples for hydrogen-2 (deuterium,  $^2\text{H}$ ) and oxygen-18 ( $^{18}\text{O}$ ) analyses were collected along with major-ion and trace-element samples and analyzed at the New Mexico Institute of Mining and Technology, Department of Earth and Environmental Sciences stable isotope laboratory on a Thermo Finnigan Delta Plus XP isotope ratio mass spectrometer. Analytical uncertainties for  $\delta^2\text{H}$  and  $\delta^{18}\text{O}$  are typically less than 1 per mil (‰) and 0.1‰, respectively. Stable isotope data are presented in Table 6. These data were merged with data from Anderholm (1994) for analysis.

### Rock Chemistry

Nine rock samples were collected from two general locations near Cieneguilla that overlap the eastern margin of the Cerrillos uplift (Fig. 8). Samples represent a variety of rock types from

the Espinaso Formation and Cieneguilla basanite that include tuffaceous and volcaniclastic sediments, phreatomagmatic breccia, monzonite, hydrothermally altered basalt and sandstone, and vein calcite. The general vicinity of these two sample locations is the only place these rocks are exposed in the western study area. Further north along the eastern boundary of the Caja del Rio horst, the units are buried beneath the Cerros del Rio volcanic field and Santa Fe Group basin fill. Whole-rock samples, including three replicates, were crushed, ground, and digested by Milestone microwave with 9 mL of trace-metal-grade nitric acid. Samples were then diluted 1:20 with purified water and analyzed on ICP-MS (Agilent 7500) for aluminum (Al), arsenic (As), boron (B), cadmium (Cd), calcium (Ca), chromium (Cr), lithium (L), magnesium (Mg), molybdenum (Mo), potassium (K), selenium (Se), sodium (Na), uranium (U), and vanadium (V). Four rock reference standards were processed and analyzed with the samples. Rock chemistry data and standard errors are presented in Table 7.

### Data Compilation and Data Quality

Geochemical data for 73 sites within the Santa Fe GFU were compiled from databases and records of the Jemez y Sangre Water Planning Council, the U.S. Geological Survey National Water Information System (NWIS), the New Mexico Environment Department (NMED) Petroleum Storage Tank, Solid Waste, and Drinking Water Bureaus, the City of Santa Fe, the County of Santa Fe, historical metropolitan water board reports, and libraries of private consultants and water users. Stable isotope data from 42 groundwater and surface water locations were compiled from Anderholm (1994). The compilation resulted in a large, assorted data set, with many locations having partial analyses or multiple sampling events. At some sites, data compiled for field parameters, ion chemistry, and/or trace-element chemistry have been combined from more than one sampling event. The data were reviewed and filtered for data quality based on several criteria including an accurate map location or geographical coordinates for the sample site, an ion balance of  $\leq \pm 5.0$ , and a report from the analyzing laboratory, a state agency, or professional consultant.

## THERMAL CONDITIONS AND GROUNDWATER FLOW IN THE TESUQUE AQUIFER SYSTEM

Temperature measurements of discharge from shallow wells near Santa Fe defined a zone with elevated (>19 °C) groundwater temperatures generally overlying the Cañada Ancha graben and Caja del Rio horst (Fig. 9) (Johnson et al., 2008). To further assess regional thermal conditions, we compiled bottomhole temperatures measured in exploration and monitoring wells (Table 8). Temperature gradients in wells were calculated by subtracting the mean annual surface temperature from the bottomhole temperature and dividing by depth. Mean surface temperatures were estimated at each site from a regional temperature-elevation

TABLE 3. FIELD PARAMETERS AND GENERAL CHEMISTRY

Site name	Sample number	Field parameters <sup>†</sup>						Alkalinity (mg/L CaCO <sub>3</sub> )	Lab pH	TDS <sup>#</sup> (mg/L)	General chemistry	Water type
		Location (SIC fault)*	T (°C)	SC (µS/cm)	pH	DO	Lab <sup>§</sup>					
El Prado	EB-058A	West	U	U	U	U	Controls for Environmental Pollution	111.5	U	156	1.4	Ca-Na-HCO <sub>3</sub>
Leyba	EB-059A	West	20.9	284	7.87	6.7	NMBGMR	127.1	8	189	-1.3	Na-Ca-HCO <sub>3</sub>
La Tierra 16	EB-065A	West	U	280	U	U	Environmental Biochemists	68.9	7.3	344	4.3	Ca-Na-HCO <sub>3</sub> -SO <sub>4</sub>
HDC1	EB-061A	West	26.2	332	8.3	2.66	NMBGMR	128.9	8.4	186	-3.5	Na-Ca-HCO <sub>3</sub>
Las Dos No. 1	EB-055BC	West	17	285.3	8.06	4.04	USGS, NMBGMR	118.1	7.95	252	-6.3	Na-Ca-HCO <sub>3</sub>
Los Dos No. 2	EB-066A	West	19	360	U	U	Environmental Biochemists	121.4	7.73	120	-3.1	Na-HCO <sub>3</sub> -SO <sub>4</sub>
Sharp	EB-093A	East	16.3	246	8.2	5.2	NMBGMR	106.6	8.3	153	-0.6	Ca-HCO <sub>3</sub>
Conron No. 2	EB-096A	West	U	U	U	U	Controls for Environmental Pollution	143.5	U	216	2.9	Ca-HCO <sub>3</sub>
Tano Vista	EB-098C	East	15.9	270	8	5.9	NMBGMR	118.9	8.0	164	-1.3	Ca-HCO <sub>3</sub>
Los Suenos Expl	EB-104A	West	U	U	U	U	Controls for Environmental Pollution	111.6	U	123	0.5	Ca-Na-HCO <sub>3</sub>
Ninos	EB-105B	West	U	U	U	U	National Testing Lab	119.7	7.7	190	2.1	Ca-Na-HCO <sub>3</sub>
Cuervos	EB-107A	East	U	U	U	U	Controls for Environmental Pollution	104.2	8.03	202	0.9	Ca-HCO <sub>3</sub>
SF Ranch HQ1	EB-121A	West	U	U	U	U	Controls for Environmental Pollution	122.2	7.74	180	7.4	Ca-Na-HCO <sub>3</sub>
Northwest	EB-122E	East	19.8	220.4	7.96	7.95	USGS	99.2	7.97	153	0.9	Ca-Mg-HCO <sub>3</sub> -Cl
New Hickox No. 2	EB-123A	East	10.5	315	8.25	U	Unknown	138.1	8.7	170	-2.3	Na-Ca-HCO <sub>3</sub>
Hearststone	EB-136A	East	16	U	U	4.78	National Testing Lab	140.3	7.7	190	-0.4	Ca-Na-HCO <sub>3</sub>
SF Shelter	EB-138A	West	U	U	U	U	Environmental Health Lab	109.9	8	140	-1.6	Ca-Na-HCO <sub>3</sub>
MWA	EB-141A	East	13.5	483.7	7.3	1.47	USGS	172.2	7.54	373	-5.8	Ca-Na-HCO <sub>3</sub> -Cl
Santa Fe MW-1	EB-150B	East	U	U	U	U	Unknown	114.9	7.4	262	19.2	Ca-HCO <sub>3</sub>
Santa Fe MW-2	EB-151B	East	U	U	U	U	Unknown	100.1	7.9	330	-6.1	Ca-HCO <sub>3</sub>
Santa Fe MW-3	EB-152B	East	U	U	U	U	Unknown	96.0	8	290	-3.4	Ca-HCO <sub>3</sub>
Santa Fe MW-4	EB-153A	East	U	U	U	U	Unknown	84.5	8.1	290	19.6	Ca-HCO <sub>3</sub>
Caja del Rio MW-1	EB-155A	West	U	U	U	U	Hall Environmental Hall	48.2	9.01	150	12.2	Ca-Na-HCO <sub>3</sub>
Caja del Rio MW-4	EB-156A	West	U	U	U	U	Hall Environmental Hall	100.1	8.04	160	-1.5	Na-Ca-HCO <sub>3</sub>
SF Ranch HQ2	EB-159A	West	19	307	8.1	U	NMBGMR	131.2	8.3	195	-1.5	Ca-Na-HCO <sub>3</sub>
Tony's WM	EB-160A	West	16.5	347	7.8	5.00	NMBGMR	127.1	8	215	-0.5	Ca-HCO <sub>3</sub>
Moss Farms	EB-165A	East	17.9	135.3	7.58	5.05	NMBGMR	135.3	7.9	194	-0.8	Ca-HCO <sub>3</sub>
Hurlucker	EB-174A	East	16	256	7.57	6.45	USGS	110.7	7.83	221	0.5	Ca-HCO <sub>3</sub>
Indian School	EB-207H	East	11	350	7.3	U	Analytical Technologies, Inc.	91.0	8.1	240	-0.5	Ca-HCO <sub>3</sub>
Hagerman Orchard	EB-219B	East	17	133	6.84	U	NM State Lab	92.7	7.5	125	3.5	Ca-Mg-HCO <sub>3</sub>
Agua Fria Park	EB-240A	West	14.9	231	7.4	5.30	NMBGMR	90.2	8.2	137	-1.3	Ca-HCO <sub>3</sub>
SF-3a (piezometer B)	EB-255A	West	18.8	178	8.27	U	NMBGMR	88.0	8.8	132	-3.4	Na-HCO <sub>3</sub>
SF-3b (piezometer B)	EB-266A	West	16.9	196	8.73	7.23	NMBGMR	75.5	9.2	108	4.4	Na-Ca-HCO <sub>3</sub>
SF-3c (piezometer B)	EB-267A	West	15	442	7.23	4.48	NMBGMR	205.0	8	290	-1.8	Na-HCO <sub>3</sub>
SF-2a (piezometer B)	EB-268A	West	U	1350	U	U	USGS	581.5	9.2	U	2.4	Na-HCO <sub>3</sub>
SF-2b (piezometer B)	EB-269A	West	18.6	1029	6.81	U	NMBGMR	467.5	7.5	570	-2.4	Na-HCO <sub>3</sub>
SF-2c (piezometer B)	EB-270A	West	19.3	417	7.97	U	Controls for Environmental Pollution	164.0	8.3	263	-1.8	Na-HCO <sub>3</sub>
La Tierra South	EB-285A	West	U	U	U	U	Controls for Environmental Pollution	116.5	7.95	161	7.2	Ca-Na-Mg-HCO <sub>3</sub>
La Tierra Kubert	EB-286A	West	U	U	U	U	Environmental Biochemists	143.5	7.44	185	-3.9	Na-HCO <sub>3</sub>
La Tierra Pinon	EB-287A	West	U	U	U	U	Controls for Environmental Pollution	137.0	7.71	239	9.4	Na-Ca-HCO <sub>3</sub>
La Tierra 32-T-3	EB-291A	On fault	U	U	U	U	Controls for Environmental Pollution	124.7	7.9	220	-1.2	Ca-Na-HCO <sub>3</sub>
Archery 1a (piezometer C)	EB-295A	East	16.3	279	7.8	6.28	NMBGMR	135.3	7.9	180	-2.1	Ca-Na-HCO <sub>3</sub>
Archery 1b (piezometer C)	EB-296A	East	12.9	322	7.4	U	NMBGMR	123.0	7.9	210	-2.3	Ca-HCO <sub>3</sub>

(Continued)

---

(Continued)

TABLE 3. FIELD PARAMETERS AND GENERAL CHEMISTRY (Continued)

Site name	Sample number	Field parameters <sup>a</sup>				General chemistry					
		Location (SIC fault)*	T (°C)	SC ( $\mu\text{S}/\text{cm}$ )	pH	DO	Lab <sup>b</sup>	Alkalinity (mg/L CaCO <sub>3</sub> )	Lab pH	TDS <sup>#</sup> (mg/L)	Charge balance (%)
Archery 1c (piezometer C)	EB-297A	East	14.2	396	7.49	U	NMBGMR	143.5	8.2	245	-0.3
Buckman SF-6a (piezometer D)	EB-298A	West	20.7	1354	6.91	0.21	NMBGMR	709.5	7.8	863	-1.3
Buckman SF-6b (piezometer D)	EB-299A	West	20.8	836	7.25	0.13	NMBGMR	406.0	8.1	516	-1.3
Buckman SF-6c (piezometer D)	EB-300A	West	18.1	363	7.34	U	NMBGMR	143.5	8.1	233	-0.5
Chalmers SFR a (piezometer E)	EB-328A	West	18	253	8.3	2.60	NMBGMR	96.9	8.3	155	1.5
SFR b (piezometer E)	EB-336A	West	19.6	551	8.45	0.58	NMBGMR	245.0	8.5	316	-0.7
SFR c (piezometer E)	EB-337A	West	18	288	8.08	7.3	NMBGMR	123.0	8.2	191	-1.7
Gold	EB-338A	West	16.3	159	8.04	U	NMBGMR	78.0	8.0	108	-2.1
Weil PNM	EB-367A	West	17.2	250	7.4	5.20	NMBGMR	110.7	8.2	157	1.2
Ferguson	EB-416A	West	22	418	7.6	U	USGS	199.3	U	272	-1.8
Osage	EB-434AB	East	U	U	U	U	Unknown, NMDWB	112.7	7.76	U	Ca-HCO <sub>3</sub>
Estancia Subdiv	EB-455AB	East	U	U	U	U	Unknown, NMDWB	106.7	7.67	U	Ca-HCO <sub>3</sub>
Santa Fe MW-7	EB-466A	East	U	U	U	U	Hall Environmental	109.9	7.71	140	Ca-HCO <sub>3</sub>
Santa Fe Ortiz-1	EB-473A	East	U	U	U	U	Unknown	113.3	8.2	170	Ca-Mg-HCO <sub>3</sub>
Santa Fe	EB-475A	East	U	U	U	U	Unknown	137.9	8	260	2.4
Buckman No. 1	EB-476B	West	13.7	U	U	U	NMDWB	109.9	7.65	264	Ca-Na-HCO <sub>3</sub>
Buckman No. 2	EB-478AD	West	U	U	U	U	Unknown, LANL	201.8	7.83	254	9.2
Buckman No. 3A	EB-479AB	West	33.1	1429	8.4	U	Unknown, Core Labs	7.32	1209	Na-HCO <sub>3</sub>	-3.1
Buckman No. 4	EB-480ABC	West	26.7	910	7.8	U	Unknown	391.5	7.32	1209	Na-HCO <sub>3</sub>
Buckman No. 5	EB-481AB	West	U	U	U	U	Unknown	330.5	7.56	420	Na-Ca-HCO <sub>3</sub>
Buckman No. 6	EB-482AB	West	U	U	U	U	Unknown	422.4	7.23	524	4.1
Buckman No. 7	EB-483AC	West	U	U	U	U	Unknown	763.6	7.15	844	3.0
Buckman No. 8	EB-484AC	West	U	U	U	U	Unknown	237.0	7.46	324	0.9
Buckman No. 9	EB-485AC	West	U	U	U	U	Unknown	221.4	7.61	342	3.0
Buckman No. 10	EB-486B	West	21.6	640	U	U	Unknown, LANL	340.4	8.14	440	-1.7
Buckman No. 11	EB-487A	West	27.0	U	U	U	Hall Environmental	260.0	7.59	340	Ca-Na-HCO <sub>3</sub>
Buckman No. 12	EB-488A	West	28.9	U	7.88	U	Hall Environmental	180.4	7.86	270	Na-Ca-HCO <sub>3</sub>
Buckman No. 13	EB-489A	West	27.2	U	U	U	Hall Environmental	130.4	8.21	200	Na-Ca-HCO <sub>3</sub>
Agua Fria No. 1	EB-490A	West	U	U	U	U	Hall Environmental	140.3	8.09	190	Na-HCO <sub>3</sub>
Village MHP No. 1	EB-505E	East	13.7	281	7.37	4.44	USGS	120.6	7.58	252	-6.9
Hyde Park, Yellow Cat	EB-562B	On fault	U	U	U	U	Unknown	82.0	7.8	200	7.0
SF Horse Park North	EB-577A	East	U	U	U	U	Controls for Environmental Pollution	226.4	7.94	315	-1.6
SF Horse Park South	EB-578B	West	U	U	U	U	Assalai	83.7	7.4	150	3.4
Althouse	EB-579B	West	U	U	U	U	Assalai	94.3	6.9	135	Ca-Na-HCO <sub>3</sub>
Leibman	EB-583A	East	15.1	254	7.9	5.3	NMBGMR	98.4	8	146	3.0
La Tierra Henry	EB-584A	On fault	16.2	282	7.5	5.8	NMBGMR	118.9	8	175	Ca-Na-HCO <sub>3</sub>
Travis Ranch	EB-585A	West	18.6	313	7.9	5.2	NMBGMR	127.1	8.1	189	0.0
C. Henry	EB-587A	West	20.4	285	7.95	4.5	NMBGMR	123.0	8.1	175	-0.5
Leyba Agua Fria	EB-588A	East	17.3	220	7.4	5.5	NMBGMR	98.4	8.1	136	Ca-HCO <sub>3</sub>
Constant 1	EB-590A	West	14.2	284	7.8	4.4	NMBGMR	102.5	7.6	164	-0.3
Homans	EB-591A	East	17.4	353	7.4	5.6	NMBGMR	118.9	8	185	-1.1
Sugarmen	EB-593A	East	16.0	189	7.8	5.0	NMBGMR	131.2	8	213	0.3
Trujillo	EB-594A	On fault	18.9	293	7.9	4.5	NMBGMR	82.0	8.1	116	Ca-HCO <sub>3</sub>
Santa Fe River above WWTP	EB-595A	West	23.2	251	8.3	4.7	NMBGMR	118.9	8	183	1.2
Centaurus Ranch	EB-596A	On fault	17.9	319	7.7	5.9	NMBGMR	77.7	8.4	141	0.7
								118.9	8	195	1.3

(Continued)

TABLE 3. FIELD PARAMETERS AND GENERAL CHEMISTRY (Continued)

Site name	Sample number	Field parameters <sup>a</sup>					General chemistry					
		Location (SIC fault)*	T (°C)	SC (µS/cm)	pH	DO	Lab <sup>b</sup>	Alkalinity (mg/L CaCO <sub>3</sub> )	Lab pH	TDS <sup>#</sup> (mg/L)	Charge balance (%)	
Mariah Ranch	EB-597A	West	21.5	378	7.9	3.4	NMBGMR	147.6	8	235	-1.4	
Leyba 600	EB-598A	West	19.5	270	7.9	6.5	NMBGMR	123.0	8.2	181	0.3	
Terwilliger	EB-599A	On fault	16.9	248	8.1	6.1	NMBGMR	98.4	7.8	152	0.5	
Preston	EB-600A	East	19.0	309	8	4.1	NMBGMR	135.3	8	192	-0.8	
Oneil	EB-601A	West	18.2	216	7.9	4.9	NMBGMR	98.4	8	138	0.4	
Borrego	EB-603A	West	18.9	444	8.45	3.7	NMBGMR	147.6	8.3	255	-2.5	
Torreón No. 2	EB-604D	East	16.1	345	7.44	7.21	USGS	125.5	7.67	248	1.7	
Jail Deep	EB-605A	West	U	U	U	U	LANL	202.7	8.09	2539	-1.7	
Las Campanas a (piezometer H)	EB-608A	West	19.8	441	7.99	0.15	NMBGMR	213.8	8.5	270	-6.3	
Las Campanas b (piezometer H)	EB-609A	West	20.4	357	8.16	0.19	NMBGMR	143.5	8.4	222	-1.1	
Las Campanas c (piezometer H)	EB-610A	West	18.8	309	7.53	7.49	NMBGMR	123.0	8	202	0.5	
Peters Expl	EB-611A	West	23.2	270	7.25	U	Hall Environmental	109.9	7.25	260	0.7	
Constant 2	EB-615A	West	U	U	8.1	U	Assaigai	99.7	8.10	137	-7.7	
Buckman No. 10 zone	EB-625A	West	29.0	544	8.57	U	Hall Environmental	236.5	8.57	300	1.5	
1900–1920	EB-626A	West	24.3	841	8.81	U	Hall Environmental	432.9	8.81	520	-4.5	
Buckman No. 10 zone	EB-627A	West	24.0	460	8.46	U	Hall Environmental	262.6	8.46	420	-5.7	
1650–1670	EB-628A	West	21.6	295	8.6	U	Hall Environmental	150.1	8.3	320	17.1	
Buckman No. 10 zone	797–817	EB-629A	West	24.7	544	8.75	U	Hall Environmental	274.6	8.75	390	2.5
Buckman No. 11 zone	1900–1920	EB-630A	West	23.4	532	8.64	U	Hall Environmental	290.6	8.64	500	-3.1
Buckman No. 11 zone	1620–1640	EB-628A	West	21.7	280	8.41	U	Hall Environmental	134.3	8.41	200	1.4
Buckman No. 11 zone	820–840	EB-631A	West	23.5	274	8.59	U	Hall Environmental	290.6	8.59	260	3.9
Buckman No. 11 zone	1780–1800	EB-632A	West	22.7	282	8.54	U	Hall Environmental	132.2	8.54	390	7.8
Buckman No. 12 zone	1430–1450	EB-633A	West	22.9	320	8.57	U	Hall Environmental	142.3	8.57	410	6.7
Buckman No. 12 zone	1110–1130	EB-634A	West	20.9	327	8.3	U	Hall Environmental	130.3	8.3	270	11.4
Buckman No. 12 zone	770–790	EB-635A	West	25.5	294	8.45	U	Hall Environmental	134.3	8.45	220	-2.4
Buckman No. 13 zone	2002–1982	EB-636A	West	22.1	262	8.46	U	Hall Environmental	124.2	8.46	220	-2.5
Buckman No. 13 zone	1290–1310	EB-637A	West	20.8	279	8.34	U	Hall Environmental	132.3	8.34	210	1.6
Buckman No. 13 zone	900–920	EB-638A	West	25.1	289	8.53	U	Hall Environmental	146.3	8.53	240	3.0
Buckman No. 13 zone	691–711	EB-639A	West	27.5	325	7.8	U	USGS	144.4	U	212	-0.3
USFS 1200 ft well	EB-642A	West	U	U	8.12	U	Assaigai	121.4	8.12	154	-3.6	
Parker	EB-671A	West	U	U	U	U						

<sup>a</sup>Location, relative to San Isidro Crossing fault.  
<sup>b</sup>Field parameters; T—temperature; SC—specific conductance; µS—microsiemens; DO—dissolved oxygen; U—undetermined, S—dissolved sulfur; Lab: NMBGMR—New Mexico Bureau of Geology and Mineral Resources; USGS—U.S. Geological Survey; NMDWB—New Mexico Drinking Water Bureau; LANL—Los Alamos National Laboratory.

# TDS—total dissolved solids; WWTP—wastewater treatment plant.

TABLE 4. MAJOR AND MINOR ION DATA

Site name	Sample number	Major ions							Minor ions				
		Ca	Mg	Na	K	Cl	SO <sub>4</sub>	HCO <sub>3</sub>	CO <sub>3</sub>	F	Fe	Mn	
El Prado	EB-058A	35.7	4.2	12.9	U	2.1	15.1	136	0	0.32	0.16	<0.03	2.3
Leyba	EB-059A	18	2.3	43	1.7	2.8	17	155	0	0.54	0.044	<0.001	5.3
La Tierra 16	EB-065A	21.65	3.4	16.8	U	4	20	84	0	0.20	<0.02	<0.01	<4
HDC1	EB-081A	14	<1	51	1.7	4.5	21	145	6	0.48	0.099	<0.001	1.7
Las Dos No. 1	EB-085C	16.6	0.78	38.8	1.7	3.47	21.6	144	0	0.44	0.02	<0.001	4
Los Dos No. 2	EB-086A	11	0.8	63	U	4.6	37.5	146.7	0.65	0.52	0.80	<0.01	15.6
Sharp	EB-093A	36	3.8	7.3	1.4	3.6	7.5	130	0	0.43	0.27	<0.001	6.7
Conron No. 2	EB-096A	45	5.2	14	U	8	<1	175	0	0.22	0.07	<0.01	U
Tano Vista	EB-098C	37	5.5	7.7	1.5	4.1	8.6	145	0	0.33	0.075	<0.001	4
Los Suenos Expl	EB-104A	32.7	4.1	13	U	1.4	10	130	3	0.37	<0.03	<0.03	0.9
Ninos	EB-105B	27	3.6	30	2	2.3	16	146	0	0.40	0.024	0.005	4.4
Cuervos	EB-107A	46.6	5.2	7.1	U	14.2	15	127	0	0.43	0.03	0.01	12
SF Ranch HQ1	EB-121A	34.1	6.5	28.3	U	4.4	17	149	0	0.47	0.023	0.006	2.7
Northwest	EB-122E	27.9	2.89	14.2	1.6	1.89	7.12	121	0	0.30	<0.01	<0.001	3.3
New Hickox No. 2	EB-123A B	24.5	4.2	46.7	1.7	10	22.8	144	12	1.40	<0.2	<0.01	14.6
Heartstone1	EB-136A	41	5.2	15	2.4	2.2	14	171	0	0.40	<0.02	0.044	2.3
SF Shelter	EB-138A	28	3.9	13	1.4	2	6.2	134	0	0.40	<0.1	0.0025	<2
MWA	EB-141A	49.8	4.93	33.7	2.87	40.6	16.3	210	0	0.37	<0.01	0.005	2
Santa Fe MW-1	EB-150B	94.6	15.3	7.8	1.8	40	11	136	2	0.40	6.7	0.49	43.4
Santa Fe MW-2	EB-151B	41	5.9	5.4	1.7	20	17	122	0	0.30	0.17	<0.03	15.5
Santa Fe MW-3	EB-152B	34	5	5.2	1.4	9.9	7.1	117	0	0.30	0.15	<0.03	11.5
Santa Fe MW-4	EB-153A	61	7.4	5.5	2	14	5.6	103	0	0.20	3.1	1	32.3
Caja del Rio	EB-155A	24	3	22	4	3.7	19	49	4.8	0.30	0.148	<0.005	29.7
MW-1													
Caja del Rio	EB-156A	17	3	32	2	3	20	122	0	0.59	0.049	<0.005	5.3
MW-4													
SF Ranch HQ2	EB-159A	33	2.7	27	2.1	3.7	18	160	0	0.44	0.24	0.001	4.9
Tony's WM	EB-160A	47	4.7	15	2.1	8.8	18	155	0	0.26	0.12	0.018	19
Moss Farms	EB-165A	40	5.7	14	2	3.2	16	165	0	0.29	2.5	0.051	2.9
Hurlocker	EB-174A	43.2	2.78	4.74	0.48	4.22	5.76	135	0	0.16	<0.01	<0.001	7.8
Indian School	EB-207H	55.2	3.7	5.9	<1	20	24	111	0	0.15	0.197	<0.01	28.4
Hagerman	EB-219B	27.1	7.78	9.2	1.17	7.1	9.32	113	0	0.23	U	U	U
Orchard	EB-240A	35	3.4	4.3	0.77	5.2	9.6	110	0	0.17	0.26	<0.001	8.7
Agua Fria Park													
SF-3a (piezometer B)	EB-265A	3.1	<1	37	1.3	2.1	3	92	7.5	0.42	0.011	<0.001	1.6
SF-3b (piezometer B)	EB-266A	0	<1	42	0.6	2.2	3	78	6.9	0.52	0.039	0.001	1.6
SF-3c (piezometer B)	EB-267A	35	2.4	58	2.7	2.3	11	250	0	0.29	0.16	<0.001	19
SF-2a (piezometer B)	EB-268A	20	2.8	310	7.6	55	49	709	0	0.4	0.031	0.49	U
SF-2b (piezometer B)	EB-269A	20	7.2	180	7.6	5.2	28	570	0	0.14	0.23	0.22	3.7
SF-2c (piezometer B)	EB-270A	3.8	<1	88	2.2	11	24	200	0	0.21	0.053	0.031	8.5
La Tierra South	EB-285A	27	7.4	29.8	U	3.4	16	142	0	0.41	<0.001	0.002	2.2
La Tierra Kubert	EB-286A	4	0.45	74	2.5	8	18.5	175	0	1.94	<0.1	<0.05	14
La Tierra Pinon	EB-287A	30.3	8.8	50.6	U	17.9	17	167	0	0.68	0.027	<0.001	2.7
La Tierra 32-T-3	EB-291A	37.2	5.1	25.7	U	10	22.6	152	0	0.18	0.003	0.008	13.7
Archery 1a (piezometer C)	EB-295A	33	3.6	20	2.2	1.6	11	165	0	0.30	0.15	<0.001	0.25
Archery 1b (piezometer C)	EB-296A	43	5.4	13	2.6	12	8.5	150	0	0.42	0.19	<0.001	24
Archery 1c (piezometer C)	EB-297A	18	2.6	62	5.5	15	25	175	0	0.43	0.071	0.078	9
Buckman SF-6a (piezometer D)	EB-298A	35	11	275	14	8.9	45	865	0	0.72	0.25	0.063	<0.1
Buckman SF-6b (piezometer D)	EB-299A	18	5.7	170	6	5.2	42	495	0	0.79	0.077	0.029	<0.1
Buckman SF-6c (piezometer D)	EB-300A	27	3	45	4.9	8.1	20	175	0	0.29	0.118	0.024	12
Chalmers	EB-328A	16.4	3.2	33	1.8	5.6	14	110	4	0.57	0.035	<0.001	4.8
SFR a (piezometer E)	EB-336A	1.9	<1	125	1	6.2	22	275	12	1.60	0.016	0.009	1.3
SFR b (piezometer E)	EB-337A	11	<1	54	1.8	3	21	150	0	0.40	0.037	0.002	3.8
SFR c (piezometer E)	EB-338A	22	2.7	6.8	0.92	1.7	3.6	95	0	0.29	0.099	<0.001	1.4
Gold	EB-367A	30	4.7	15	2.2	1.7	11	135	0	0.35	0.2	<0.001	1.8
Weil PNM	EB-416A	36	3.9	53	3.6	3.4	16	243	0	0.40	<0	ND	15.1
Ferguson	EB-434A B	51.3	5.2	3.7	0.2	13.5	17	135.4	1	U	U	U	22.2
Osage	EB-455A B	46.9	3.2	3.3	1.1	11.2	13	128.1	1	U	U	U	14.9
Estancia Subdiv	EB-466A	33	3.8	6.8	1.5	5.7	8.3	134	0	0.40	<0.05	0.012	10.2

(Continued)

TABLE 4. MAJOR AND MINOR ION DATA (*Continued*)

Site name	Sample number	Major ions							Minor ions				
		Ca	Mg	Na	K	Cl	SO <sub>4</sub>	HCO <sub>3</sub>	CO <sub>3</sub>	F	Fe	Mn	
Santa Fe MW-7	EB-473A	41	7.6	5.5	1.5	10	4.1	130	4	0.40	1.1	0.073	25.3
Santa Fe Ortiz-1	EB-475A	51	5.5	24	1.1	21	13	160	4	0.20	0.26	0.34	16.4
Santa Fe	EB-476B	64	1.2	8	2	7.4	18.3	134	0	U	<0.1	<0.05	17.4
Buckman No. 1	EB-478A D	6.8	0.391	90.2	2.13	2.68	12.3	246	0	0.67	U	U	U
Buckman No. 2	EB-479A B	19.1	3.4	326	1.9	41.7	340	477.3	0	0.61	0.4	U	U
Buckman No. 3 A	EB-480ABC	50	7.2	100	18	6	23	403	0	U	U	U	U
Buckman No. 4	EB-481A B	84	13	96	14	6	20	515	0	U	<0.1	<0.05	U
Buckman No. 5	EB-482A B	172	25	132	19	7	21	931	0	U	U	U	U
Buckman No. 6	EB-483A C	48	7.1	56	11	5	19	309	0	0.48	<0.1	<0.05	U
Buckman No. 7	EB-484A C	35	5.5	76	8.9	5	24	289	0	0.38	<0.01	<0.01	U
Buckman No. 8	EB-485A C	13.5	2.11	82.3	2.49	2.69	12.5	270	0	0.66	U	U	U
Buckman No. 9	EB-486B	17.2	2.6	145	2.7	8.1	29	415	0	0.72	0.816	0.058	7.1
Buckman No. 10	EB-487A	39.4	6.4	72.7	4.3	7.8	27	317	0	0.61	0.107	0.013	4.9
Buckman No. 11	EB-488A	22	2.4	68	2.1	5.8	29	220	0	0.92	0.031	0.016	6.6
Buckman No. 12	EB-489A	16	1.1	57	1.7	4.5	26	159	0	0.54	<0.02	0.009	6.6
Buckman No. 13	EB-490A	17.1	<1	47.3	1.7	5.4	27	171	0	0.47	<0.03	0.012	3.3
Agua Fria No. 1	EB-505E	41.3	3.48	5.15	0.6	5.03	12.4	147	0	0.17	<0.01	<0.001	9.7
Village MHP No. 1	EB-562B	53.5	3.59	5	5	14.9	23.6	100	0	U	<0.1	<0.05	20.2
Hyde Park, Yellow Cat	EB-571A	52.5	20	19	U	11.8	15	276	0	0.54	0.38	0.024	4
SF Horse Park North	EB-578B	31.1	4.5	9.5	U	6.6	7.1	102	0	<0.5	<0.05	<0.01	11.1
SF Horse Park South	EB-579B	29.5	3.5	13.6	U	5.3	6.4	115	0	<0.5	<0.01	<0.01	3.1
Althouse Leibman	EB-583A	29	8.7	7.9	0.88	8.8	4.8	120	0	0.15	0.085	<0.001	9.7
La Tierra Henry	EB-584A	32	5.8	17	2.2	4.4	12	145	0	0.21	0.059	<0.001	7.4
Travis Ranch	EB-585A	34	3.5	23	2.2	3.8	17	155	0	0.49	0.065	0.001	4.9
C. Henry	EB-587A	30	4.2	20	2.3	2.6	13	150	0	0.28	0.055	<0.001	4.9
Leyba Agua Fria	EB-588A	31	3.2	7.5	1.4	1.7	8.3	120	0	0.46	0.056	<0.001	1.7
Constant 1	EB-589A	42	4.2	6.6	0.93	12	8.9	125	0	0.17	0.1	<0.001	12
Homans	EB-590A	39	5.8	11	2.4	7.1	12	145	0	0.30	0.087	<0.001	12
Sugarman	EB-591A	44	8.2	13	2.6	12	12	160	0	0.38	0.098	<0.001	16
Trujillo	EB-593A	27	2.7	6.4	1.6	3.2	4	100	0	0.21	0.05	<0.001	1.2
Santa Fe River above WWTP	EB-594A	38	4	16	1.8	3.9	13	145	0	0.27	0.12	0.001	8.7
EB-595A	31	5	9.6	1.6	12	23	87	3.8	0.27	0.24	0.02	0.19	
Centaurus Ranch	EB-596A	43	6.4	11	2.5	9.4	9.4	145	0	0.21	0.12	<0.001	18
Mariah Ranch	EB-597A	25	3.1	50	2.8	6.4	29	180	0	0.72	0.067	<0.001	6.2
Leyba 600	EB-598A	30	4.4	24	2.4	2.9	14	150	0	0.27	0.21	<0.001	6.6
Terwilliger	EB-599A	31	4.5	11	2.3	4.3	8.4	120	0	0.38	0.11	<0.001	10
Preston	EB-600A	39	4.8	17	1.9	3.8	13	165	0	0.33	0.12	<0.001	5.6
Oneil	EB-601A	30	3.4	9.3	1.6	1.6	8.4	120	0	0.26	0.092	<0.001	0.88
Borrego	EB-603A	31	4.2	50	2.4	38	12	180	0	0.20	0.079	<0.001	4.1
Torreón No. 2	EB-604D	50.1	6.33	6.68	0.95	10.7	3.24	153	0	0.13	<0.01	<0.001	22
Jail Deep	EB-605A	18.8	2.13	824	4.63	632	768	231	7.92	3.49	<0.01	0.065	0.07
Las Campanas a (piezometer H)	EB-608A	7.1	0.74	92	1.8	4.6	29	220	20	1.50	0.15	0.008	0.37
Las Campanas b (piezometer H)	EB-609A	7.1	0.61	71	1.2	4.9	27	175	0	0.75	0.088	0.026	0.5
Las Campanas c (piezometer H)	EB-610A	31	3.3	30	2.1	3.3	15	150	0	0.36	0.27	<0.001	17
Peters Expl	EB-611A	23	1.6	31	1.7	1.7	17	134	0	0.28	0.04	0.0071	1.9
Constant 2	EB-615A	26.6	3.4	7.8	2.4	3.21	7.53	121.5	0	<0.05	<0.05	<0.01	6.6
Buckman No. 10 zone 1900–1920	EB-625A	21	3.2	99	3.3	5.2	29	268.8	9.6	1.2	<0.02	0.028	U
Buckman No. 10 zone 1650–1670	EB-626A	27	7.1	160	6.1	7.2	48	488.8	19.2	0.87	0.055	0.059	U
Buckman No. 10 zone 1080–1100	EB-627A	25	5.7	83	4.2	4.2	33	305.5	7.2	0.68	0.083	0.025	U
Buckman No. 10 zone 797–817	EB-628A	68	4.7	25	3.1	4.4	18	183	0	0.27	0.85	0.34	U
Buckman No. 11 zone 1900–1920	EB-629A	24	4.1	120	4.1	5.7	40	305.5	14.4	0.85	<0.02	0.056	U
Buckman No. 11 zone 1620–1640	EB-630A	20	3.6	120	4	6.2	49	329.9	12	0.85	0.13	0.037	U
Buckman No. 11 zone 820–840	EB-631A	30	2.3	37	1.8	4.1	20	158.9	2.4	0.63	0.026	0.025	U
Buckman No. 12 zone 1780–1800	EB-632A	9.5	0.56	70	1.9	4	29	146.6	6	0.50	0.037	0.025	U
Buckman No. 12 zone 1430–1450	EB-633A	17	1.2	68	2.3	4	29	146.6	7.2	0.56	0.084	0.017	U

(Continued)

TABLE 4. MAJOR AND MINOR ION DATA (*Continued*)

Site name	Sample number	Major ions							Minor ions				
		Ca	Mg	Na	K	Cl	SO <sub>4</sub>	HCO <sub>3</sub>	CO <sub>3</sub>	F	Fe	Mn	
Buckman No. 12 zone 1110–1130	EB-634A	17	2	72	2.3	4.5	32	158.8	7.2	0.71	<0.02	0.029	U
Buckman No. 12 zone 770–790	EB-635A	37	4	38	3.1	3.8	18	158.9	0	0.39	0.065	0.016	U
Buckman No. 13 zone 2002–1982	EB-636A	11	<1	61	1.5	4.6	27	158.86	2.4	0.47	0.063	0.029	U
Buckman No. 13 zone 1290–1310	EB-637A	22	0.85	39	1.8	3.8	22	146.6	2.4	0.30	<0.02	0.047	U
Buckman No. 13 zone 900–920	EB-638A	38	2.9	24	2.2	3.6	18	158.9	1.2	0.32	<0.02	0.035	U
Buckman No. 13 zone 691–711	EB-639A	39	4.8	28	2.5	3.4	18	171.1	3.6	0.37	<0.02	0.058	U
USFS 1200 ft well Parker	EB-642A	18	2	50	4.5	4.4	15	176	0	0.20	0.14	U	2.2
	EB-671A	23.7	2.18	23.9	U	1.86	2.88	148	0	U	<0.5	0.003	4.4

Key: All units in mg/L; U—undetermined; WWTP—wastewater treatment plant.

regression (Manning, 2009). The mean surface temperature at Santa Fe (elevation 2100 m above sea level) is ~10 °C based on this regression. Temperature gradients vary from 24 °C/km near Santa Fe to over 40 °C/km over the Caja del Rio horst, with the highest gradient increase aligning along the faulted eastern boundary of the horst (Fig. 10). A temperature gradient of 40 °C/km is one deviation above the mean for New Mexico oil-well data and is the recognized threshold indicating geothermal activity (Swanberg, 1981).

We offer three possible conceptual flow scenarios to explain thermal anomalies in the shallow Tesuque aquifer system. First, the Cañada Ancha graben is characterized by strong, vertically upward hydraulic gradients and discharge of warm, fossil groundwater. The anomalously high groundwater temperatures and thermal gradients may simply be caused by groundwater discharge through high permeability zones in the Tesuque Formation aquifer, as described by Domenico and Palciauskas (1973) and Anderson (2005) (Fig. 11). Second, the Caja del Rio horst thins the Tesuque aquifer system and constricts flow in the Santa Fe GFU, creating a forced convection system that drives upward flow of warm groundwater through the Tesuque aquifer (Fig. 12A) (Witcher et al., 1992; Kilty and Chapman, 1980). Third, deep thermal water flowing upward along horst-bounding basement faults discharges into the Tesuque aquifer and causes or contributes to thermal anomalies (Fig. 12B). Examples of forced convection systems and upflow of thermal groundwater along faults have been confirmed in field studies in the Rio Grande rift (Mailloux et al., 1999) and at Yucca Mountain, Nevada (Sass et al., 1988, 1995; Fridrich et al., 1994). Each of these scenarios entails mixing of warm upflow with cooler groundwater near the water table.

### Defining Thermal Waters in the Santa Fe GFU

Investigations involving water-rock interactions require accurate subsurface temperatures, and in this study we first establish a method of classifying thermal waters in the Santa Fe GFU. In applied geothermal assessments the definition of “ther-

mal water” has often been arbitrary and subjective. For example, the U.S. Department of Energy has used 20 °C as the minimum temperature for designating a “geothermal” well, while geothermal evaluations in New Mexico have arbitrarily established 30 °C as the minimum temperature for identifying thermal water (Swanberg, 1981). However, what is important in our study is to distinguish anomalous water temperatures that exceed what is expected given well depth and regional thermal gradient. For the Santa Fe GFU, we modify a method that uses the mean annual air temperature (MAT) as a baseline from which to define a thermal spring (Witcher, 1981; Swanberg, 1981; Steele and Wagner, 1981; Swanberg and Morgan, 1978). In Arizona, Witcher (1981) established one standard deviation (7.5 °C) above the MAT as the quantitative criteria for defining a “warm” spring, and two standard deviations (15 °C) to define a “hot” spring. We extend this method to groundwater wells in the Santa Fe GFU by applying an average temperature gradient of 25 °C/km (Fig. 10), a mean surface temperature of 10 °C, and the sample depth (Table 2) to calculate expected sample temperatures (Fig. 13). Using this approach, we identify seven warm wells with discharge temperatures of 25.1–28.9 °C, and one hot well with a discharge temperature of 33.1 °C. However, because temperature data are not always present for wells in the compiled data set, additional unidentified thermal wells may exist in our database.

### CHEMICAL AND ISOTOPIC COMPOSITION OF GROUNDWATER

Chemical and isotopic data for groundwater from the Tesuque Formation in the Santa Fe GFU were examined for relations and spatial patterns useful in determining sources of groundwater, groundwater flow patterns, recharge and discharge zones, and geochemical processes. We focus on parameters that help distinguish between shallow and deep groundwater flow in the Tesuque aquifer, including total dissolved solids (TDS), calcium (Ca), sodium (Na) and deuterium ( $\delta^2\text{H}$ , in per mil [%]). We also examine the trace element arsenic (As) and possible linkages with the geothermal indicators boron (B), lithium (Li),

TABLE 5. TRACE-ELEMENT DATA

Site name	Sample number	Al	As	B	Ba	Br	Cr	Cu	Li	Ni	Pb	SiO <sub>2</sub>	Sr	U	Zn	
El Prado Leyba	EB-059A	U	<0.001	U	0.16	U	<0.03	U	U	U	0.0163	U	U	<0.03	U	
HDC1	EB-081A	<0.001	0.007	0.082	0.13	0.04	0.002	0.035	<0.001	0.061	0.031	20	0.31	0.006	0.01	
Las Dos No. 1	EB-085C	0.0059	0.0049	0.047	0.086	0.05	0.0015	0.0025	0.001	0.043	0.008	U	18	0.3	0.008	
Sharp	EB-093A	<0.001	0.003	0.03	0.15	<0.1	<0.001	0.008	<0.001	0.001	0.001	U	18.8	0.61	0.0086	
Contron No. 2	EB-096A	<0.1	0.004	U	<0.1	<0.1	<0.01	0.03	U	<0.001	0.001	U	21	0.12	0.002	
Tarjo Vista	EB-098C	<0.001	0.011	0.031	0.16	<0.1	0.001	0.002	U	<0.001	0.001	U	23	0.18	0.002	
Los Suenos Expl Ninos	EB-104A	U	0.015	<0.1	0.11	U	<0.03	<0.03	U	<0.003	0.002	U	U	U	<0.03	
Northwest	EB-105B	0.06	0.015	0.02	0.23	0.03	<0.001	<0.002	U	<0.001	0.001	U	25.3	0.17	<0.004	
New Hickox No. 2	EB-122E	0.0036	0.0046	0.007	U	0.18	<0.04	0.04	U	<0.001	<0.0002	U	U	0.0015	0.005	
Heartstone 1	EB-123AB	<0.5	U	U	U	U	<0.04	0.021	U	<0.002	<0.0002	U	U	U	<0.1	
SF Shelter	EB-136A	<0.05	0.003	<0.1	<0.1	<2	<0.001	U	U	U	0.0015	<0.0001	U	U	U	0.008
MWA	EB-138A	<0.002	0.0089	0.0031	0.043	0.15	0.03	0.0029	0.001	0.008	0.0044	0.0003	U	0.18	0.0021	0.018
Santa Fe MW-1	EB-141A	<0.05	<0.001	<0.001	<0.5	0.025	0.025	0.0027	0.0039	0.01	0.0016	<0.005	0.1	0.11	0.0009	0.009
Santa Fe MW-2	EB-150B	<3	<0.01	<0.5	0.21	U	<0.01	0.08	U	<0.05	0.005	U	U	U	<2.5	1.82
Santa Fe MW-3	EB-152B	<3	<0.01	<0.5	0.34	U	<0.01	0.06	U	<0.05	0.006	U	U	U	<2.5	<0.05
Santa Fe MW-4	EB-153A	<3	<0.01	<0.5	0.65	U	<0.01	U	U	<0.05	0.015	U	U	U	<2.5	0.06
Caja del Rio MW-1	EB-155A	U	U	0.054	U	U	U	U	U	<0.004	U	U	U	U	U	2.3
Caja del Rio MW-4	EB-156A	U	U	0.029	U	U	U	U	U	<0.004	U	U	U	U	U	0.003
SF Ranch HQ2	EB-159A	<0.001	0.012	0.074	0.11	<0.1	0.002	0.001	U	0.025	0.001	U	U	U	U	0.036
Tony's WM	EB-160A	<0.001	0.004	0.044	0.14	0.12	0.001	<0.001	U	0.017	0.004	U	U	U	U	0.083
Moss Farms	EB-165A	0.015	0.007	0.039	0.18	<0.1	0.006	0.001	U	0.016	0.001	U	U	U	U	0.014
Hurlucker	EB-174A	0.0072	0.0016	0.011	0.3	0.03	<0.001	0.0019	U	0.004	<0.001	U	U	U	U	0.099
Indian School	EB-207H	<0.005	U	U	U	0.218	U	<0.01	U	<0.004	U	U	U	U	U	0.13
Hagerman Orchard	EB-219B	U	U	U	U	U	U	U	U	<0.001	U	U	U	U	U	0.0011
Agua Fria Park	EB-240A	<0.001	0.001	0.01	0.1	<0.1	<0.001	U	U	0.002	<0.001	U	U	U	U	0.057
SF-3a (piezometer B)	EB-265A	0.002	0.006	0.044	0.016	0.016	0.001	0.007	U	0.0037	0.001	U	U	U	U	0
SF-3b (piezometer B)	EB-266A	0.014	0.016	0.052	0.02	0.01	0.001	0.007	U	0.0012	0.001	U	U	U	U	0.001
SF-3c (piezometer B)	EB-267A	<0.001	0.003	0.064	0.014	0.014	0.001	0.003	U	0.002	0.001	U	U	U	U	<0.003
SF-2a (piezometer B)	EB-268A	U	U	U	U	U	U	U	U	0.038	0.001	U	U	U	U	0.001
SF-2b (piezometer B)	EB-269A	<0.001	0.001	0.16	0.075	0.11	<0.001	0.006	U	0.2	0.002	U	U	U	U	0.002
SF-2c (piezometer B)	EB-270A	0.004	0.002	0.063	0.034	0.15	<0.001	0.004	U	0.007	<0.001	U	U	U	U	0.001
Archery 1a (piezometer C)	EB-295A	0.001	0.003	0.042	0.023	<0.1	<0.001	0.001	U	0.016	<0.001	U	U	U	U	0.003
Archery 1b (piezometer C)	EB-296A	0.001	0.002	0.028	0.28	0.18	<0.001	0.001	U	0.015	0.001	U	U	U	U	0.002
Archery 1c (piezometer C)	EB-297A	0.005	0.006	0.052	0.12	0.12	<0.001	0.003	U	0.022	0.001	U	U	U	U	0.016
Buckman SF-6a (piezometer D)	EB-298A	<0.001	0.007	0.18	0.21	<0.1	0.001	0.008	U	0.024	0.002	U	U	U	U	0.001
Buckman SF-6b (piezometer D)	EB-299A	0.002	0.019	0.19	0.13	0.11	0.001	0.005	U	0.019	0.012	U	U	U	U	0.004
Buckman SF-6c (piezometer D)	EB-300A	0.002	0.004	0.062	0.11	0.15	<0.001	0.002	U	0.026	0.001	U	U	U	U	0.008
Chalmers	EB-328A	0.001	0.004	0.071	0.055	<0.1	0.013	0.001	U	0.015	<0.001	U	U	U	U	0.008
SFR a (piezometer E)	EB-336A	0.016	0.042	0.17	0.029	0.14	0.006	0.005	U	0.069	<0.001	U	U	U	U	0.003
SFR b (piezometer E)	EB-337A	0.002	0.018	0.061	0.11	0.11	0.005	0.003	U	0.03	<0.001	U	U	U	U	0.008
SFR c (piezometer E)	EB-338A	0.001	0.001	0.009	0.17	<0.1	<0.001	0.001	U	0.004	<0.001	U	U	U	U	0.001
Gold	EB-367A	<0.001	0.014	0.057	0.12	<0.1	0.001	0.001	U	0.013	<0.001	U	U	U	U	0.004
Weil PNM Ferguson	EB-416A	U	U	0.07	U	U	U	U	U	U	U	U	U	U	U	U
Osage	EB-434AB	U	U	0.004	U	0.535	U	0.0011	U	U	0.0012	U	U	U	U	U
Estancia Subdiv	EB-455AB	0.037	0.002	U	0.2	U	<0.006	<0.006	U	<0.01	<0.005	U	U	U	U	0.0018
	EB-466A	U	U	U	U	U	U	U	U	U	U	U	U	U	U	0.0001

(Continued)

TABLE 5. TRACE-ELEMENT DATA (Continued)

Site name	Sample number	Al	As	B	Ba	Br	Cr	Cu	Li	Ni	Pb	SiO <sub>2</sub>	Sr	U	Zn
Santa Fe Mn-7	EB-473A	<3	<0.01	<0.5	0.4	U	<0.01	0.06	<0.05	<0.05	<0.01	23.5	0.0115	<0.05	<0.05
Santa Fe Ortiz-1	EB-475A	<3	<0.01	<0.5	0.38	<0.1	<0.007	U	ND	ND	<0.01	33	0.008	<0.05	<0.05
Buckman No. 1	EB-478AD	U	0.005	U	0.1	U	0.006	U	U	U	U	ND	0.0159	U	U
Buckman No. 2	EB-479AB	U	0.005	U	0.1	U	0.006	U	U	U	U	ND	0.0159	U	U
Buckman No. 3A	EB-480ABC	U	0.002	U	0.2	U	0.004	U	U	U	U	ND	0.009	U	U
Buckman No. 4	EB-481AB	U	0.003	U	0.4	U	0.003	U	U	U	U	ND	0.01	U	U
Buckman No. 5	EB-482AB	U	0.008	U	0.2	U	0.004	U	U	U	U	ND	0.016	U	U
Buckman No. 6	EB-483AC	U	0.004	U	0.1	U	0.007	U	U	U	U	ND	0.006	U	U
Buckman No. 7	EB-484AC	U	0.007	U	<0.1	U	0.006	U	U	U	U	ND	0.006	U	U
Buckman No. 8	EB-485AC	U	0.013	U	0.068	U	0.012	U	U	U	U	ND	0.0149	U	U
Buckman No. 9	EB-486B	0.587	0.006	0.004	0.089	U	0.002	U	U	U	U	ND	0.0115	0.0001	0.0001
Buckman No. 10	EB-487A	0.006	0.004	0.011	0.099	U	0.002	U	U	U	U	ND	0.008	0.023	0.0005
Buckman No. 11	EB-488A	<0.02	0.018	0.1	0.1	U	<0.006	U	U	U	U	ND	0.005	0.243	<0.1
Buckman No. 12	EB-489A	0.014	0.016	0.004	0.007	U	0.003	U	U	U	U	ND	0.004	0.424	0.008
Buckman No. 13	EB-490A	0.0081	<0.001	0.001	0.08	U	<0.001	0.02	U	U	U	ND	0.0017	0.058	0.042
Aguia Fria No. 1	EB-505E	U	0.004	U	0.13	U	<0.01	U	U	U	U	ND	U	U	U
SF Horse Park North	EB-578B	<0.1	<0.001	U	0.08	U	<0.01	U	U	U	U	ND	U	U	U
SF Horse Park South	EB-579B	<0.1	<0.001	U	0.13	U	<0.01	U	U	U	U	ND	U	U	U
Aithouse	EB-583A	0.001	0.005	0.014	0.62	0.17	<0.001	U	U	U	U	ND	U	U	U
Leibman	EB-584A	<0.001	0.009	0.036	U	0.036	<0.001	U	U	U	U	ND	U	U	U
La Tierra Henry	EB-585A	<0.01	0.016	0.071	0.13	<0.1	0.002	U	U	U	U	ND	U	U	U
Travis Ranch	EB-587A	<0.001	0.014	0.064	0.15	<0.1	0.001	U	U	U	U	ND	U	U	U
C. Henry	EB-588A	<0.001	0.004	0.031	0.16	<0.1	0.001	U	U	U	U	ND	U	U	U
Leyba Agua Fria	EB-589A	0.001	0.001	0.017	0.1	<0.1	<0.001	U	U	U	U	ND	U	U	U
Constant 1	EB-590A	0.001	0.007	0.042	0.17	0.14	0.001	U	U	U	U	ND	U	U	U
Homans	EB-591A	<0.001	0.005	0.048	0.17	0.23	0.001	U	U	U	U	ND	U	U	U
Sugarman	EB-593A	0.001	0.002	0.01	0.4	<0.1	<0.001	U	U	U	U	ND	U	U	U
Trujillo	EB-594A	<0.001	0.004	0.039	0.17	<0.1	0.001	U	U	U	U	ND	U	U	U
Santa Fe River above WWTP	EB-595A	0.013	0.001	0.017	0.055	<0.1	0.001	U	U	U	U	ND	U	U	U
Centaurus Ranch	EB-596A	0.001	0.007	0.04	0.24	0.18	0.001	U	U	U	U	ND	U	U	U
Mariah Ranch	EB-597A	0.001	0.008	0.11	0.087	0.11	0.001	U	U	U	U	ND	U	U	U
Leyba 600	EB-598A	0.002	0.002	0.066	0.16	<0.1	0.002	U	U	U	U	ND	U	U	U
Terwilliger	EB-599A	0.001	0.008	0.031	0.2	<0.1	<0.001	U	U	U	U	ND	U	U	U
Preston	EB-600A	0.001	0.005	0.044	0.16	<0.1	0.001	U	U	U	U	ND	U	U	U
O'Neill	EB-601A	0.001	0.008	0.028	0.23	<0.1	0.001	U	U	U	U	ND	U	U	U
Borrego	EB-603A	0.001	0.014	0.049	0.19	<0.1	0.001	U	U	U	U	ND	U	U	U
Torreón No. 2	EB-604D	0.0025	0.0049	0.01	0.78	0.06	<0.001	U	U	U	U	ND	U	U	U
Jail Deep	EB-605A	0.005	0.0122	3.7	0.006	0.94	0.001	U	U	U	U	ND	U	U	U
Las Campanas a (piezometer H)	EB-608A	0.14	0.017	0.14	0.11	0.1	0.001	U	U	U	U	ND	U	U	U
Las Campanas b (piezometer H)	EB-609A	0.051	0.03	0.086	0.088	<0.1	0.001	U	U	U	U	ND	U	U	U
Las Campanas c (piezometer H)	EB-610A	0.002	0.016	0.085	0.12	<0.1	0.004	U	U	U	U	ND	U	U	U
Peters Expl	EB-611A	0.039	0.011	0.043	0.13	U	<0.006	U	U	U	U	ND	U	U	U
Constant 2	EB-615A	<0.1	0.0092	0.18	<0.01	U	<0.006	U	U	U	U	ND	U	U	U
Buckman No. 10	EB-625A	0.006	U	U	U	U	<0.01	U	U	U	U	ND	U	U	U
zone 1900-1920															

(Continued)

TABLE 5. TRACE-ELEMENT DATA (Continued)

Site name	Sample number	Al	As	B	Ba	Br	Cr	Cu	Li	Ni	Pb	SiO <sub>2</sub>	Sr	U	Zn
Buckman No. 10 zone 1650–1670	EB-626A	U	0.003	U	U	U	U	U	U	U	U	U	U	<0.1	U
Buckman No. 10 zone 1080–1100	EB-627A	U	0.008	U	U	U	U	U	U	U	U	U	U	<0.1	U
Buckman No. 10 zone 797–817	EB-628A	U	0.002	U	U	U	U	U	U	U	U	U	U	<0.1	U
Buckman No. 11 zone 1900–1920	EB-629A	U	0.003	U	U	U	U	U	U	U	U	U	U	<0.1	U
Buckman No. 11 zone 1620–1640	EB-630A	U	0.011	U	U	U	U	U	U	U	U	U	U	<0.1	U
Buckman No. 11 zone 820–840	EB-631A	U	0.014	U	U	U	U	U	U	U	U	U	U	<0.1	U
Buckman No. 12 zone 1780–1800	EB-632A	U	0.021	U	U	U	U	U	U	U	U	U	U	<0.1	U
Buckman No. 12 zone 1430–1450	EB-633A	U	<0.02	U	U	U	U	U	U	U	U	U	U	<0.1	U
Buckman No. 12 zone 1110–1130	EB-634A	U	<0.02	U	U	U	U	U	U	U	U	U	U	<0.1	U
Buckman No. 12 zone 770–790	EB-635A	U	<0.02	U	U	U	U	U	U	U	U	U	U	<0.1	U
Buckman No. 13 zone 2002–1982	EB-636A	U	0.013	U	U	U	U	U	U	U	U	U	U	<0.1	U
Buckman No. 13 zone 1290–1310	EB-637A	U	0.01	U	U	U	U	U	U	U	U	U	U	<0.1	U
Buckman No. 13 zone 900–920	EB-638A	U	0.007	U	U	U	U	U	U	U	U	U	U	<0.1	U
Buckman No. 13 zone 691–711	EB-639A	U	0.009	U	U	U	U	U	U	U	U	U	U	<0.1	U
USFS 1200 ft well Parker	EB-642A	U	0.07	U	U	U	U	U	U	U	U	U	U	21	U
	EB-671A	<0.05	0.01	U	0.105	U	0.003	U	U	U	<0.002	<0.005	U	U	U

Key: All units in mg/L; U—undetermined; WWTP—wastewater treatment plant.

TABLE 6. HYDROGEN AND OXYGEN ISOTOPE DATA

Site name	Site number	Location (UTM, NAD83)			Data source	Sample date (m/d/yyyy)	$\delta^2\text{H}$ (‰)	$\delta^{18}\text{O}$ (‰)
		Easting (m)	Northing (m)	Water source				
Leyba	059	403151	3949549	GW	NMBGMR	6/2/2005	-92.93	-13.27
Las Dos No. 1	085	407663	3958060	GW	NMBGMR	5/11/2005	-116.66	-15.85
Sharp	093	412794	3955412	GW	NMBGMR	5/11/2005	-84.91	-12.43
Tano Vista	098	412169	3957033	GW	NMBGMR	5/25/2005	-80.78	-11.53
SF Ranch HQ2	159	405295	3956594	GW	NMBGMR	5/10/2005	-97.99	-13.53
Tony's WM	160	405117	3959307	GW	NMBGMR	6/6/2005	-78.18	-10.79
Moss Farms	165	410472	3957919	GW	NMBGMR	3/1/2006	-99.00	-13.00
Aqua Fria Park	240	406983	3946736	GW	NMBGMR	5/12/2005	-83.22	-12.05
SF-3a (piezometer B)	265	395131	3966203	GW	NMBGMR	3/31/2005	-86.86	-12.55
SF-3b (piezometer B)	266	395137	3966202	GW	NMBGMR	3/30/2005	-86.85	-12.71
SF-3c (piezometer B)	267	395127	3966201	GW	NMBGMR	3/31/2005	-77.17	-11.34
SF-2a (piezometer B)	268	395376	3966090	GW	Anderholm, 1994	7/27/1986	-112.00	-15.00
SF-2b (piezometer B)	269	395390	3966086	GW		4/5/2005	-116.59	-15.78
SF-2c (piezometer B)	270	395376	3966092	GW	NMBGMR	4/6/2005	-92.38	-12.78
Archery 1a (piezometer C)	295	413152	3953989	GW	NMBGMR	4/4/2005	-79.22	-12.06
Archery 1b (piezometer C)	296	413146	3953983	GW	NMBGMR	4/5/2005	-84.08	-12.61
Archery 1c (piezometer C)	297	413146	3953983	GW	NMBGMR	4/4/2005	-84.77	-12.40
Buckman SF-6a (piezometer D)	298	398587	3961476	GW	NMBGMR	3/29/2005	-104.20	-14.71
Buckman SF-6b (piezometer D)	299	398587	3961476	GW	NMBGMR	3/30/2005	-110.08	-15.02
Buckman SF-6c (piezometer D)	300	398587	3961476	GW	NMBGMR	4/6/2005	-84.65	-12.02
Chalmers	328	397578	3942243	GW	NMBGMR	6/7/2005	-94.12	-12.89
SFR a (piezometer E)	336	403199	3944575	GW	NMBGMR	4/8/2005	-103.58	-14.27
SFR b (piezometer E)	337	403199	3944575	GW	NMBGMR	4/8/2005	-113.33	-15.65
SFR c (piezometer E)	338	403199	3944575	GW	NMBGMR	4/9/2005	-83.23	-12.34
Gold	367	405580	3948470	GW	NMBGMR	5/12/2005	-80.30	-12.03
Santa Fe River 2	493	418999	3949504	SW	Anderholm, 1994	11/30/1988	-76.00	-10.00
Santa Fe River 2	493	418999	3949504	SW		9/19/1988	-76.00	-11.00
Santa Fe River 2	493	418999	3949504	SW	Anderholm, 1994	11/10/1988	-77.00	-10.00
Santa Fe River 2	493	418999	3949504	SW	Anderholm, 1994	4/28/1988	-79.00	-11.00
Santa Fe River 2	493	418999	3949504	SW	Anderholm, 1994	8/26/1987	-79.00	-11.00
Santa Fe River 2	493	418999	3949504	SW	Anderholm, 1994	5/28/1987	-85.00	-12.00
Little Tesuque Creek	495	417501	3954784	SW	Anderholm, 1994	8/26/1987	-68.00	-10.00
Little Tesuque Creek	495	417501	3954784	SW	Anderholm, 1994	4/27/1988	-86.00	-12.00
Little Tesuque Creek	495	417501	3954784	SW	Anderholm, 1994	6/3/1987	-90.00	-13.00
Tesuque Creek 2	497	417124	3955895	SW	Anderholm, 1994	6/3/1987	-91.00	-13.00
Tesuque Creek 2	497	417124	3955895	SW	Anderholm, 1994	4/27/1988	-92.00	-13.00
Rio Tesuque 1	498	416528	3956339	SW	Anderholm, 1994	6/3/1987	-90.00	-13.00
Althouse	583	409986	3948497	GW	NMBGMR	6/3/2005	-76.77	-11.20
Leibman	584	407524	3949892	GW	NMBGMR	5/26/2005	-96.64	-13.15
La Tierra Henry	585	403853	3955866	GW	NMBGMR	5/24/2005	-96.70	-13.08
Travis Ranch	587	404110	3949025	GW	NMBGMR	5/24/2005	-89.47	-12.50
C. Henry	588	412444	3954655	GW	NMBGMR	5/25/2005	-84.19	-11.91
Leyba Agua Fria	589	407442	3946750	GW	NMBGMR	6/2/2005	-80.89	-12.04
Constant 1	590	406448	3950465	GW	NMBGMR	5/25/2005	-93.32	-12.93
Homans	591	410125	3950744	GW	NMBGMR	5/26/2005	-72.01	-10.48
Heartstone2	592A	411191	3954720	GW	NMBGMR	5/26/2005	-80.62	-11.42
Trujillo	594	409294	3955311	GW	NMBGMR	6/1/2005	-98.75	-13.31
Centaurus Ranch	596	408677	3950763	GW	NMBGMR	6/1/2005	-83.39	-11.59
Mariah Ranch	597	405067	3962076	GW	NMBGMR	6/3/2005	-106.75	-14.19
Leyba 600	598	403236	3949568	GW	NMBGMR	5/10/2005	-88.26	-12.48
Terwilliger	599	407830	3948618	GW	NMBGMR	6/2/2005	-76.65	-10.96
Preston	600	409825	3956335	GW	NMBGMR	6/1/2005	-94.19	-12.79
Oneil	601	406530	3951847	GW	NMBGMR	6/1/2005	-84.64	-12.04
Borrego	603	403984	3950389	GW	NMBGMR	6/7/2005	-88.55	-12.06
Las Campanas a (piezometer H)	608A	402225	3952079	GW	NMBGMR	9/28/2006	-114.00	-15.80
Las Campanas b (piezometer H)	609A	402225	3952079	GW	NMBGMR	9/27/2006	-112.00	-15.50
Las Campanas c (piezometer H)	610A	402225	3952079	GW	NMBGMR	9/26/2006	-88.00	-12.80
Rio Grande at Otowi	621	396940	3970664	SW	Mills, 2003	8/22/2002	-78.00	-10.00
Rio Grande at Otowi	621	396940	3970664	SW	Mills, 2003	8/16/2003	-86.00	-11.00

(Continued)

TABLE 6. HYDROGEN AND OXYGEN ISOTOPE DATA (*Continued*)

Site name	Site number	Location (UTM, NAD83)			Data source	Sample date (m/d/yyyy)	$\delta^2\text{H}$ (‰)	$\delta^{18}\text{O}$ (‰)
		Easting (m)	Northing (m)	Water source				
Rio Grande at Otowi	621	396940	3970664	SW	Mills, 2003	8/18/2001	-88.00	-12.00
Rio Grande at Otowi	621	396940	3970664	SW	Mills, 2003	1/12/2003	-95.00	-13.00
Rio Grande at Otowi	621	396940	3970664	SW	Mills, 2003	1/5/2002	-100.00	-14.00
	353913106011801	407465	3946015	GW	Anderholm, 1994	1/11/1988	-77.00	-11.60
	353934106002101	408905	3946647	GW	Anderholm, 1994	1/11/1988	-68.00	-10.30
	353942106005801	407977	3946903	GW	Anderholm, 1994	1/11/1988	-74.00	-11.50
	353947105595201	409638	3947040	GW	Anderholm, 1994	1/11/1988	-76.00	-11.40
	353959105592701	410270	3947403	GW	Anderholm, 1994	1/11/1988	-77.00	-10.40
	353959106003901	408460	3947422	GW	Anderholm, 1994	1/11/1988	-79.00	-11.40
	354006106004101	408412	3947638	GW	Anderholm, 1994	1/11/1988	-80.00	-12.30
	354012105590801	410752	3947799	GW	Anderholm, 1994	1/11/1988	-73.00	-10.70
	354034105590501	410834	3948476	GW	Anderholm, 1994	1/11/1988	-71.00	-10.70
	354040106001801	409001	3948679	GW	Anderholm, 1994	1/11/1988	-72.00	-10.90
	354049105545401	417148	3948877	GW	Anderholm, 1994	1/11/1988	-79.00	-12.00
	354052105583501	411594	3949023	GW	Anderholm, 1994	1/11/1988	-74.00	-11.10
	354105105541601	418108	3949361	GW	Anderholm, 1994	1/11/1988	-78.00	-11.50
	354119105553301	416177	3949811	GW	Anderholm, 1994	1/11/1988	-77.00	-11.00
	354134105575101	412713	3950306	GW	Anderholm, 1994	1/11/1988	-75.00	-11.50
	354208105585101	411215	3951369	GW	Anderholm, 1994	1/11/1988	-92.00	-12.65
	354258106034501	403843	3952986	GW	Anderholm, 1994	1/11/1988	-87.00	-12.40
	354320105544501	417418	3953527	GW	Anderholm, 1994	1/11/1988	-80.00	-10.95
	354346105570801	413833	3954362	GW	Anderholm, 1994	1/11/1988	-80.50	-11.10
	354433105571701	413621	3955812	GW	Anderholm, 1994	1/11/1988	-81.50	-11.70
	354457106060601	400342	3956691	GW	Anderholm, 1994	1/11/1988	-77.00	-11.10
	354746106022101	406048	3961836	GW	Anderholm, 1994	1/11/1988	-116.00	-15.80
	354935106085301	396248	3965304	GW	Anderholm, 1994	1/11/1988	-111.00	-15.00
	354944106091801	395624	3965589	GW	Anderholm, 1994	1/11/1988	-104.50	-14.25
	355000106092801	395379	3966085	GW	Anderholm, 1994	1/11/1988	-111.50	-15.00
	355006106094802	394879	3966276	GW	Anderholm, 1994	1/11/1988	-81.50	-11.95

Key: SW—surface water; GW—groundwater; NMBGMR—New Mexico Bureau of Geology and Mineral Resources.

and fluoride (F). Contours of chemical data were constructed by kriging of concentration values followed by manual smoothing. Statistical analyses identify a unique assemblage of chemical constituents that characterize warm groundwater in the discharge zone of the Santa Fe GFU.

### Ion and Trace-Element Chemistry

Water analyses from wells (Table 3) indicate that groundwater in the Santa Fe GFU is generally  $<30$  °C, ranges in pH between 7 and 9.2, and has alkalinites between 50 and 800 mg/L CaCO<sub>3</sub>. The distribution of TDS (Fig. 14) ranges between 90 and 860 mg/L. Concentrations are locally high in the Sangre de Cristo Mountains, near the Buckman well field, and generally increase with depth indicating vertical stratification. Dilute groundwater is found in some shallow wells far into the basin, beyond the Agua Fria and Barrancos fault systems, suggesting that recharge from stream loss occurs along distal reaches of major water courses. Water type is equally distributed between Ca- and Na-rich water. The cation content (Fig. 15) is generally Ca rich east of the San Isidro Crossing fault and Na rich west of the fault, except in the vicinity of the Santa Fe River. Depth

specific sampling in piezometers west of the San Isidro Crossing fault shows Na dominance in all intermediate and deep intervals. Shallow samples near the top of the water table contain mixed Na-Ca waters (Fig. 15, Tables 2 and 3), indicating mixing in the upper aquifer between deep upflowing discharge and shallow recharge. Bicarbonate (HCO<sub>3</sub>) groundwater dominates the entire basin and contributions of SO<sub>4</sub> and Cl are rare (Table 3).

Concentrations of As, B, and Li, like TDS and Na, also increase from east to west in the Tesuque aquifer, with greatest concentrations occurring west of the San Isidro Crossing fault in the discharge zone of the Santa Fe GFU. A plume of As with concentrations as high as 0.054 mg/L (Fig. 16) is present in the Cañada Ancha graben. Limited data for B (Fig. 17) and Li (Fig. 18) show a similar spatial distribution, with concentrations increasing with depth and increasing westward across the Cañada Ancha graben and Caja del Rio horst. In general, areas with high As also have relatively high TDS, Na, B, F, Li, and temperature. The chemical constituents As, B, F and Li are usually present at much higher concentrations in hydrothermal waters than in low-temperature waters (Ellis and Mahon, 1977; Arnórsson, 2000a). B and As also associate with thermal waters near recent volcanic systems (Tello et al., 2000).

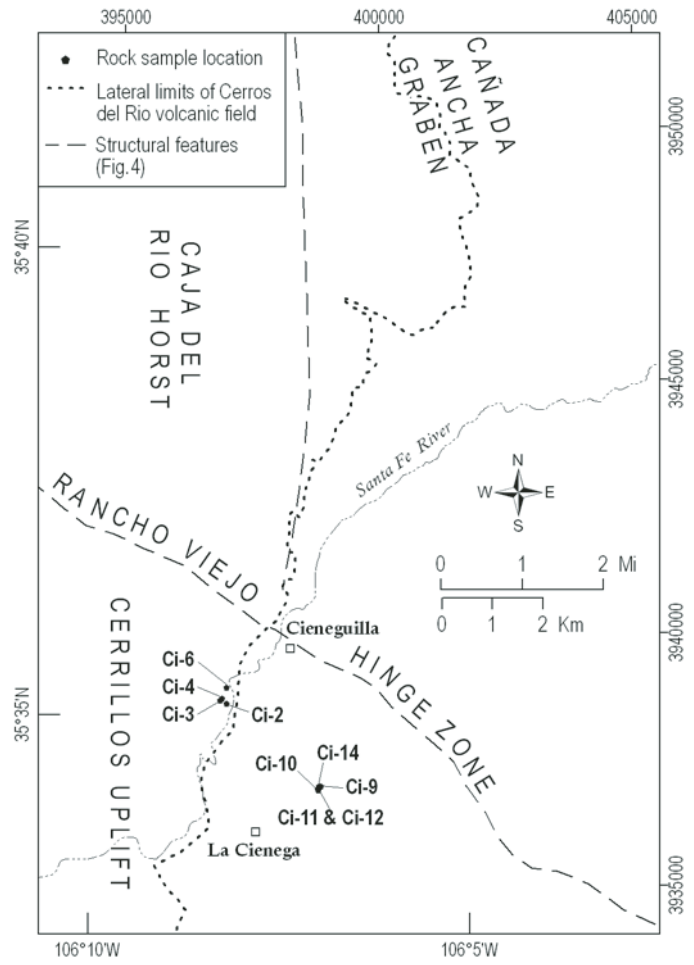


Figure 8. Locations of rock samples collected for major- and trace-element analysis. Samples are from exposures in the Espinaso Formation and Cieneguilla basanite that generally overlie the deformed eastern margin of the Cerillos uplift near the intersection with the Rancho Viejo hinge zone and the Caja del Rio horst. Chemistry results are presented in Table 7.

### Hydrogen-2 ( $\delta^2\text{H}$ ) and Oxygen-18 ( $\delta^{18}\text{O}$ ) Isotopes

Stable isotope values (Table 6) from 44 groundwater samples in the Santa Fe GFU were merged with data from Anderholm (1994), which include surface water samples from the Santa Fe River, the Rio Tesuque watershed, and Arroyo Hondo, and data from Mills (2003) that include five seasonal samples from the Rio Grande at Otowi. The data are shown in Figure 19 with a local meteoric water line (LMWL) for the Santa Fe area (Anderholm, 1994). Streams from the Sangre de Cristo Mountains have  $\delta^2\text{H}$  values of  $-92\text{\textperthousand}$  to  $-68\text{\textperthousand}$  (Anderholm, 1994). Winter flows in the Rio Grande are depleted in  $\delta^2\text{H}$  ( $-100\text{\textperthousand}$  to  $-95\text{\textperthousand}$ ) but relatively enriched the remainder of the year ( $-88\text{\textperthousand}$  to  $-78\text{\textperthousand}$ ) (Mills, 2003). Groundwater in the Santa Fe GFU has  $\delta^2\text{H}$  values of  $-117\text{\textperthousand}$  to  $-68\text{\textperthousand}$  and  $\delta^{18}\text{O}$  values of  $-15.8\text{\textperthousand}$  to  $-10.3\text{\textperthousand}$ . Most groundwater sampled from the Santa Fe GFU falls within

TABLE 7. MAJOR- AND TRACE-ELEMENT DATA FOR ROCK SAMPLES NEAR CIENEGUILLA

Lab sample ID	Field sample ID	Sample lithology	Analyte (mg/kg)															
			Al	As	B	Cd	Ca	Cr	Li	Mg	Mn	Mo	K	Se	Na	U	V	
08-1476	Ci-2	Tuffaceous sandstone with basalt, monzonite and calcite cement (Tc)	2.0	2.0	5.0	2.0	100	1.5	2.0	50	10	1.0	100	5.0	100	1.5	1.0	
08-1477	Ci-3	Hydrothermally altered basalt with 1–3% calcite veining (Tc)	17,560	2.3	<5.0	2.0	40,920	62	26	27,280	565	<1.0	5,421	<5.0	1,462	1.9	80	
08-1478	Ci-4	Phreatomagmatic basaltic breccia (Tc)	13,850	0.2	<5.0	2.0	81,920	1.2	0.8	325	6	121	33	0.03	1.3			
08-1478R	Ci-4	Phreatomagmatic basaltic breccia (Tc)	25	<2.0	<5.0	2.0	213	0.1	0.1	6160	683	<1.0	7560	<5.0	1,734	<1.5	25	
08-1479	Ci-6	Hydrothermally altered basalt with vein and vug calcite (Tc)	14,060	<2.0	<5.0	2.0	60,250	29	30	13,510	698	<1.0	4168	<5.0	2078	<1.5	29	
08-1480	Ci-9	Volcaniclastics with monzonite, latite and tuff (Te)	18,020	<2.0	<5.0	2.0	66,850	38	35	16,490	855	<1.0	4319	<5.0	2301	1.5	36	
08-1481	Ci-10	Volcanic tuff (Te)	29	<2.0	<5.0	2.0	41,120	0.1	1,070	0.7	94	4	58	11	0.01	0.5		
08-1482	Ci-11	Volcaniclastics with monzonite, latite and tuff (Te)	63	0.1	<5.0	2.0	6499	0.2	382	1.1	265	612	<1.0	3872	<5.0	1804	<1.5	81
08-1483	Ci-12	Monzonite intrusive (Te)	6515	<2.0	<5.0	2.0	7403	52	23	4230	427	<1.0	3294	<5.0	1,663	<1.5	46	
08-1484	Ci-14	Hydrothermally altered sandstone with vein calcite (Te)	182.2	<2.0	<5.0	2.0	180.7	0.3	0.4	21.2	2.8	100	16	16	0.6			
08-1484R	Ci-14R	Hydrothermally altered sandstone with vein calcite (Te)	2091	2.3	<5.0	2.0	3138	31	5.5	1506	349	<1.0	1,417	<5.0	500	<1.5	22	
			11.5	0.1	0.4	9.4	0.2	0.5	24.2	2.5		3,4		9.8	0.1			
			5183	2.8	<5.0	2.0	5179	23	16	3537	1976	<1.0	2177	<5.0	647	<1.5	36	
			55.5	0.1	0.3	28.0	0.2	1.3	44.2	28.8		4029	39.8	6.3	0.4			
			5924	2.9	<5.0	2.0	5384	26	18	2003	<1.0	2371	<5.0	663	<1.5	40		
			78.8	0.0	0.2	78.6	0.5	0.4	78.2	48.5		45.0	12.1					

Second line of each sample entry is percent relative standard deviation (RSD%), which equals (standard deviation / average measurement) \* 100.

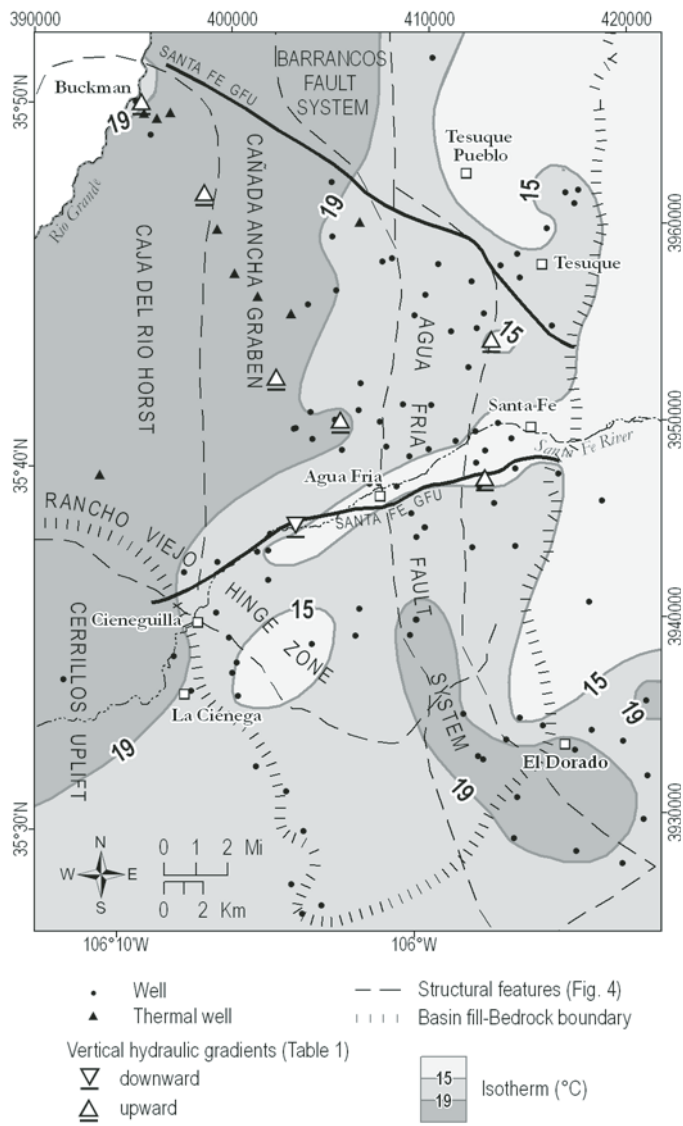


Figure 9. Groundwater isotherms based on bulk temperature measurements in shallow wells in the Tesuque aquifer system. Small black dots indicate locations of measurements. Downward- and upward-pointing triangles depict vertical hydraulic gradients (Fig. 6). Boundaries of major structural features (Fig. 4) are shown as an underlay. Modified from Johnson et al. (2008). GFU—groundwater-flow unit.

a  $\delta^2\text{H}$  range of  $-70\text{\textperthousand}$  to  $-95\text{\textperthousand}$ , similar to the composition of the mountain streams. Anderholm (1994) interpreted this relationship to indicate that groundwater recharge originates primarily from winter precipitation and mountain-front streams.

About 20% of groundwater samples ( $n = 18$ ) have a deuterium composition  $<-95\text{\textperthousand}$ , which is more depleted than any modern stream source but within the range of winter flows in the Rio Grande at Otowi (Mills, 2003). Samples with  $\delta^2\text{H} < -100\text{\textperthousand}$  are significantly lighter than the rest and most plot below the LMWL (Fig. 19), indicating a slight positive shift in  $\delta^{18}\text{O}$ . Deuterium-depleted groundwater is generally found west of the

Barrancos and Agua Fria fault systems in the discharge zone of the Santa Fe GFU (Fig. 20). In the Middle Rio Grande Basin to the south, similar deuterium-depleted water was found with radiocarbon ages greater than 20,000 years (Plummer et al., 2004a, 2004b), but comprehensive radiocarbon data are lacking in the Española Basin. A regression of limited carbon-14 ages and  $\delta^2\text{H}$  values gathered by Manning (2009) from the Española Basin (Fig. 21) indicates that groundwater with a  $\delta^2\text{H}$  value  $\leq -95\text{\textperthousand}$  should have a radiocarbon age of  $\geq 12,800$  years. The deuterium-age correlation indicates that, west of the San Isidro Crossing fault, groundwater discharging from depths of more than  $\sim 160$  m (525 ft) below the water table in nested piezometers has an age range of  $\sim 13,000$ – $30,000$  years (Figs. 20, 21). Enriched deuterium values from shallow piezometers at the water-table surface in the discharge zone (Fig. 20) reflect modern or mixed modern-fossil sources. In the Santa Fe River recharge zone east of the San Isidro Crossing fault,  $\delta^2\text{H}$  values remain constant or are slightly enriched with depth in the aquifer (Manning, 2009) (Fig. 20).

#### Links between Thermal, Chemical, and Isotopic Parameters and Structural Features

Spatial distributions of temperature, ion, trace-element, and isotopic parameters in groundwater show general similarities (Figs. 9, 14–18). Temperature, TDS, Na, F, As, and Li all increase westward from Santa Fe toward Buckman and with depth in the Tesuque aquifer while  $\delta^2\text{H}$  becomes more depleted and groundwater age increases to more than 13,000 years. As groundwater flows from east to west in the Santa Fe GFU, flow lines sequentially cross several north-trending structures including the Agua Fria fault system and San Isidro Crossing (SIC) fault, the synclinal folding at the southern end of the Cañada Ancha graben, and the Caja del Rio horst (Fig. 4).

The change in concentration of select cations and elements along east-to-west flow lines are examined in plots of chemical parameters versus UTM easting, with locations of structural features noted (Fig. 22). All parameters show westerly increasing trends, but not always in a similar pattern. Groundwater temperature (Fig. 22A) increases steadily from  $10\text{ }^\circ\text{C}$  at the mountain front to a maximum of  $33\text{ }^\circ\text{C}$  over the Caja del Rio horst. All thermal wells are situated west of the basin syncline axis, near the Caja del Rio horst. Na and K (Figs. 22B–22C) have uniform distributions between the mountain front and the basin syncline axis, but about half the samples show a three- to fourfold concentration increase approaching the Caja del Rio horst. Trace elements As, Li, and B (Figs. 22D–22F) have uniform distributions between the mountain front and the San Isidro Crossing fault, then increase four- to fivefold approaching the syncline axis and the Caja del Rio horst. These chemical trends appear to associate spatially with structural features.

Statistical correlations reveal links between chemical parameters in the Santa Fe GFU and suggest a possible fluid origin. Spearman rank-order correlation for chemical parameters in

TABLE 8. THERMAL GRADIENTS CALCULATED FROM BOTTOMHOLE TEMPERATURES

Site name	Site number	Location (UTM, NAD83)		Elevation (ft asl)	Elevation (m asl)	Mean annual surface temperature (°C)*	Bottomhole temperature (°C)	Well depth (m)	Temperature gradient (°C/km)	Source of bottomhole temperature data
		Easting (m)	Easting (m)							
SF-2 piezometer B	EB-268	395376	3966090	5521	1683	11.8	25.7	241	58	A. Manning, 2009, personal commun.
Buckman No. 3A	EB-480	396172	3965366	5618	1713	11.6	26.1	457	32	City of Santa Fe well records
Buckman No. 9	EB-486	396848	3965659	5738	1749	11.4	22.2	435	25	John Shomaker & Associates, 2003
SF-6 piezometer D	EB-298	398587	3961476	5963	1818	11.0	37.9	671	40	A. Manning, 2009, personal commun.
Buckman No. 10	EB-487	399250	3959720	6043	1842	10.8	26.1	614	25	John Shomaker & Associates, 2004
Buckman No. 11	EB-488	400130	3957460	6152	1876	10.6	22.8	610	20	John Shomaker & Associates, 2004
Buckman No. 12	EB-489	401300	3956280	6249	1905	10.4	25.9	584	27	John Shomaker & Associates, 2004
Yates La Mesa No. 3	YLM#3	406009	3932807	6320	1927	10.3	51.7	1448	29	NMBGMR Subsurface Data Center
SFR piezometer E	EB-336	403199	3944575	6363	1940	10.2	30.1	570	35	A. Manning, 2009, personal commun.
Rancho Viejo- OWC	EB-667	407135	3939493	6418	1957	10.1	20.6	426	25	Balleau Groundwater, 2008
Buckman No. 13	EB-490	402980	3955400	6429	1960	10.1	26.1	610	26	John Shomaker & Associates, 2004
Rancho Viejo- OWA	EB-663	407765	3939546	6483	1977	10.0	21.4	442	26	Balleau Groundwater, 2008
Yates La Mesa No. 2	YLM#2	405562	3949704	6610	2015	9.7	82.3	2348	31	NMBGMR Subsurface Data Center
Fairgrounds piezometer F	EB-413	409790	3944508	6649	2027	9.6	22.5	511	25	A. Manning, 2009, personal commun.
SF-1 piezometer A	EB-244	412838	3946969	6881	2098	9.2	21.5	524	24	A. Manning, 2009, personal commun.
Hickox	EB-123	414198	3949035	6959	2122	9.0	21.4	352	35	City of Santa Fe well records
Northwest	EB-122	412026	3952585	7129	2173	8.7	21.6	534	24	City of Santa Fe well records
Archery piezometer C	EB-295	413149	3953989	7195	2194	8.6	18.7	333	30	A. Manning, 2009, personal commun.
PUB-A	PUB-A	390446	3937007	6170	1881	10.6			40	Shearer and Reiter, 1978 <sup>†</sup>
PUB-B	PUB-B	393099	3946637	6688	2039	9.6			49	Shearer and Reiter, 1978 <sup>†</sup>
PUB-C	PUB-C	395728	3968459	5747	1752	11.4			40	Shearer and Reiter, 1978 <sup>†</sup>
PUB-D	PUB-D	395882	3970066	5524	1684	11.8			34	Shearer and Reiter, 1978 <sup>†</sup>

Key: asl—above sea level; NMBGMR—New Mexico Bureau of Geology and Mineral Resources.

\*Estimated using temperature-elevation regression for Española Basin (Manning, 2009):  $T(\text{°C}) = -0.0064 * \text{elevation(m)} + 22.6$ .

<sup>†</sup>Published data for conductive thermal gradient.

groundwater (Table 9) shows a strong positive covariance (0.42–0.88) among B, F, Li,  $\text{SO}_4^{2-}$ , and temperature, as well as between Na and these parameters (0.62–0.90). Significant positive covariance also exists among trace elements As, Cr, Mo, U, and V, and between As, Na, and the thermal water indicators B, F, Li,  $\text{SO}_4^{2-}$ , and temperature (0.36–0.67). Hydrogen-2 shows a strong negative covariance (−0.32 to −0.67) with B, Li,  $\text{SO}_4^{2-}$ , the trace elements As, Cr, Mo, and U, and temperature, indicating that

groundwater is increasingly depleted in  $^2\text{H}$  as concentrations of these constituents increase. No significant correlations with chloride or bromide are indicated.

Boron and lithium are commonly elevated in thermal wells and springs and used as geothermal indicators and tracers of thermal fluids (Arnórsson, 2000a; Shaw and Sturchio, 1992). Neither B nor Li elevates in low-temperature waters via cation exchange, aluminosilicate weathering, or dissolution of carbonate

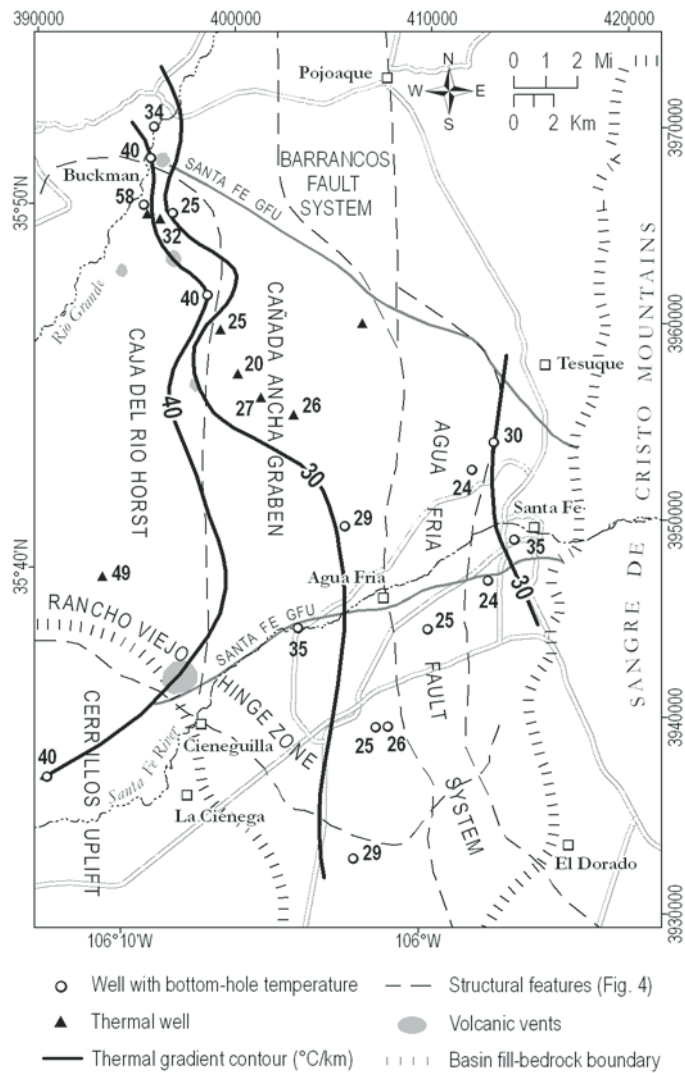


Figure 10. Thermal gradients ( $^{\circ}\text{C}/\text{km}$ ) in the Santa Fe area, south-eastern Espanola Basin, estimated from bottomhole temperatures measured in exploration and monitoring wells. Open circles indicate well locations; black triangles indicate thermal well locations (from Fig. 13); solid black lines represent contours of thermal gradient. Well information and thermal calculations are presented in Table 8. GFU—groundwater-flow unit.

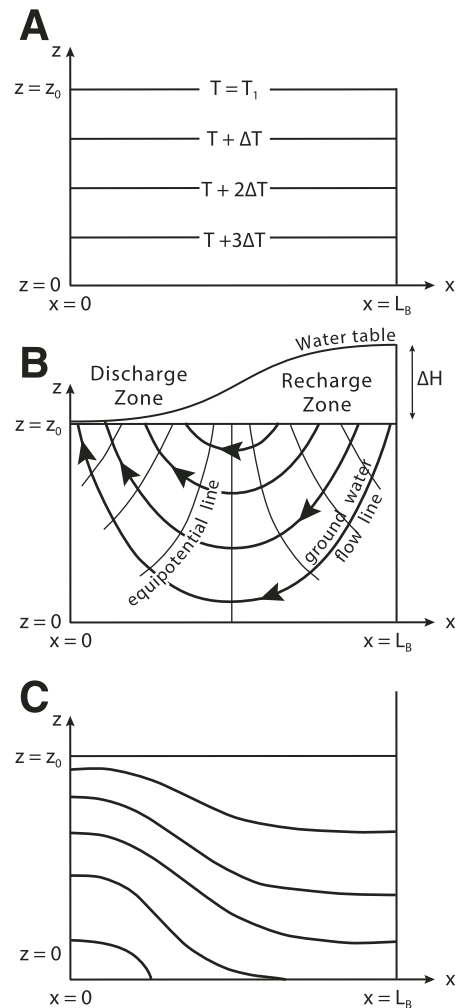


Figure 11. Two-dimensional schematic cross sections of a basin of length  $L_B$  and thickness  $z_0$  showing: (A) horizontal isotherms in a basin with no convection; (B) water table configuration, equipotential lines, and groundwater flow lines for a regional flow system under a topographic gradient; and (C) upward deflection of isotherms for the flow system portrayed in B (modified from Domenico and Palciauskas, 1973). T—temperature;  $\Delta H$ —change in hydraulic head.

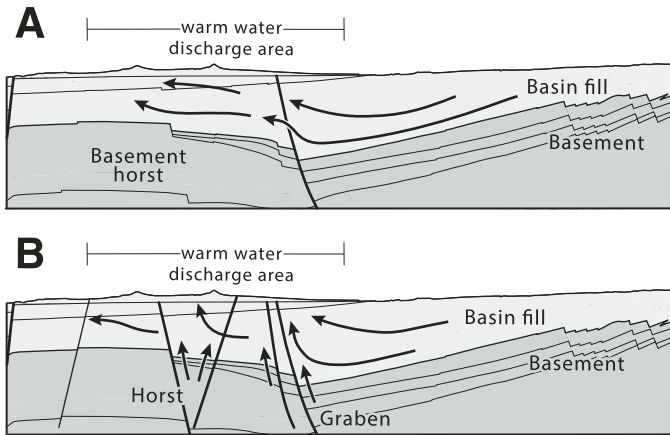


Figure 12. Two-dimensional schematic cross sections of hydrogeologic settings associated with forced convection systems: (A) constriction model with hypothetical groundwater flow over a horst and graben in impermeable bedrock; and (B) upward-flowing thermal water along horst-bounding normal faults. Cross-section models are based on the west-to-east geologic section on Figure 3. Black arrows indicate groundwater flow.

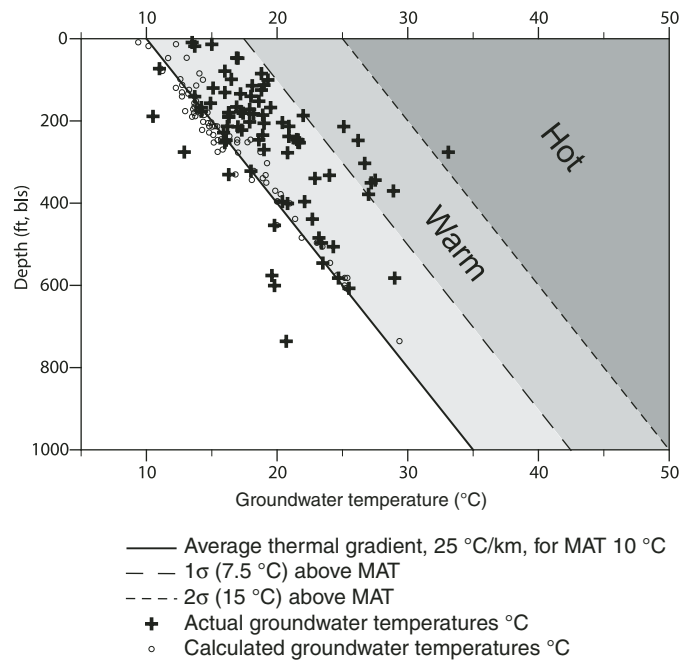


Figure 13. Plot of groundwater temperature versus sample depth (below land surface) for samples in the Santa Fe groundwater-flow unit assuming an average thermal gradient of 25 °C/km and a mean annual air temperature (MAT) of 10 °C. Deviations in actual groundwater temperature of more than one standard deviation above MAT (7.5 °C) define anomalously warm wells, following Witcher (1981). bls—below sea level.

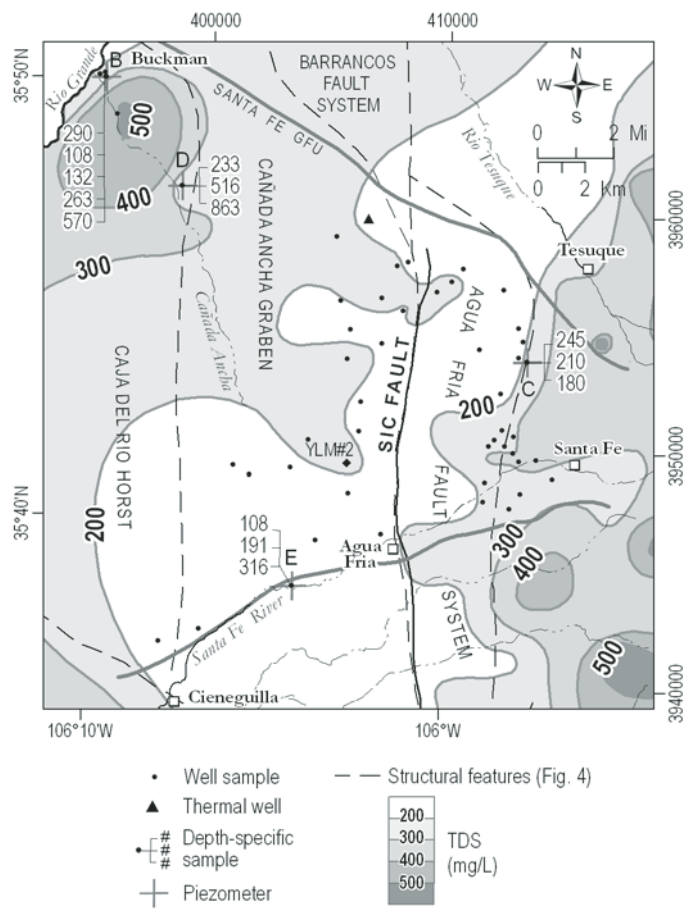


Figure 14. Distribution of total dissolved solids (TDS) in the Santa Fe groundwater-flow unit (GFU) with boundaries of structural features (Fig. 4) shown as an underlay. Stacked values show the vertical distribution of TDS from depth-specific sampling. Modified from Johnson et al. (2008). YLM#2—Yates La Mesa No. 2 exploration well; SIC fault—San Isidro Crossing fault.

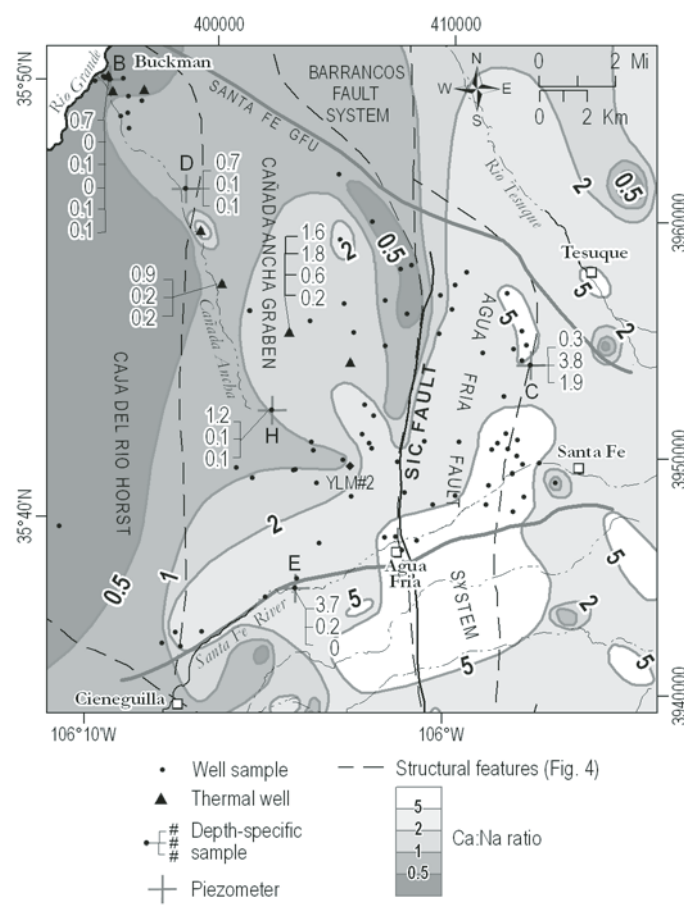


Figure 15. Ratios of Ca to Na (milliequivalents per liter, meq/L) in the Santa Fe groundwater-flow unit (GFU). The Ca:Na isocon of 2 demarcates the zone of significant Na enrichment, which aligns with the margins of the Barrancos and Agua Fria fault systems. Structural features (Fig. 4) are shown as an underlay. Stacked values show the vertical distribution of Ca:Na from depth-specific sampling. Modified from Johnson et al. (2008). YLM#2—Yates La Mesa No. 2 exploration well; SIC fault—San Isidro Crossing fault.

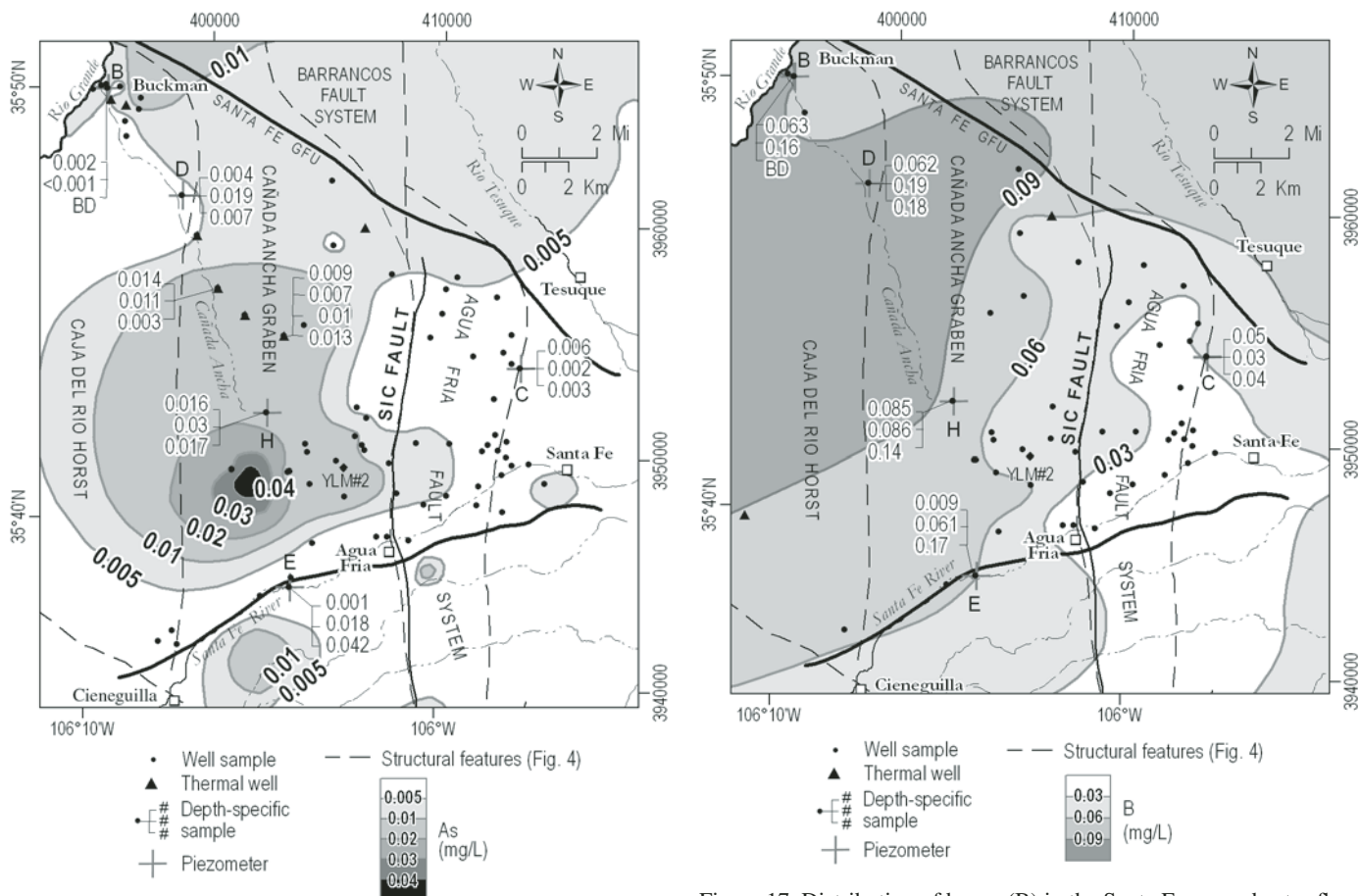


Figure 16. Distribution of arsenic (As) in the Santa Fe groundwater-flow unit (GFU) with boundaries of structural features (Fig. 4) shown as an underlay. Stacked values show the vertical distribution of As from depth-specific sampling; BD—below detection. YLM#2—Yates La Mesa No. 2 exploration well; SIC fault—San Isidro Crossing fault. Modified from Johnson et al. (2008).

or sulfate minerals. The presence of these trace elements in spatial proximity with thermal anomalies suggests that upwelling of element-laden thermal waters may affect shallow water quality in the Santa Fe GFU. The presence of this chemical assemblage—As, B, F, Li,  $\text{SO}_4^{2-}$ —in warm groundwater west of the San Isidro Crossing fault suggests that mixing of deep thermal fluids may influence water quality in the discharge zone of the Tesuque aquifer west of Santa Fe.

#### Boron and Lithium in Cieneguilla Hydrothermal Deposits

Boron is a conservative, highly mobile component of geothermal systems, and remains mobile at lower temperatures and during mixing. It is easily dissolved from volcanic or sedimentary rocks by thermal waters to become a major, nonreactive constituent of aqueous systems (Arnórsson and D’Amore, 2000; Shaw and Sturchio, 1992). Lithium is also removed from

Figure 17. Distribution of boron (B) in the Santa Fe groundwater-flow unit (GFU) with boundaries of structural features (Fig. 4) shown as an underlay. Stacked values show the vertical distribution of B from depth-specific sampling; BD—below detection. YLM#2—Yates La Mesa No. 2 exploration well; SIC fault—San Isidro Crossing fault. Modified from Johnson et al. (2008).

minerals during hydrothermal alteration to become a highly mobile constituent of high-temperature geothermal waters. Unlike B, Li is reactive and can be adsorbed by illite and other clays (Shaw and Sturchio, 1992; Hounslow, 1995), particularly clays generated by pervasive alteration (Sturchio et al., 1986) and during mixing of hot and cold waters in upflow (Arnórsson, 2000a).

Hydrothermal alteration of igneous rocks typically does not involve large changes in the chemical composition of the rock, but some elements show enrichment or depletion. Extensive studies of alteration in rhyolitic rocks in Yellowstone National Park show progressive depletion of B and enrichment of Li with increased alteration (Shaw and Sturchio, 1992). Trace elements such as As may be added to or taken from the rock so that their concentrations in altered rock differ significantly from those in fresh rock. Whole-rock analyses of samples from the Espinaso Formation and Cieneguilla basanite near the eastern margin of the Cerrillos

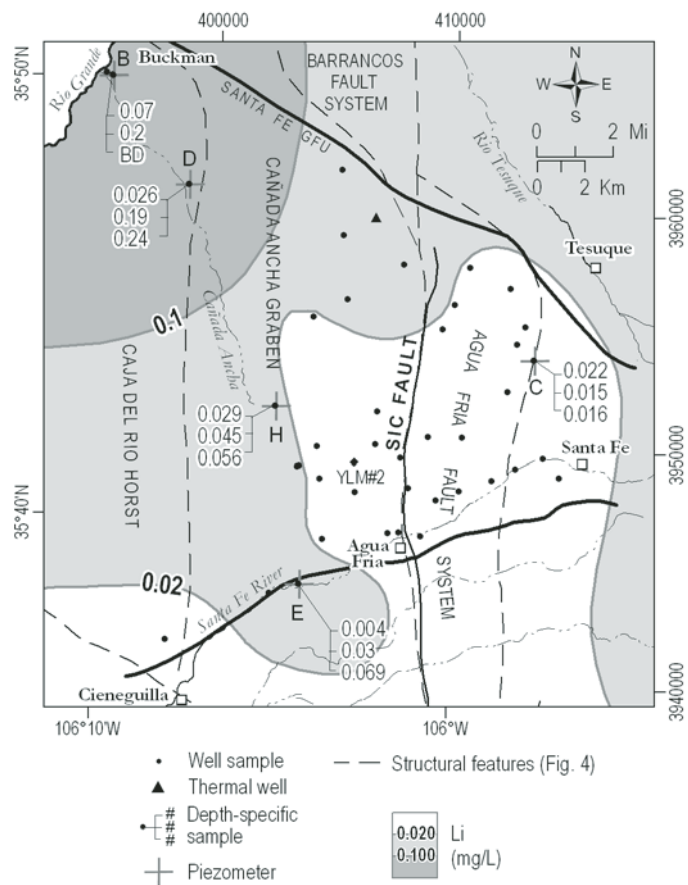


Figure 18. Distribution of lithium (Li) in the Santa Fe groundwater-flow unit (GFU) with boundaries of structural features (Fig. 4) shown as an overlay. Stacked values show the vertical distribution of Li from depth-specific sampling; BD—below detection; YLM#2—Yates La Mesa No. 2 exploration well; SIC fault—San Isidro Crossing fault. Modified from Johnson et al. (2008).

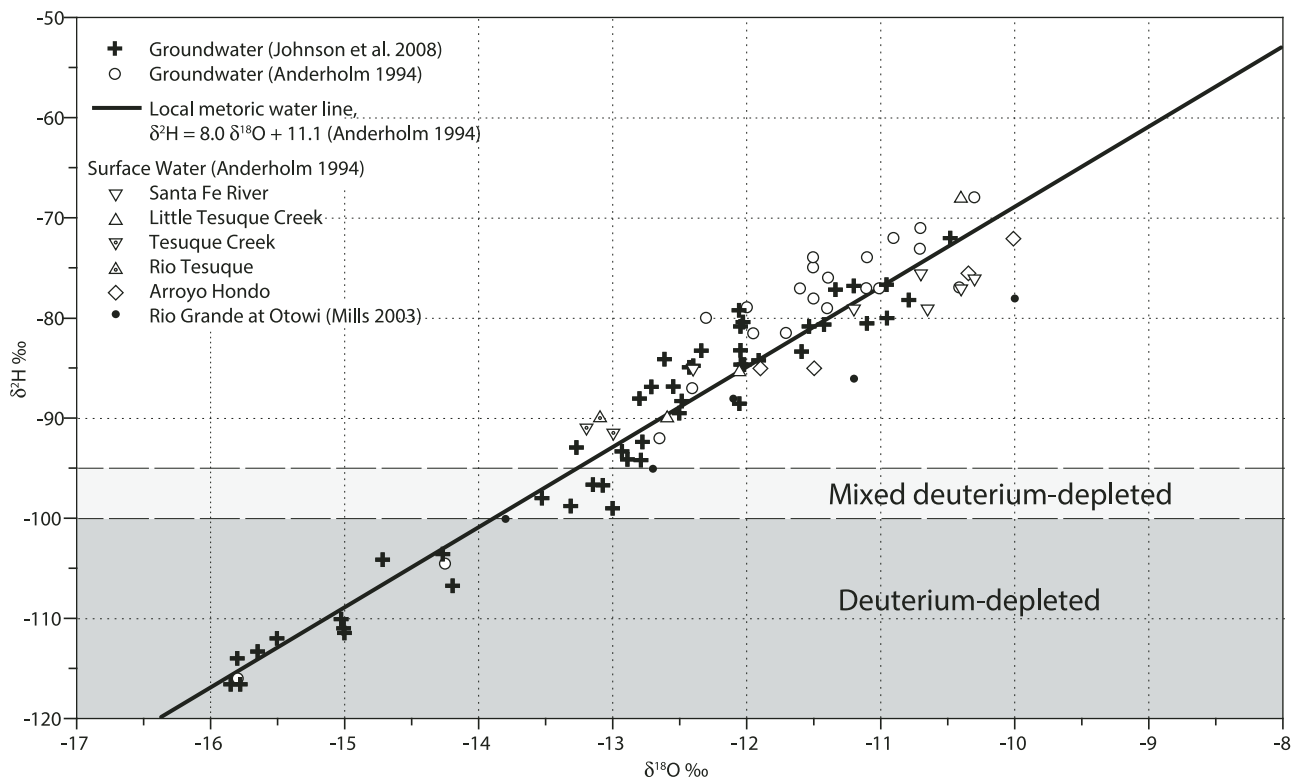


Figure 19. Values of  $\delta^2\text{H}$  and  $\delta^{18}\text{O}$  for groundwater from the Santa Fe groundwater-flow unit and surface water from the southern Es-pañola Basin in relation to the local meteoric water line of Anderholm (1994).

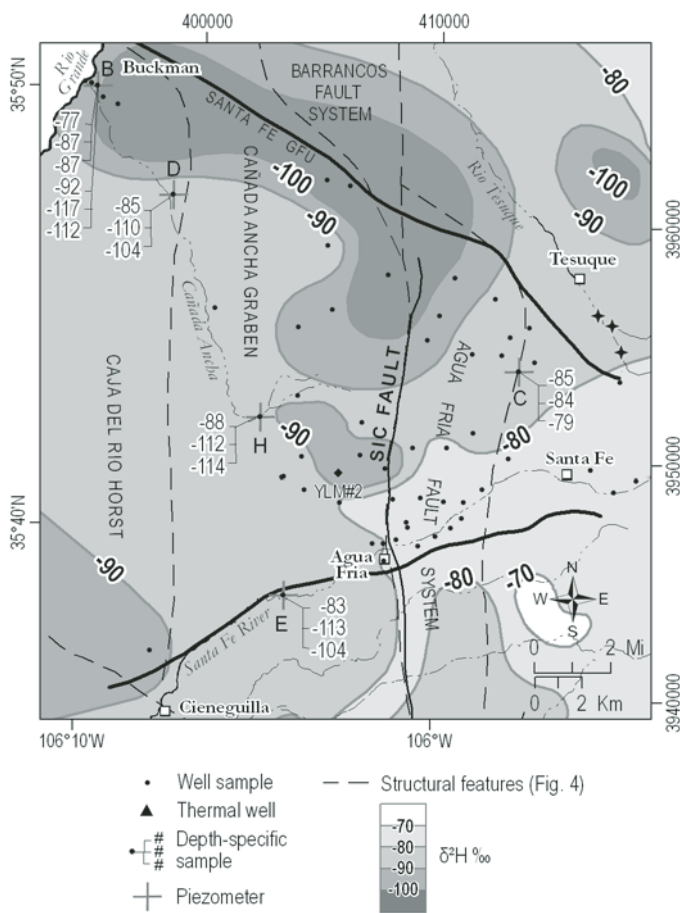


Figure 20. Distribution of deuterium-hydrogen ratios ( $\delta^2\text{H}$ ) in the Santa Fe groundwater-flow unit (GFU) with boundaries of structural features (Fig. 4) shown as an underlay. Stacked values show the vertical distribution of  $\delta^2\text{H}$  from depth-specific sampling. YLM#2—Yates La Mesa No. 2 exploration well; SIC fault—San Isidro Crossing fault. Modified from Johnson et al. (2008).

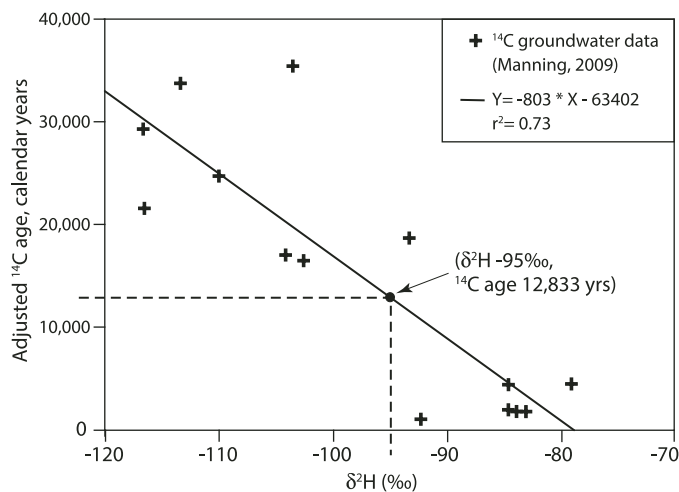


Figure 21. Regression of  $^{14}\text{C}$  ages and  $\delta^2\text{H}$  values collected by Manning (2009) from the Española Basin. A  $\delta^2\text{H}$  value of  $-95\text{\textperthousand}$  corresponds to a radiocarbon age of 12,833 years.

uplift (Fig. 8) show relatively high levels of As, Li, and trace elements Cr, U, and V (Table 7). Hydrothermally altered basalt with vein calcite (sample Ci-6) and calcite-cemented tuffaceous sediments (sample Ci-2) from the Cieneguilla basanite (Fig. 5) generally show the highest relative concentrations. Arsenic, lithium, and other elevated trace elements may have been mobilized in hydrothermal fluids then adsorbed on the surfaces of clays and metal oxides present in the hydrothermally altered rocks. Boron was not detected in the rock samples, as expected from its conservative behavior in aqueous systems.

## GEOCHEMICAL CONTROLS ON GROUNDWATER COMPOSITION

The chemical characteristics of groundwater in the Santa Fe GFU may be affected by several processes: (1) dissolution and precipitation of calcite, which raises or lowers Ca concentration; (2) Ca-Na cation exchange, which raises Na and lowers Ca concentration; (3) weathering of plagioclase feldspar, which raises Na and Ca concentrations; (4) dissolution of carbonate, gypsum, or silicate minerals; and (5) mixing with a chemically or thermally different fluid source. To evaluate the effect of rock-water interactions and possible mixing of thermal and nonthermal fluid sources on observed geochemical patterns we: (1) construct Piper and bivariate ion plots to assess Na enrichment in discharge waters; (2) calculate mineral saturation indices along a flow line; and (3) apply Mg-Li ratios to evaluate chemical and thermal evolution in samples along a flow line.

Changes in ion composition from east to west (Fig. 15) generally show shallow Ca-HCO<sub>3</sub>-type meteoric waters evolving into Ca-Na-HCO<sub>3</sub>-type recharge waters, and ultimately into Na-HCO<sub>3</sub>- or Na-Ca-HCO<sub>3</sub>-type discharge waters. The average compositions of meteoric (Rm), recharge (Rgw), and discharge (Dgw) waters (Table 10) define geochemical and flow zones (Fig. 23) for the Santa Fe GFU. Chemical evolution from recharge to discharge zones involves enrichment of TDS, Na, K, HCO<sub>3</sub>, SO<sub>4</sub>, and SiO<sub>2</sub>, an increase in temperature and pH, and depletion of Ca, Mg, and Cl. Discharge-zone groundwater exhibits a 14-fold increase in Na and a 16-fold increase in Na-to-Cl ratio, relative to shallow meteoric groundwater. We analyze groundwater samples representing each geochemical zone along a southeast-to-northwest flow line (Fig. 23) to assess which processes control chemical composition.

## Assessing Na Enrichment

A Piper diagram of major-ion chemistry (Fig. 24) shows a trend between Ca-Mg-HCO<sub>3</sub> waters and Na-HCO<sub>3</sub> waters, which documents replacement of Ca and Mg in solution by Na, with little change in anion content. The Na-enrichment trend is consistent with cation exchange. The Ca-type groundwater is generally limited to shallow wells near the Santa Fe River, where it is similar in composition to river water. Waters in the Santa Fe River recharge zone are shown in a shaded field in

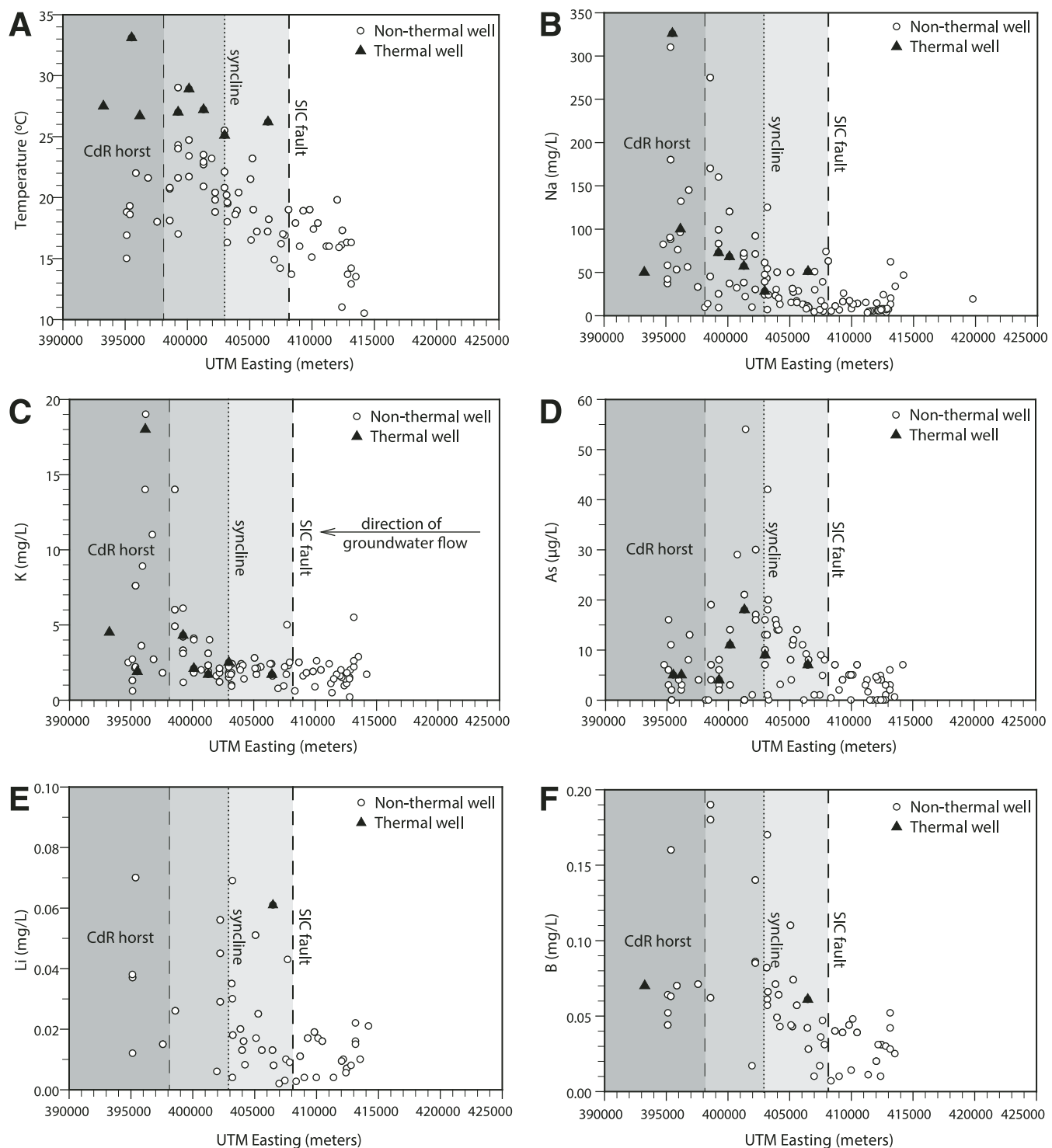


Figure 22. Spatial plots of chemical parameters in the Santa Fe groundwater-flow unit versus UTM easting: (A) temperature, (B) sodium, (C) potassium, (D) arsenic, (E) lithium, and (F) boron. Plots illustrate changes in thermal, ion, and trace-element parameters along generalized east-to-west flow paths that cross north-trending structural features: the San Isidro Crossing (SIC) fault, the basin syncline, and the Cerillos uplift or Caja del Rio (CdR) horst.

**TABLE 9. SPEARMAN RANK ORDER CORRELATION FOR CHEMICAL PARAMETERS IN GROUNDWATER FROM THE SANTA FE GFU**

	B	Ca	Cl	Cr	F	$^{2}\text{H}/\text{H}$	K	Li	Mo	Na	$\text{SiO}_2$	$\text{SO}_4$	Sr	T (°C)	U	V		
As	0.67	-0.53	-0.39	0.54	0.36	-0.32		0.40	0.5	0.42		0.32	0.32	0.31	0.27	0.64	As	
B		-0.62			0.55	0.42	-0.50	0.54	0.88	0.69	0.82	0.31	0.66	0.58	0.63	0.90	0.38	B
Ca			0.40		-0.48	0.38		-0.49	-0.46	-0.60		-0.35		-0.38		-0.39	Ca	
Cl				-0.23												-0.45	Cl	
Cr					0.38	-0.33	0.26	0.31	0.42	0.51		0.35		0.40	0.56	0.50	Cr	
F						0.29	0.54	0.59	0.62		0.51			0.52			F	
$^{2}\text{H}/\text{H}$							-0.53	-0.33	-0.52		-0.59		-0.67	-0.50			$^{2}\text{H}/\text{H}$	
K							0.57	0.45	0.61	0.38	0.52	0.63	0.48	0.35			K	
Li								0.59	0.90	0.39	0.80	0.58	0.55	0.89			Li	
Mo									0.62		0.52	0.28		0.70			Mo	
Na										0.27	0.72	0.46	0.70	0.39	0.25		Na	
$\text{SiO}_2$											0.34			0.33			$\text{SiO}_2$	
$\text{SO}_4$											0.59	0.59					$\text{SO}_4$	
Sr											0.38	0.61					Sr	
T (°C)												-0.30					T (°C)	
U													0.29				U	

blank cells—no significant correlation, P value > 0.05

correlation coefficient > ± 0.40

thermal–water tracers—correlation coefficient > 0.40

GFU—groundwater-flow unit

Figure 24. Location of samples relative to the San Isidro Crossing fault (east or west) illustrates that chemical evolution of Ca-type waters toward the Na apex develops with westward groundwater flow across the Agua Fria fault system and the San Isidro Crossing fault. Sodium excess exists primarily west of the fault in the discharge zone of the Santa Fe GFU. All thermal wells are located in the discharge zone and generally produce Na-type water with  $\text{SO}_4$  enrichment (Fig. 24), which indicates a process other than ion exchange, such as mixing with a different sulfate-rich water or gypsum dissolution.

Although the Piper diagram demonstrates Na enrichment consistent with a cation exchange reaction, weathering of Na-rich aluminosilicates may also contribute to Na excess. To assess the relative importance of cation exchange versus other rock–water weathering and dissolution reactions, we use bivariate plots of  $(\text{Ca} + \text{Mg})$ ,  $(\text{HCO}_3 + \text{SO}_4)$ , and  $(\text{Na} - \text{Cl})$  (Fig. 25). Possible contributions of  $\text{Ca}^{2+}$  and  $\text{Mg}^{2+}$  from dissolution of calcite, dolomite, gypsum, and anhydrite are evaluated by subtracting equivalent concentrations of  $\text{HCO}_3^-$  and  $\text{SO}_4^{2-}$ , and

contributions of  $\text{Na}^+$  from halite dissolution are evaluated by subtracting equivalent concentrations of  $\text{Cl}^-$  (Nkotagu, 1996; McLean and Jankowski, 2000). In a plot of  $(\text{Ca} + \text{Mg})$  minus  $(\text{HCO}_3 + \text{SO}_4)$  versus  $(\text{Na} - \text{Cl})$  (Fig. 25A), water undergoing ion exchange falls along a line with a slope of -1 (Jankowski et al., 1998). Water samples from the Santa Fe GFU plot very close to a line with a -1 slope ( $r^2 = 0.99$ ) indicating that ion exchange is the primary source of Na enrichment. Plots of Ca, Mg, and  $(\text{Ca} + \text{Mg})$  versus  $(\text{Na} - \text{Cl})$  (Fig. 25B) indicate which cation(s), Ca and/or Mg, dominate the ion-exchange reaction. Calcium provides the best fit of the three plots ( $r^2 = 0.37$ ) indicating that Na exchange for Ca, as opposed to Mg, controls water composition in the Santa Fe GFU.

#### Mineral Saturation Indices in Recharge and Discharge Waters

Mineral saturation was evaluated in water samples along an east-to-west flow path (Fig. 26) to better understand

**TABLE 10. AVERAGE CHEMICAL COMPOSITION OF RECHARGE AND DISCHARGE WATERS IN THE SANTA FE GFU**

Zone	n	TDS	pH	Na	K	Ca	Mg	$\text{HCO}_3$	Cl	$\text{SO}_4$	Na/Cl	Average concentrations*		
												SI	$\text{SiO}_2$	Temp (°C)
Rm, meteoric groundwater	11	172	8.0	7	1.0	42	4.0	128	8.0	11	1	-0.016	19	15
Rgw, groundwater recharge zone	10	250	8.1	20	2.0	29	3.0	133	5.0	14	6	0.206	19	17
Dgw, groundwater discharge zone	10	357	8.3	93	4.2	25	3.9	299	5.3	26	16	0.466	26	22

\*TDS, ions, and  $\text{SiO}_2$  in mg/L; pH in pH units; Na/Cl ratio in meq/L; SI = saturation index; GFU—groundwater-flow unit.

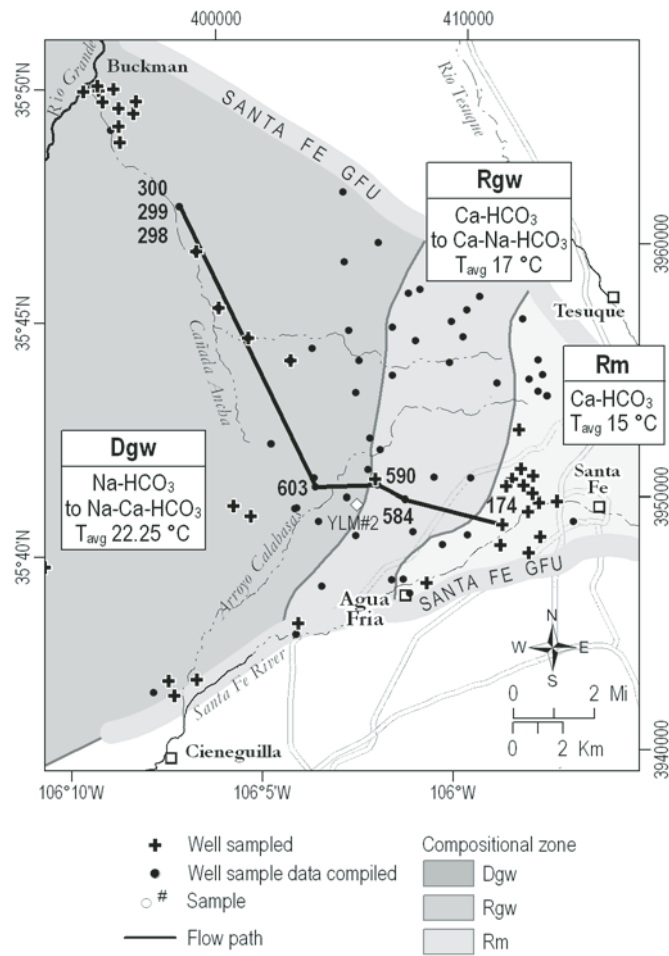


Figure 23. Index map of sample sites, compositional zones, and flow pathways utilized in geochemical analyses (Figs. 26 and 27). GFU—groundwater-flow unit; YLM#2—Yates La Mesa No. 2 exploration well;  $T_{\text{avg}}$ —average water temperature; Rm—meteoric groundwater; Rgw—groundwater recharge zone; Dgw—groundwater discharge zone.

thermodynamic controls on groundwater composition and mineral equilibrium in recharge and discharge waters. The modeled flow line (Fig. 23) begins with meteoric recharge water (well EB-174) and continues to piezometer D in the discharge zone. All three completion intervals of piezometer D (EB-298, EB-299, EB-300) are analyzed to assess aquifer stratification and mixing. Saturation indices for carbonate, silicate, and sulfate minerals were determined using the speciation modeling application in PHREEQC for Windows version 2.14.3.2411 (Parkhurst and Appelo, 1999).

Calcite and aragonite saturation (Fig. 26A) increases steadily from near equilibrium (saturation index [SI] = 0.06, EB-174) at recharge to oversaturation (SI = 0.51–0.64) in the discharge zone (EB-603, EB-298). The vertical trend in piezometer D shows a linear decrease in carbonate saturation from the deep (EB-298) to shallow (EB-300) intervals. The observed trends indicate that, in addition to ion exchange, pre-

cipitation of carbonate minerals also contributes to Ca and Mg depletion in the discharge zone. However, even with multiple sinks for Ca and Mg, we observe oversaturation with respect to carbonates, probably because of long groundwater residence times and input of Ca and Na from progressive dissolution of feldspars. The upward decrease in carbonate saturation in piezometer D demonstrates mixing of deep Ca-poor waters and shallow Ca-rich waters near the water table. The implication of these trends is that Na enrichment in the discharge zone may also be affected by feldspar weathering.

In low-temperatures systems, feldspar weathering is the primary control for silica saturation. Saturation indices for silicate minerals (Fig. 26B) show that quartz silica is oversaturated but relatively stable along the flow line, whereas chalcedony is near equilibrium throughout the system. Chrysotile is undersaturated due to limited Mg availability. Average silica concentration increases from 19 mg/L in the recharge zone to 26 mg/L in the discharge zone (Table 10). Elevated silica concentrations (>30 mg/L) occur in several wells and piezometers near Buckman. While dissolved silica in low-temperature waters typically derives from weathering of silicate minerals, silica oversaturation and concentrations exceeding 30 mg/L (0.5 mmol/L) suggest that an additional hydrothermal source (Hounslow, 1995) may influence both deep and shallow groundwaters near Buckman.

Limited sulfate availability in recharge waters holds barite near equilibrium along most of the flow line and triggers barium excess as noted in Johnson et al. (2008). However, barite is oversaturated at depths of 400 and 740 m (EB-299 and EB-298, piezometer D) in the discharge zone (Fig. 26C). Gypsum and anhydrite are consistently undersaturated, consistent with the lack of these minerals in the Tesuque Formation, but show a slight increase in saturation along the flow line. An increase in sulfate-mineral saturation in the discharge zone is consistent with  $\text{SO}_4^{2-}$  enrichment in discharge-zone thermal wells demonstrated in the Piper diagram (Fig. 24).

## Thermal Evolution of Groundwater in the Santa Fe GFU

We evaluate the thermal evolution of groundwater along a flow line in the Santa Fe GFU using Mg/Li ratios and groundwater temperature. Concentrations of Mg in subsurface waters are known to decrease with increasing temperature, while Li concentrations increase with increasing temperature (Kharaka and Mariner, 1989), making the Mg/Li ratio a sensitive indicator of temperature and a reliable geothermometer for low-temperature thermal systems. A plot of Mg/Li ratio versus temperature (Fig. 27) constructed for wells along a flow line between shallow meteoric recharge (EB-174) and deep groundwater discharge (EB-299) shows a strong linear relation between low Mg/Li ratios and elevated temperatures. Well samples along the flow line fall sequentially on a regression line with a correlation coefficient ( $r$ ) of 0.94. The strong linear correlation indicates that the Mg-Li geothermometer should be

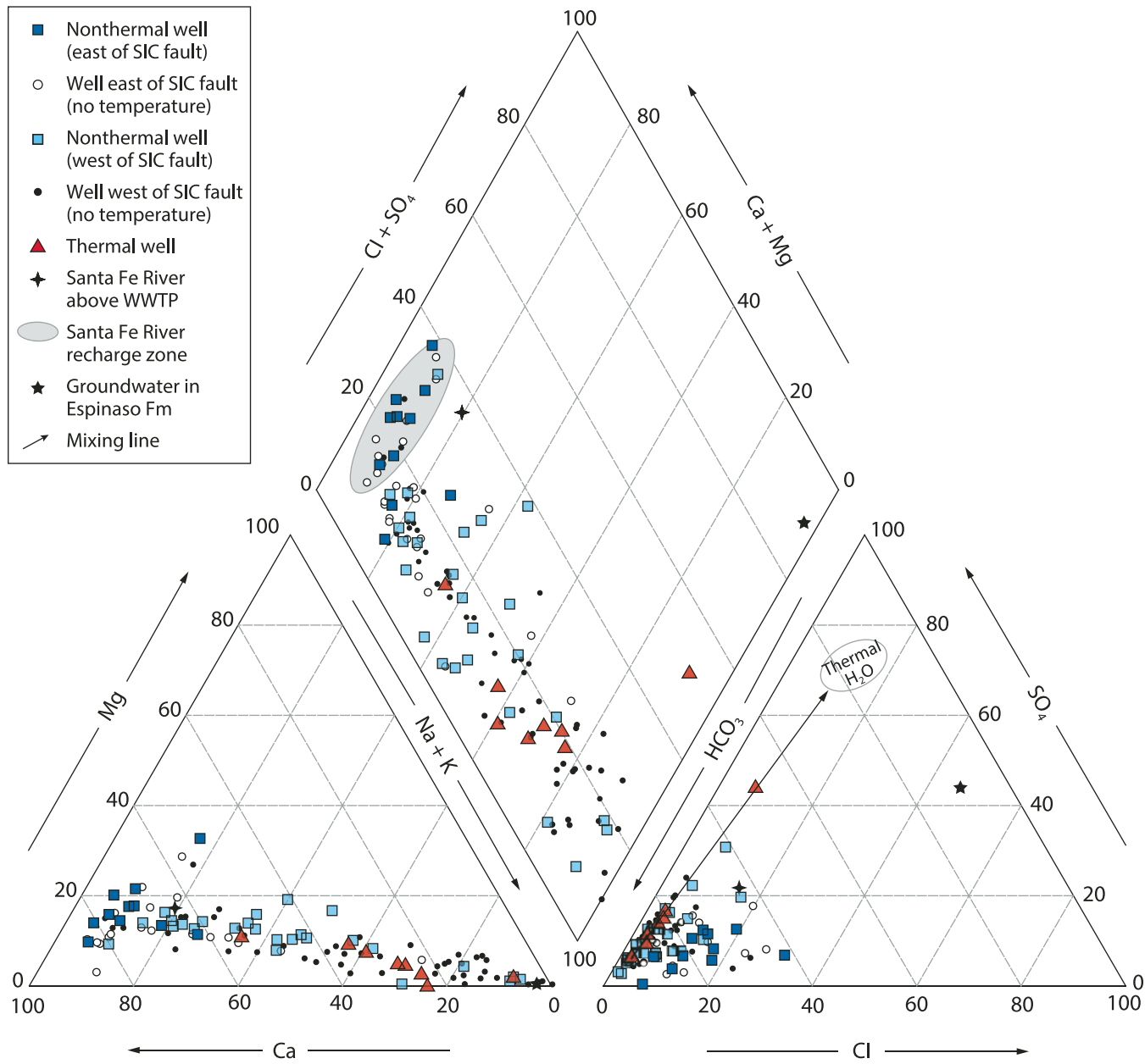


Figure 24. Piper diagram displaying percentages of major cations and anions (computed in milliequivalents per liter [meq/L]) (after Piper, 1944) in samples from the Santa Fe ground-water-flow unit. Symbols indicate sample location east (upgradient) or west (downgradient) of the San Isidro Crossing (SIC) fault and thermal status of the well water (see Fig. 13 and text discussion). Thermal wells shown in red triangles are all located west of the San Isidro Crossing fault. Ca-Mg recharge waters (gray zone) evolve along a westward flow path toward Na-rich discharge waters. WWTP—wastewater treatment plant.

a reliable gauge of temperatures for deep circulating ground-water in the Santa Fe GFU.

The Mg-Li chemical geothermometer provides estimates of thermal reservoir temperatures based on the chemical composition of discharging hot or cold springs or well samples. Kharaka and Mariner (1989) demonstrated superior results for the Mg-Li geothermometer over other methods when applied to well samples from geothermal and oil-field waters with a temperature range of

33 °C to 170 °C, and suggested the geothermometer could be used successfully for all subsurface waters, giving the best results for low-temperature systems (30 °C to 70 °C). Whereas other chemical geothermometers relying on Na, K, Ca, or silica give poor results in low-temperature systems where thermal fluids mix with surface or other underground waters in upflow zones (Fournier, 1981; Arnórsson, 2000b), the Mg-Li geothermometer appears much more robust, possibly because fast exchange reactions involving

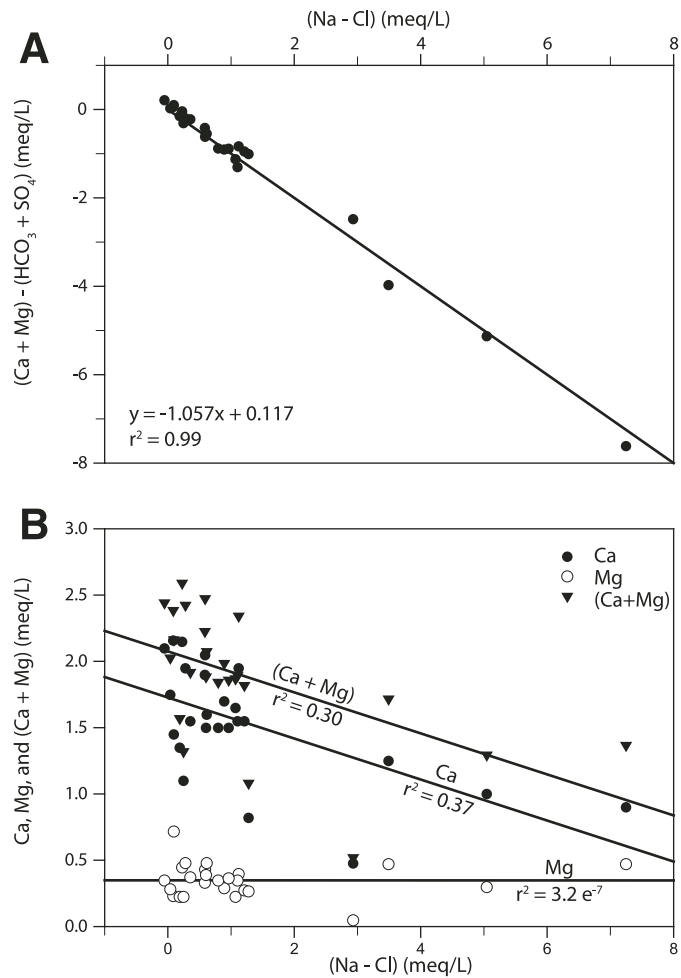


Figure 25. Bivariate plots assessing ion contributions in milliequivalents per liter (meq/L) from dissolution of calcite, dolomite, gypsum, anhydrite, and halite: (A)  $(\text{Ca} + \text{Mg}) - (\text{HCO}_3 + \text{SO}_4)$  versus  $(\text{Na} - \text{Cl})$ ; and (B) Ca, Mg, and  $(\text{Ca} + \text{Mg})$  versus  $(\text{Na} - \text{Cl})$ . This method (after Jankowski et al., 1998) evaluates the relative importance of cation exchange versus weathering and dissolution reactions in causing Na excess.

clay minerals, rather than temperature-dependent equilibrium reactions, control the Mg-Li content (Kharaka and Mariner, 1989).

We apply the following equation for the Mg-Li geothermometer (Kharaka and Mariner, 1989) to well samples from the Santa Fe GFU:

$$T_{\text{Mg}-\text{Li}} = \frac{2,200}{\log \left( \frac{\sqrt{C_{\text{Mg}}}}{C_{\text{Li}}} \right) + 5.47} - 273, \quad (1)$$

where  $C$  is the concentration in mg/L of the subscripted cation, and  $T$  is temperature in °C. Results for the Mg-Li geothermometer characterize the temperature distribution associated with deep circulating groundwater beneath the Santa Fe GFU. Estimated

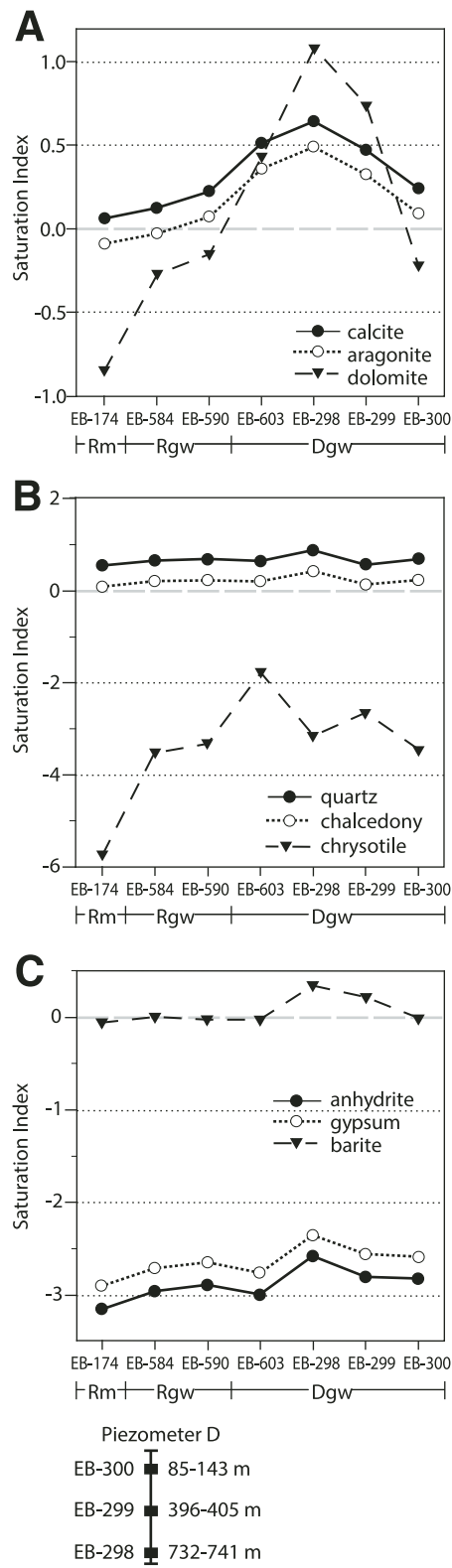


Figure 26. Saturation indices for (A) carbonate, (B) silicate, and (C) sulfate minerals along an east-to-west flow path (Fig. 23). Rm—meteoric groundwater; Rgw—groundwater recharge zone; Dgw—groundwater discharge zone.

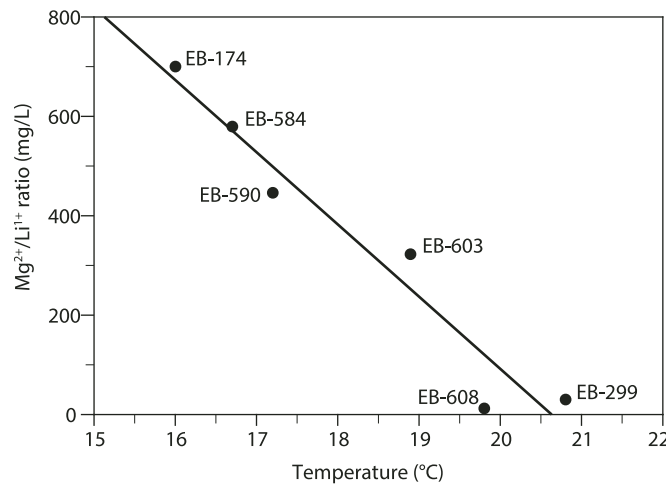


Figure 27. Mg/Li ratio versus temperature along a groundwater flow path (Fig. 23).

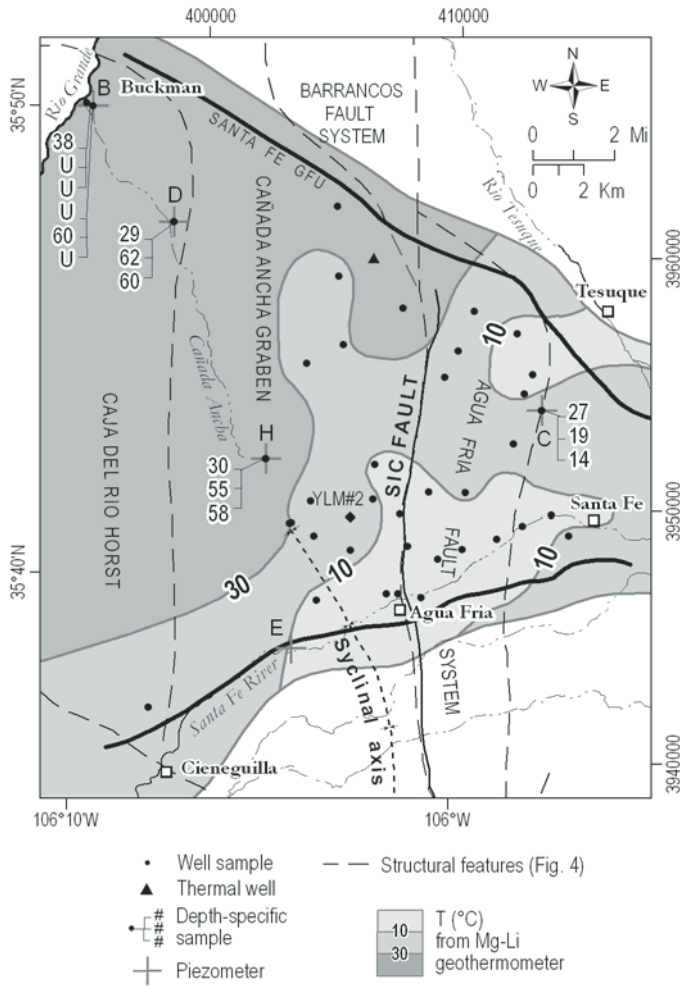


Figure 28. Spatial distribution of deep reservoir temperatures in the Santa Fe groundwater-flow unit (GFU), predicted from Mg-Li geothermometry. U—undetermined; YLM#2—Yates La Mesa No. 2 exploration well; SIC fault—San Isidro Crossing fault.

reservoir temperatures range from 62 °C to <0 °C and delineate a heat-flow distribution pattern (Fig. 28) similar to measured groundwater temperatures (Fig. 9) and Ca-Na content (Fig. 15). The highest temperatures (30 °C to 60 °C) align with the western margin of the Barrancos fault system and along the transition between the Cañada Ancha graben and Caja del Rio horst. Temperatures of <10 °C estimated for shallow recharge waters adjacent to the Santa Fe River are below the temperature range for the geothermometer. Results of Mg-Li geothermometry support the conceptual model that upflow and mixing of thermal waters from low-temperature geothermal systems, coincident with major rift-related fault systems, locally affect both the thermal and chemical quality of shallow groundwater in this discharge zone of the Tesuque aquifer system.

## SUMMARY OF FINDINGS

Measurements of chemical, isotopic, and thermal properties of groundwater from 120 wells were used to examine links between groundwater flow, temperature, water chemistry, and major fault structures in the southeastern Española Basin. Study focused on a single groundwater-flow unit (GFU) of the Tesuque aquifer system near Santa Fe, where groundwater flows east to west across several north-trending rift structures. Synthesis of hydrologic, thermal, geochemical, isotopic, and structural data from the Santa Fe GFU resulted in delineation of recharge and discharge areas, mapping of the spatial extent of chemical and thermal properties of groundwater, and demonstration of the spatial correspondence between the chemical and thermal properties and major rift structures. The chemical and thermal data set improves characterization of hydrochemical processes and enhances understanding of the Tesuque groundwater system. Important findings include:

1. The chemical composition and thermal properties of recharge from the Sangre de Cristo Mountains and the Santa Fe River change rapidly along an east-to-west flow line from cool (<15 °C) Ca-HCO<sub>3</sub> waters to warm (>19 °C) Na or mixed Na-Ca-HCO<sub>3</sub> waters west of the San Isidro Crossing fault. The discharge zone overlying the Cañada Ancha graben and Caja del Rio horst is delineated by the spatial extent of dominantly upward hydraulic gradients and warm, Na-rich water. Sodium enrichment along the flow line results primarily from Na-Ca ion exchange, but feldspar weathering and mixing with a deep thermal source of SO<sub>4</sub>-rich water also affects shallow-water chemistry.
2. Eight thermal wells with anomalously warm temperatures are identified in the discharge zone of the Santa Fe GFU. Most are located in close proximity to the faulted boundary between the Cañada Ancha graben and Caja del Rio horst. Thermal wells have discharge temperatures from 25.1 to 33.1 °C and display a prominent trend of SO<sub>4</sub> enrichment. Spearman coefficients indicate

- a strong, positive covariance among several trace elements and thermal water indicators (F, B, Li, As, SO<sub>4</sub>, and temperature).
3. Thermal mapping based on bottomhole temperatures in wells establishes a regional trend in thermal gradients. Results demonstrate a normal thermal gradient of ~25 °C/km near Santa Fe and a thermal gradient high (> 40 °C/km) coincident with the Caja del Rio horst. The magnitude of thermal gradients over the horst is sufficient to indicate geothermal activity at depth.
  4. Spatial coincidence of chemical, temperature, and thermal-gradient anomalies with the eastern margin of the Caja del Rio horst suggests that intersecting chemical and thermal anomalies have a structural control.
  5. Whole-rock analyses of hydrothermal deposits from the Espinaso Formation and Cieneguilla basanite near the eastern margin of the Cerrillos uplift show relatively high levels of As, Li, and other trace elements, indicating mobilization of these elements in hydrothermal fluids. Absence of boron in the deposits is consistent with its conservative behavior in aqueous systems.
  6. The suitability of the Mg-Li geothermometer in the Santa Fe GFU is demonstrated by strong linear correlation between Mg/Li ratios and discharge temperatures in wells. The geothermometer is applied to well samples to estimate reservoir temperatures for thermal waters contributing to chemical and thermal anomalies in the discharge zone. Results show a temperature distribution associated with deep circulating groundwater. The highest temperatures (30 °C to 60 °C) align with the western margin of the Barrancos fault system and along the transition between the Cañada Ancha graben and Caja del Rio horst.

In summary, hydrologic, geochemical, thermal, and structural data are used to construct a conceptual model of the Tesuque aquifer system near Santa Fe. The Caja del Rio horst constricts westward groundwater flow and creates a forced convection system that drives upward flow and discharge of warm, Na-rich groundwater through the Tesuque Formation in the western half of the Cañada Ancha graben. The Barrancos fault system and major faults bounding the Cañada Ancha graben and Caja del Rio horst focus vertical flow of deep, NaSO<sub>4</sub> thermal waters, which also contribute to chemical anomalies and thermal disturbances in the shallow Tesuque aquifer.

## ACKNOWLEDGMENTS

The authors thank the numerous individual landowners near Santa Fe who allowed access to their wells and the numerous professional consultants and agency scientists who generously shared their data. John Shomaker & Associates, Inc., Balleau Groundwater and Associates, Inc., Glorieta Geoscience, Inc., and many individuals from the City of Santa Fe, Santa Fe County, and the New Mexico Environment Department (Solid Waste and UST Bureaus) provided access to both wells and

data. Special thanks go to Claudia Borchert, Casey Cook, Dennis Cooper, Jim Corbin, Paul Drakos, and John Shomaker for their many contributions.

We thank our colleagues with the New Mexico Bureau of Geology and Mineral Resources (New Mexico Tech) for assistance in many tasks: Brigitte Kludt for crafting illustrations, Stacy Timmons in field sampling and data management, Bonnie Frey in laboratory analysis, Gretchen Hoffman in data management, and Talon Newton, Paul Bauer, and Greer Price in manuscript preparation. We thank Tien Grauch, Sean Connell, Andrew Manning, Paul Bauer, Marshall Reiter, Adam Read, and J. Michael Timmons for sharing their knowledge about the geology and hydrology of the basin. The manuscript was improved significantly at several stages by the constructive reviews and insight of colleagues Laura Crossey, Talon Newton, Jim Witcher, Jonathan Caine, and Paul Bauer. This work was supported in part by funds from the New Mexico Office of the State Engineer and the Aquifer Mapping Program at New Mexico Bureau of Geology and Mineral Resources, New Mexico Tech.

## REFERENCES CITED

- Anderholm, S.K., 1994, Ground-Water Recharge near Santa Fe, North-Central New Mexico: U.S. Geological Survey Water-Resources Investigations Report 94-4078, 68 p.
- Anderson, M.P., 2005, Heat as a ground water tracer: *Ground Water*, v. 43, p. 951–968, doi:10.1111/j.1745-6584.2005.00052.x.
- Arnórsson, S., 2000a, Reactive and conservative components, in Arnórsson, S., ed., Isotopic and Chemical Techniques in Geothermal Exploration, Development and Use: Vienna, International Atomic Energy Agency, p. 40–48.
- Arnórsson, S., 2000b, Mixing process in upflow zones and mixing models, in Arnórsson, S., ed., Isotopic and Chemical Techniques in Geothermal Exploration, Development and Use: Vienna, International Atomic Energy Agency, p. 200–211.
- Arnórsson, S., and D'Amore, F., 2000, The source of chemical and isotopic components in geothermal fluids, in Arnórsson, S., ed., Isotopic and Chemical Techniques in Geothermal Exploration, Development and Use: Vienna, International Atomic Energy Agency, p. 66–72.
- Balleau Groundwater, Inc., 2008, Unpublished consultant's subdivision report prepared for Rancho Viejo de Santa Fe, Inc.
- Bauer, P.W., Ralser, S., Daniel, C., and Ilg, B., 1997, Geology of the McClure Reservoir 7.5-Minute Quadrangle: New Mexico Bureau of Geology and Mineral Resources Open-File Geologic Map 7, scale 1:24,000.
- Biehler, S., Ferguson, J., Baldridge, W.S., Jiracek, G.R., Aldern, J.L., Martinez, M., Fernandez, R., Romo, J., Gilpin, B., Braile, L.W., Hersey, D.R., Luyendyk, B.P., and Aiken, C.L.V., 1991, A geophysical model of the *Española* Basin, Rio Grande rift, New Mexico: *Geophysics*, v. 56, p. 340–353, doi:10.1190/1.1443048.
- Chapin, C.E., and Cather, S.M., 1994, Tectonic setting of the axial basins of the northern and central Rio Grande rift, in Keller, G.R., and Cather, S.M., eds., Basins of the Rio Grande Rift: Structure, Stratigraphy and Tectonic Setting: Geological Society of America Special Paper 291, p. 5–25.
- Domenico, P.A., and Palciauskas, V.V., 1973, Theoretical analysis of forced convective heat transfer in regional groundwater flow: *Geological Society of America Bulletin*, v. 84, p. 3803–3814, doi:10.1130/0016-7606(1973)84<3803:TAOFCH>2.0.CO;2.
- Ellis, A.J., and Mahon, W.A.J., 1977, Chemistry and Geothermal Systems: New York, Academic Press, 392 p.
- Erskine, D.W., and Smith, G.A., 1993, Compositional characterization of volcanic products from a primarily sedimentary record—The Oligocene Espinaso Formation, north-central New Mexico: *Geological Society of America Bulletin*, v. 105, p. 1214–1222, doi:10.1130/0016-7606(1993)105<1214:CCOVPF>2.3.CO;2.
- Fournier, R.O., 1981, Application of water geochemistry to geothermal exploration and reservoir engineering, in Rybach, L., and Muffler, L.J.P., eds.,

- Geothermal Systems: Principles and Case Histories: New York, John Wiley & Sons, 359 p.
- Fridrich, C.J., Dudley, W.W., Jr., and Stuckless, J.S., 1994, Hydrogeological analysis of the saturated-zone ground-water system under Yucca Mountain, Nevada: *Journal of Hydrology* (Amsterdam), v. 154, p. 133–168, doi:10.1016/0022-1694(94)90215-1.
- Galusha, T., and Blick, J.C., 1971, Stratigraphy of the Santa Fe Group, New Mexico: *Bulletin of the American Museum of Natural History*, v. 144, 127 p.
- Goff, F., Laughlin, A., Aldrich, J., Ander, M., Arney, B., Decker, E., Gardner, J., Heiken, G., Kron, A., LaDelfe, C., Pettitt, R., and Shannon, S., 1981, Hot dry rock geothermal prospects: *Geothermal Resources Council Transactions*, v. 5, p. 173–176.
- Grauch, V.J.S., and Hudson, M.R., 2007, Guides to understanding the aeromagnetic expression of faults in sedimentary basins—Lessons learned from the central Rio Grande rift, New Mexico: *Geosphere*, v. 3, p. 596–623, doi:10.1130/GES00128.1.
- Grauch, V.J.S., Phillips, J.D., Koning, D.J., Johnson, P.S., and Bankey, V., 2009, Geophysical Interpretations of the Southern Española Basin, New Mexico, That Contribute to Understanding Its Hydrogeologic Framework: U.S. Geological Survey Professional Paper 1761, 88 p.
- Harder, V., Morgan, P., and Swanberg, C.A., 1980, Geothermal resources in the Rio Grande rift: Origins and potential: *Geothermal Resources Council Transactions*, v. 4, p. 61–64.
- Hounslow, A.W., 1995, Water Quality Data Analysis and Interpretation: New York, CRC Lewis Publishers, 379 p.
- Jankowski, J., Acworth, R.I., and Shekarforoush, S., 1998, Reverse ion exchange in a deeply weathered porphyritic dacite fracture aquifer system, Yass, New South Wales, Australia, in Arehart, G.B., and Hulston, J.R., eds., *Proceedings, Ninth International Symposium on Water-Rock Interaction*, Taupo, New Zealand, March 1998: Rotterdam, A.A. Balkema, p. 243–246.
- John Shomaker & Associates, Inc., 2003, Well Report: Drilling, Construction, and Testing of Buckman Well No. 9, City of Santa Fe: unpublished report to the City of Santa Fe.
- John Shomaker & Associates, Inc., 2004, Well Report: Buckman Wells No. 10 through 13, City of Santa Fe, New Mexico: unpublished report to the City of Santa Fe.
- Johnson, P.S., 2009, Water-Level Elevation Contours and Groundwater-Flow Conditions (2000 to 2005) for the Santa Fe Area, Southern Española Basin, New Mexico: New Mexico Bureau of Geology and Mineral Resources Open-File Report 520 (CD-ROM).
- Johnson, P.S., Koning, D.J., Timmons, S.W., and Felix, B., 2008, Geochemical Characterization of Groundwater in the Southern Española Basin, Santa Fe County, New Mexico: New Mexico Bureau of Geology and Mineral Resources Open-File Report 511, 49 p.
- Kautz, P.F., Ingersoll, R.V., Baldridge, W.S., Damon, P.E., and Shafiqullah, M., 1981, Geology of the Espinaso Formation (Oligocene), north-central New Mexico: *Geological Society of America Bulletin*, v. 92, Part I, p. 980–983, and Part II, p. 2318–2400.
- Kharaka, Y.K., and Mariner, R.H., 1989, Chemical geothermometers and their application to formation waters from sedimentary basins, in Naeser, N.D., and McCulloch, T.H., eds., *Thermal History of Sedimentary Basins*: New York, Springer-Verlag, p. 99–117.
- Kilty, K., and Chapman, D.S., 1980, Convective heat transfer in selected geologic situations: *Ground Water*, v. 18, p. 386–394, doi:10.1111/j.1745-6584.1980.tb03413.x.
- Koning, D.J., and Hallett, R.B., 2001 (orig. publ. 2000), Geologic Map of the Turquoise Hill 7.5-Minute Quadrangle, Santa Fe County, New Mexico: New Mexico Bureau of Geology and Mineral Resources Open-File Geologic Map 41, scale 1:24,000.
- Koning, D.J., and Johnson, P.S., 2006, Locations and textural contrasts of Tesuque Formation lithostratigraphic units in the southern Española Basin, NM, and hydrogeologic implications, in McKinney, K.C., ed., *Proceedings, Española Basin Workshop*, 5th, Santa Fe, March 2006: U.S. Geological Survey Open-File Report 2006-1134, p. 24.
- Koning, D.J., and Maldonado, F., 2003 (orig. publ. 2001), Geologic Map of the Horcado Ranch 7.5-Minute Quadrangle, Santa Fe County, New Mexico: New Mexico Bureau of Geology and Mineral Resources Open-File Geologic Map 44, scale 1:24,000.
- Koning, D.J., and Read, A.S., 2010, Geologic Map of the Southern Española Basin: New Mexico Bureau of Geology and Mineral Resources Open-File Report 531, scale 1:48,000 (CD-ROM).
- Koning, D.J., Smith, G., Lyman, J., and Paul, P., 2004, Lithosome S of the Tesuque Formation: Hydrostratigraphic and tectonic implications of a newly delineated lithosome in the southern Española Basin, New Mexico, in Hudson, M., ed., *Proceedings, Española Basin Workshop*, 3rd, Santa Fe, March 2004: U.S. Geological Survey Open-File Report 2004-1093, p. 17.
- Koning, D.J., Broxton, D., Sawyer, D., Vaniman, D., and Shomaker, J., 2007, Surface and subsurface stratigraphy of the Santa Fe Group near White Rock and the Buckman areas of the Española Basin, north-central New Mexico, in Kues, B., Kelley, S., and Leuth, V., eds., *Geology of the Jemez Region II: New Mexico Geological Society Guidebook 58*, p. 209–224.
- Koning, D.J., Grauch, V.J.S., Connell, S.D., Ferguson, J., McIntosh, W., Slate, J.L., Wan, E., and Baldridge, W.S., 2013, this volume, Structure and tectonic evolution of the eastern Española Basin, Rio Grande rift, north-central New Mexico, in Hudson, M.R., and Grauch, V.J.S., eds., *New Perspectives on Rio Grande Rift Basins: From Tectonics to Groundwater*: Geological Society of America Special Paper 494, doi:10.1130/2013.2494(08).
- Mailloux, B.J., Person, M., Kelley, S., Dunbar, N., Cather, S., Strayer, L., and Hudleston, P., 1999, Tectonic controls on the hydrogeology of the Rio Grande Rift, New Mexico: *Water Resources Research*, v. 35, p. 2641–2659, doi:10.1029/1999WR900110.
- Manley, K., 1978, Cenozoic geology of the Española basin, in Hawley, J.W., ed., *Guidebook to Rio Grande Rift in New Mexico and Colorado*: New Mexico Bureau of Mines and Mineral Resources Circular 163, p. 201–210.
- Manley, K., 1979, Stratigraphy and structure of the Española Basin, Rio Grande rift, New Mexico, in Riecker, R.E., ed., *Rio Grande Rift—Tectonics and Magmatism*: Washington, D.C., American Geophysical Union, p. 71–86.
- Manning, A.H., 2009, Ground-Water Temperature, Noble Gas, and Carbon Isotope Data from the Española Basin, New Mexico: U.S. Geological Survey Scientific Investigations Report 2008-5200, 69 p.
- McAda, D.P., and Wasilek, M., 1988, Simulation of the Regional Geohydrology of the Tesuque Aquifer System near Santa Fe, New Mexico: U.S. Geological Survey Water-Resources Investigations Report 87-4056, 69 p.
- McLean, W., and Jankowski, J., 2000, Groundwater quality and sustainability in an alluvial aquifer, Australia, in Sililo et al., eds., *Proceedings, 30th Congress of the International Association of Hydrogeologists, Groundwater: Past Achievements and Future Challenges*, Cape Town, South Africa, November 2000: Rotterdam, A.A. Balkema.
- Mills, S.K., 2003, Quantifying Salinization of the Rio Grande Using Environmental Tracers [M.S. thesis]: Socorro, New Mexico Institute of Mining and Technology, 397 p.
- Minor, S.A., ed., 2006, The Cerrillos Uplift, the La Bajada Constriction, and Hydrogeologic Framework of the Santo Domingo Basin, Rio Grande Rift, New Mexico: U.S. Geological Survey Professional Paper 1720, 189 p.
- Minor, S.A., Hudson, M.R., Grauch, V.J.S., and Sawyer, D.A., 2006, Structure of the Santo Domingo Basin and La Bajada constriction area, New Mexico, in Minor, S.A., ed., *The Cerrillos Uplift, the La Bajada Constriction, and Hydrogeologic Framework of the Santo Domingo Basin, Rio Grande Rift, New Mexico*: U.S. Geological Survey Professional Paper 1720-E, p. 91–120.
- Moore, S.J., 2007, Streamflow, infiltration, and recharge in Arroyo Hondo, New Mexico, in Stonestrom, D.A., Constantz, J., Ferre, T., and Leake, S.A., eds., *Ground-Water Recharge in the Arid and Semiarid Southwestern United States*: U.S. Geological Survey Professional Paper 1703, p. 137–156.
- Morgan, P., Harder, V., Swanberg, C.A., and Daggett, P.H., 1981, A groundwater convection model for Rio Grande rift geothermal resources: *Geothermal Resources Council Transactions*, v. 5, p. 193–196.
- Mourant, W.A., 1980, Hydrologic Maps and Data for Santa Fe County, New Mexico: Santa Fe, New Mexico State Engineer Basic Data Report, 180 p.
- Myer, C., and Smith, G.A., 2006, Stratigraphic analysis of the Yates #2 La Mesa well and implications for southern Española Basin tectonic history: *New Mexico Geology*, v. 28, p. 75–83.
- Nkotagu, H., 1996, The groundwater geochemistry in a semi-arid, fractured crystalline basement area of Dodoma, Tanzania: *Journal of African Earth Sciences*, v. 23, p. 593–605, doi:10.1016/S0899-5362(97)00021-3.
- Parkhurst, D.L., and Appelo, C.A.J., 1999, User's Guide to PHREEQC (Version 2)—A Computer Program for Speciation, Batch-Reaction, One-Dimensional Transport, and Inverse Geochemical Calculations: U.S. Geological Survey Water-Resources Investigations Report 99-4259, 310 p.
- Pearson, C., and Goff, F., 1981, A Schlumberger resistivity study of the Jemez Springs region of northwestern New Mexico: *Geothermal Resources Council Transactions*, v. 5, p. 119–122.

- Piper, A.M., 1944, A graphical procedure in the geochemical interpretation of water analyses: *Transactions of the American Geophysical Union*, v. 25, p. 914–923.
- Plummer, L.N., Bexfield, L.M., Anderholm, S.K., Sanford, W.E., and Busenberg, E., 2004a, Geochemical Characterization of Ground-Water Flow in the Santa Fe Group Aquifer System, Middle Rio Grande Basin, New Mexico: U.S. Geological Survey Water-Resources Investigations Report 03-4131, 395 p.
- Plummer, L.N., Bexfield, L.M., Anderholm, S.K., Sanford, W.E., and Busenberg, E., 2004b, Hydrochemical tracers in the Middle Rio Grande Basin, U.S.A., I. Conceptualization of groundwater flow: *Hydrogeology Journal*, v. 12, p. 359–388, doi:10.1007/s10040-004-0324-6.
- Read, A.S., Koning, D.J., Smith, G.A., Ralser, S., Rogers, J., and Bauer, P.W., 2003 (orig. publ. 2000), Geology of the Santa Fe 7.5-Minute Quadrangle, Santa Fe County, New Mexico: New Mexico Bureau of Geology and Mineral Resources Open-File Geologic Map 32, scale 1:24,000.
- Read, A.S., Koning, D.J., and Johnson, P.S., 2005 (orig. publ. 2004), Generalized Geologic Map of the Southern Española Basin, Santa Fe County, New Mexico: New Mexico Bureau of Geology and Mineral Resources Open-File Report 481, scale 1:50,000 (CD-ROM).
- Reiter, M., Edwards, C.L., Hartman, H., and Weidman, C., 1975, Terrestrial heat flow along the Rio Grande rift: New Mexico and southern Colorado: *Geological Society of America Bulletin*, v. 86, p. 811–818, doi:10.1130/0016-7606(1975)86<811:THFATR>2.0.CO;2.
- Rodriguez, B.D., and Sawyer, D.A., 2013, this volume, Geophysical constraints on Rio Grande rift structure and stratigraphy from magnetotelluric models and borehole resistivity logs, northern New Mexico, in Hudson, M.R., and Grauch, V.J.S., eds., *New Perspectives on Rio Grande Rift Basins: From Tectonics to Groundwater*: Geological Society of America Special Paper 494, doi:10.1130/2013.2494(13).
- Sass, J.H., Lachenbruch, A.H., Dudley, W.W., Jr., Priest, J.J., and Munroe, R.J., 1988, Temperature, Thermal Conductivity, and Heat Flow near Yucca Mountain, Nevada: Some Tectonic and Hydrologic Implications: U.S. Geological Survey Open-File Report 87-649, 118 p.
- Sass, J.H., Dudley, W.W., Jr., and Lachenbruch, A.H., 1995, Regional thermal setting, Chapter 8, in Oliver, H.W., Ponce, D.A., and Hunter, W.C., eds., *Major Results of Geophysical Investigations at Yucca Mountain and Vicinity, Southern Nevada*: U.S. Geological Survey Open-File Report 95-74, 184 p.
- Sawyer, D.A., and Minor, S.A., 2006, Geologic setting of the La Bajada constriction and Cochiti Pueblo area, New Mexico, in Minor, S.A., ed., *The Cerrillos Uplift, the La Bajada Constriction, and Hydrogeologic Framework of the Santo Domingo Basin, Rio Grande Rift, New Mexico*: U.S. Geological Survey Professional Paper 1720-A, p. 1–23.
- Seager, W.R., 1975, Cenozoic tectonic evolution of the Las Cruces area, New Mexico, in Seager, W.R., Clemons, R.E., and Callender, J.F., eds., *Guidebook of the Las Cruces Country: New Mexico Geological Society Guidebook* 26, p. 241–250.
- Shaw, D.M., and Sturchio, N., 1992, Boron-lithium relationships in rhyolites and associated thermal waters of young silicic calderas, with comments on incompatible element behavior: *Geochimica et Cosmochimica Acta*, v. 56, p. 3723–3731, doi:10.1016/0016-7037(92)90165-F.
- Shearer, C.R., and Reiter, M.A., 1978, Basic Heat-Flow Data in New Mexico: New Mexico Bureau of Mines and Mineral Resources Open-File Report 93, 395 p.
- Smith, G.A., Larsen, D., Harlan, S.S., McIntosh, W.C., Erskine, D.W., and Taylor, S., 1991, A tale of two volcanoclastic aprons: Field guide to the sedimentology and physical volcanology of the Oligocene Espinaso Formation and Miocene Peralta Tuff, north-central New Mexico, in Julian, B., and Zidek, J., eds., *Field Guide to Geologic Excursions in New Mexico and Adjacent Areas of Texas and Colorado*: New Mexico Bureau of Mines and Mineral Resources Bulletin 137, p. 87–103.
- Spiegel, Z., and Baldwin, B., 1963, Geology and Water Resources of the Santa Fe Area, New Mexico: U.S. Geological Survey Water-Supply Paper 1525, 258 p.
- Stearns, C.E., 1953, Early Tertiary volcanism in the Galisteo-Tonque area, north-central New Mexico: *American Journal of Science*, v. 251, p. 415–452, doi:10.2475/ajs.251.6.415.
- Steele, K.F., and Wagner, G.H., 1981, Warm springs of the western Ouachita Mountains, Arkansas: *Geothermal Resources Council Transactions*, v. 5, p. 137–140.
- Sturchio, N.C., Muehlenbachs, K., and Seitz, M.G., 1986, Element redistribution during hydrothermal alteration of rhyolite in an active geothermal system: Yellowstone drill cores Y-7 and Y-8: *Geochimica et Cosmochimica Acta*, v. 50, p. 1619–1631, doi:10.1016/0016-7037(86)90125-0.
- Sun, M., and Baldwin, B., 1958, Volcanic rocks of the Cienega area, Santa Fe County, New Mexico: New Mexico Bureau of Geology and Mineral Resources Bulletin 54, 80 p., map scale 1:15,840.
- Swanberg, C.A., 1981, Subsurface temperatures of geothermal resources—Catalogue of thermal waters, in Iceman, L., Starkey, A., and Trentman, N., eds., *State-Coupled Low Temperature Geothermal Resource Assessment Program, Fiscal Year 1979*: Las Cruces, New Mexico Energy Research and Development Program, New Mexico State University, p. 1-18–1-30.
- Swanberg, C.A., 1984, Temperature gradient studies near two groundwater constrictions in northern New Mexico, in Iceman, L., ed., *Regional Geothermal Exploration in North Central New Mexico*: Las Cruces, New Mexico Energy Research and Development Institute, p. 114–148.
- Swanberg, C.A., and Morgan, P., 1978, The linear relation between temperatures based on the silica content of groundwater and regional heat flow: A new heat flow map of the United States: *Pure and Applied Geophysics*, v. 117, p. 227–241, doi:10.1007/BF00879749.
- Tello, E.H., Verma, P.M., and Tovar, R.A., 2000, Chemical and isotopic study to define the origin of acidity in the Los Humeros (Mexico) geothermal reservoir: *Geothermal Resources Council Transactions*, v. 24, p. 441–449.
- Thomas, C.L., Stewart, A.E., and Constantz, J., 2000, Determination of Infiltration and Percolation Rates along a Reach of the Santa Fe River near La Bajada, New Mexico: U.S. Geological Survey Water-Resources Investigations Report 00-4141, 65 p.
- Trainer, F.W., and Lyford, F.P., 1979, Geothermal hydrology in the Rio Grande rift, north-central New Mexico, in Ingersoll, R.V., Woodward, L.A., and James, H.L., eds., *Guidebook of Santa Fe Country: New Mexico Geological Society Guidebook* 30, p. 299–306.
- Witcher, J.C., 1981, Thermal springs of Arizona: *Fieldnotes from the State of Arizona Bureau of Geology and Mineral Technology*, v. 11, no. 2, p. 1–4.
- Witcher, J.C., Reiter, M., Bland, D., and Barroll, M.W., 1992, Geothermal resources in New Mexico: *New Mexico Geology*, v. 14, p. 14–16.
- Witcher, J.C., King, J.P., Hawley, J.W., Kennedy, J.F., Williams, J., Cleary, M., and Bothern, L.R., 2004, Sources of Salinity in the Rio Grande and Mesilla Basin Groundwater: *New Mexico Water Resources Research Institute Technical Completion Report* 330, 168 p.

MANUSCRIPT ACCEPTED BY THE SOCIETY 20 JULY 2012

Printed in the USA

